Kinesin-2 Motors Regulate GLI Protein Function

by

Brandon S. Carpenter

A dissertation submitted in partial fulfillment
of the requirements for the degree of
Doctor of Philosophy
(Cell and Developmental Biology)
in the University of Michigan
2015

Doctoral Committee:

Assistant Professor Benjamin L. Allen, Chair
Associate Professor Ivan P. Maillard
Associate Professor Kristen J. Verhey
Assistant Professor Sunny Y. Wong

To my baby girls, Abigail Jane and Caroline Mary Carpenter, who couldn't wait until

Daddy defended his dissertation to come into this world:

You're gonna make the finest mommas someday
Some man will take you away
But until then
Chase down your dreams
Laugh all the time and believe
That love's going to conquer all things
So until then
I'll be your man

Modified for twins from "I'll be your Man" by Zac Brown Band

To my wife, my rock, and the real reason I survived graduate school:

Happy is the man who finds a true friend,
and far happier is he who finds that true friend in his wife

- Franzs Schubert

ACKNOWLEDGEMENTS

My success in graduate school and the completion of my doctorate degree would not have been possible without a strong support team both in and outside of the laboratory.

First, I would like to thank Dr. Benjamin Allen for being an encouraging mentor. Ben's attention to detail and ability to think critically about science are unprecedented and contagious. I could not have asked for a more supportive environment to continue my scientific training and will apply what I have learned through Ben's mentorship to my own future mentoring relationships. After difficult weeks both in and outside of the lab, I always walked out of our weekly meetings feeling motivated and excited about science. No matter where my academic future leads, I am confident that I will be prepared, and for that I thank Ben Allen.

I would also like to thank my thesis committee members, Dr. Sunny Wong, Dr. Ivan Maillard, and Dr. Kristen Verhey. Through committee meetings and personal conversations, each member has provided excellent feedback and suggestions throughout my graduate career. Prior to submitting the work in Chapter II for publication, Sunny's experimental suggestions were helpful in the successful publication of Chapter II. Ivan Maillard accepted me as a rotation student when I first arrived in Ann Arbor. His early mentorship helped me transition into the University of Michigan as a thoughtful scientist. Since this invaluable experience, Ivan has continued to provide insightful experimental and career advice, and for that I thank you. Kristen Verhey has been a constant source of kinesin-2 expertise and an essential component to the

success of my doctoral work. In addition, Kristen gave me the opportunity to teach along side of her in the Physician Science Training Program; this experience has further inspired my passion for teaching.

Our CDB administrative staff members are amazing, Thanks for making me feel like family and for always being patient regardless of the situation. Along with our CDB administrators, I would also like to thank the MIL staff for being a continual source of microscopy information and training. Thanks you Sasha, Dottie, Bruce and last but certainly not least Chris Edwards. Chris I consider you an awesome colleague and even better friend. I will miss our conversations and those days we almost skipped out of work to hit the links.

It would have been a rough journey without awesome lab mates, luckily the Allen lab was full of intelligent and kind people that helped me make it through the "ups and downs" of graduate school. Thank you Jane, Irene, Alex, Justine, Martha, Ariell, Renee, Katarina, Diane, Jake, Will, and Allie. You guys rock, I wish you success in all you life endeavors.

I would like to thank all the people who were intellectually and experimentally invested in my research project. In particular I would like to thank the Billy Tsai and Kristen Verhey labs, especially Jeff, Taka, John and Lynne, for all of the reagents and help with biochemistry and kinesin biology. Further, I would like to thank Dr. Joe Besharse (Medical College of Wisconsin) for sharing the KIF17 mice. Renee Barry worked along side of me while applying for medical school and in the process performed the difficult biochemical experiments in Chapter II with KAP3B. Thank you Renee, it was fun to mentor such a wonderful personality and I will miss our poetry sessions.

I would like to especially thank my Mom and Dad for their continuous support throughout my graduate education. You have always been there for me, and I am blessed to have

you in my life. I am the person, and the scientist, I am today because of the values that you instilled in me from a young age. I can't thank you enough for all that you have done and I promise I will get a real job before I start drawing Social Security. I want to thank my sister, Brittany, for forgiving me for being a mean older brother, and always making her ride in the back seat. I love you and I am so proud of the beautiful woman you have become. I would also like to thank my grandparents for their unyielding support and relentless motivation. My grandparents are the rock that kept me strong and always encouraged me to not give up and work hard; Thank you Maw Maw, Paw Paw, and Granny.

Last, but not least, I want to thank my wife, Heather. Without you I have no idea where I would be in my life and science career. After long days, you always know what to say to put things into perspective. It seems like yesterday that we coasted into Ann Arbor on fumes with less than 100 dollars to our names. Look at us now! We are headed back to the south with two beautiful twin baby girls. I thank you for your love and patience; I can’t wait to see where this journey takes us.

TABLE OF CONTENTS

LIST OF FIGURES

ABSTRACT

Hedgehog (HH) signaling is an evolutionary conserved pathway that is indispensable for embryonic development and adult tissue homeostasis. GLI proteins are the transcriptional effector molecules of the HH signaling pathway that act in the nucleus to both activate and repress HH target gene expression. GLI proteins traffic between multiple subcellular compartments including the nucleus, cytoplasm, and primary cilium. Disruption in GLI trafficking results in defects in GLI protein activity, yet the mechanisms regulating these trafficking events are unclear. Kinesin-2 motor complexes, namely the heterotrimeric KIF3A/KIF3B/KAP3 complex and the homodimeric KIF17 complex, regulate both ciliary and non-ciliary transport of protein cargo, but whether these motor complexes regulate GLI proteins directly has not been tested. To examine a role for the heterotrimeric KIF3A/KIF3B/KAP3 kinesin-2 motor complex in regulating GLI activity, I performed a series of structure-function analyses using biochemical, cell signaling and in vivo approaches that define novel, specific interactions between GLI proteins and two components of this complex, KAP3 and KIF3A. I find that all three mammalian GLI proteins interact with KAP3 and map specific interaction sites in both proteins. Further, I find that GLI proteins interact selectively with KIF3A, but not KIF3B and that GLI interacts synergistically with KAP3 and KIF3A. Using a combination of cell signaling assays and chicken *in ovo* electroporations, I demonstrate that KAP3 interactions restrict GLI activator, but not GLI repressor function. These data suggest that GLI interactions with KIF3A/KIF3B/KAP3 complexes are essential for proper GLI transcriptional activity.

Further, I provide evidence that homodimeric KIF17 interacts with all mammalian GLI proteins and that GLI1 protein expression is decreased in cells stably expressing a dominant-negative version of KIF17. Finally, I show that KIF17 and GLI proteins are expressed in overlapping cell layers in the developing cerebellum, and that *Kif17*$^{-/-}$ mice display smaller cerebella. These data suggest a model in which KIF17 is playing a tissue-specific role in regulating HH signaling through interactions with GLI proteins. Together, my findings define novel interactions between GLI proteins and two distinct kinesin-2 motor complexes and further demonstrate that these interactions are required for proper GLI transcriptional activity.

CHAPTER I:

Introduction

Complex regulation of GLI proteins, the effector molecules of the Hedgehog signaling pathway

1.1 Abstract

Hedgehog (HH) signaling plays indispensible and diverse roles in regulating vertebrate embryonic development. GLI proteins are the effector molecules of the HH signaling pathway, modulating HH target gene transcription. Understanding the mechanisms that regulate GLI protein function is essential to treating severe developmental defects and adult cancers that arise from defects in GLI protein function. Within the mammalian GLI family of transcription factors, there are three vertebrate GLI proteins, GLI1-3. Here, I discuss how vertebrate HH signaling is regulated, specifically at the level of GLI proteins, and how GLI proteins function as molecular "switches" to activate and repress HH target gene expression. Our understanding of HH signal transduction drastically changed with the discovery that primary cilia, once thought to be vestigial structures, play essential roles in regulating HH signaling. With this discovery came the finding that GLI proteins traffic in and out of primary cilia, and that these trafficking events are necessary for proper GLI protein function. In Chapter I, I review how primary cilia and

intraflagellar trafficking (IFT) proteins regulate GLI protein ciliary localization and function. Finally, GLI proteins traffic between multiple subcellular compartments including the nucleus, cytoplasm, and primary cilia. How these trafficking events are coordinated, and what molecules regulate these trafficking events is not well understood. Thus far, two kinesin motor families, kinesin-4 and kinesin-2, have been implicated in regulating HH signaling. In the final section of Chapter I, I discuss how kinesin-4 family members, KIF7 and KIF27, regulate GLI proteins and provide justification for why I dedicate my doctoral work to understanding a role for kinesin-2 motor complexes, namely the heterotrimeric KIF3A/KIF3B/KAP3A and the homodimeric KIF17, in regulating GLI protein function.

1.2 Hedgehog signaling: pathway regulation from a "GLI" point of view

1.2.1 Identification of GLI proteins as effector molecules of the Hedgehog signaling pathway

Vertebrate HH signaling initiates when secreted HH ligands bind to the twelve-pass transmembrane receptor Patched (PTCH1) (Allen et al., 2011; Stone et al., 1996; Marigo et al., 1996a) and to the co-receptors GAS1, CDON, and BOC (Allen et al., 2011); this relieves inhibition of Smoothened (SMO), a seven-pass transmembrane GPCR-like protein that initiates a signal transduction cascade culminating in modulation of the GLI family of zinc-finger transcription factors (GLI1-3) (Hui and Angers, 2011) (Figure 1.1). The first human *GLI* gene, *GLI1*, was amplified from a glioblastoma (Kinzler et al., 1987) and subsequent GLI family members, *GLI2* and *GLI3*, were identified based on sequence similarity (J M Ruppert, 1988). Additional studies revealed that each GLI family member contains a highly conserved zinc-finger DNA-binding domain and is closely related to the *Kruppel* family of zinc-finger proteins (Kinzler et al., 1988). This finding suggested that, like other *Kruppel* family members, GLI

proteins could play important roles in regulating embryonic development. Further support for GLI proteins as transcription factors came when researchers observed that GLI1 is predominantly localized to the nucleus in tumor cells where it binds specific DNA sequences (Kinzler and Vogelstein, 1990).

Early expression analysis of GLI1-3 showing that *Gli1*, *Gli2*, and *Gli3* are expressed in both overlapping and distinct tissues during mouse embryonic development provided further evidence that GLI proteins may function in embryonic development (Hui et al., 1994). Interestingly, just prior to this expression analysis by Hui and colleagues, reports emerged showing that *extra-toes (Xt)* mutant mice display mutations in *Gli3* and that these mice are phenotypically similar to human patients suffering from Greig cephalopolysyndactyly syndrome, a syndrome in which *GLI3* was suggested to be the candidate gene (Vortkamp et al., 1991; Hui and Joyner, 1993). Together, these studies identified GLI proteins as zinc-finger transcription factors that are required for proper embryonic development and are unregulated in human cancers.

A decade after the discovery of the *Hh* gene in *Drosophila* (Nüsslein-Volhard and Wieschaus, 1980) it was determined that HH was a secreted signaling molecule that plays an important role in patterning embryos (Mohler and Vani, 1992; Lee et al., 1992; Tabata et al., 1992). Later it was revealed that three HH ligands exist in mice, Sonic Hedgehog (SHH), Indian Hedgehog (IHH), and Desert Hedgehog (DHH), demonstrating that, like GLI proteins, these molecules have been expanded in vertebrates (Echelard et al., 1993; Riddle et al., 1993; Krauss et al., 1993; Roelink et al., 1994). In *Drosophila*, *Cubitus interruptus* (*ci*) encodes the fly homolog of the vertebrate *GLI* genes and acts downstream of all other identified HH pathway components in flies to regulate HH target gene transcription (Domínguez et al., 1996; Alexandre

et al., 1996; Ingham, 1998; Orenic et al., 1990; Hepker et al., 1997; Slusarski et al., 1995). In parallel to these findings, roles for GLI proteins as regulators of HH signaling in mice were starting to surface. GLI1 was the first identified as a mediator of HH signaling because, unlike GLI2 and GLI3, GLI1 is expressed close to SHH ligand-expressing cells during gastrulation and neurulation (Sasaki et al., 1997; Lee et al., 1997; Hui et al., 1994; Platt et al., 1997). In addition to being expressed in close proximity to HH-ligand, misexpression of GLI1 mimicked the effects of ectopic HH-signaling in ventral progenitor cells within the neural tube (Hynes et al., 1997; Lee et al., 1997). In contrast to GLI1, GLI3 is down-regulated in the posterior mesenchyme of chick limb buds in an area where *Shh* is expressed, suggesting that, unlike GLI1, GLI3 represses HH activity (Marigo et al., 1996b). This idea was further supported in mice, where loss of *Gli3* results in ectopic *Shh* expression (Masuya et al., 1997; Büscher et al., 1997). Shortly after GLI1 and GLI3 were implicated as regulators of the HH signaling pathway, evidence that the third GLI family member, GLI2, was also regulating HH signaling came from a study that showed that HH-responsive genes, *Ptch1* and *Gli1*, are down-regulated in mice lacking *Gli2* (Ding et al., 1998). These authors and others, go on to show that that GLI2 is essential for high level but not low level HH signal transduction in the developing neural tube (Ding et al., 1998; Altaba, 1998).

Taken together, these studies implicated, for the first time, GLI1, GLI2, and GLI3 in regulating vertebrate HH signal transduction and further suggested that these proteins function as the transcriptional regulators of a highly conserved signaling pathway that plays important roles regulating multiple developmental processes.

1.2.2 GLI proteins display distinct and overlapping function as transcriptional activators and transcriptional repressors

With the realization that GLI1, GLI2, and GLI3 all regulate vertebrate HH transduction, came many studies dedicated to deciphering the mechanisms regulating GLI protein transcriptional activity. Evidence that GLI proteins could function as both transcriptional activators and transcriptional repressors was suggested by early reports in *Drosophila* showing that the GLI homolog, Ci, functions as both a transcriptional repressor and a transcriptional activator (Domínguez et al., 1996). Insight into vertebrate GLI protein function came with structure-function experiments in cultured cells showing that GLI3, like the *Drosophila* homolog Ci, contains both an N-terminal repressor and C-terminal activation domains, where as, GLI1 contains only the C-terminal activation domain (Dai et al., 1999) (Figure 1.2). Dai et al. further demonstrated that GLI3, but not GLI1, is processed into a transcriptional repressor and that in the presence of recombinant SHH ligand this processing event is inhibited, allowing full-length GLI3 to directly bind and activate the GLI1 promoter (Dai et al., 1999). These data suggested that *Gli1* is a direct target of the HH signaling pathway and that GLI3 can function as an activator and a repressor to mediate Hh signaling. However, the observation by these authors that *Gli1* mRNA is still present in *Gli3* homozygous mutant embryos provided an additional reason to investigate whether GLI2 could also regulate HH signaling as a transcriptional activator during vertebrate embryogenesis (Dai et al., 1999). In support of this, studies in *Gli2* and *Gli3* double mutant mice suggested that GLI2 and GLI3 play both specific and redundant roles during skeletal development (Mo et al., 1997). Analysis of GLI2 transcriptional activity showed that like GLI3, GLI2 contains both transcriptional activation and repressor domains, (Sasaki et al., 1999) (Figure 1.2). Further, these authors showed that full-length GLI2 and GLI3 function as weak activators, and that deletion of the N-terminal repression domain significantly increases the transcriptional activation function of both GLI2 and GLI3 (Sasaki et al., 1999). Together these

studies highlight GLI2 and GLI3 as the major effector molecules of the HH signaling pathway.

In contrast, to GLI2 and GLI3, GLI1 lacks a transcriptional repressor domain and is not processed, but instead is transcriptionally upregulated by GLI2 and GLI3 to propagate the HH signal once the pathway is activated (Bai et al., 2004). Unlike *Drosophila*, where Ci functions as the sole transcriptional activator and repressor in the HH signaling pathway, this function has been divided between GLI1, GLI2 and GLI3 in vertebrates. After the discovery that GLI1-3 all contain activation domains and that GLI2 and GLI3 contain additional repressor domains, the next major goal was to address the extent to which these vertebrate GLIs play overlapping and distinct roles as transcriptional activators and repressors during embryonic development.

Although GLI2 and GLI3 are the major effector molecules of HH signaling, all three vertebrate GLI proteins play overlapping activator roles. For example, during lung, trachea, and esophagus formation mutant mice lacking GLI2 display stenosis of the esophagus and trachea in addition to lung hypoplasia (Motoyama et al., 1998). Removing one copy of *Gli3* in a $Gli2^{-/-}$ mouse exacerbates these defects and complete loss of GLI3 in the same $Gli2^{-/-}$ mouse results in complete loss of the lung, trachea, and esophagus (Motoyama et al., 1998). In addition to foregut formation, HH-dependent neural tube patterning involves GLI1, GLI2, and GLI3 activator functions (Bai et al., 2004). SHH ligand is secreted from the notochord and later from the ventral most floor plate cells of the neural tube setting up a gradient of HH signaling that is important for specifying ventral progenitor cell populations (Figure 1.3). Strikingly, $Gli1^{-/-}$ mice do not display developmental defects or decreased HH signaling, unless one copy of *Gli2* is removed from the $Gli1^{-/-}$ background (Park et al., 2000; Bai et al., 2002). However, $Gli1^{-/-};Gli2^{-/-}$ mutant mice display slight defects in floor plate and V3 interneuron progenitor cells that require the highest level of HH signaling, suggesting that GLI1 enhances the activator function of GLI2 in these

most ventral cell types (Bai et al., 2004). Consistent with GLI3 functioning as a transcriptional repressor of HH signaling, *Gli3*$^{-/-}$ mice display dorsal expansion of V0-V2 indicative of over active HH signaling (Persson et al., 2002). While loss of *Gli3* in mice results in phenotypes resembling ectopic HH signaling, Bai and colleagues showed that in the ventral neural tube GLI3 functions as an activator and can induce some floor plate and V3 interneurons; however, unlike GLI2, GLI3 activator activity is dependent on *Gli1* transcription (Bai et al., 2004).

Together, these studies highlight overlapping roles for GLI proteins as transcriptional activators in multiple developmental contexts. While GLI2 and GLI3 can both act as transcriptional activators and repressors, GLI3 appears to be playing the major transcriptional repressor role in regulating HH target genes in vivo. However, reports of GLI2 functioning as a transcriptional repressor have been reported both *in vivo* and in cell culture (Buttitta et al., 2003a; Pan et al., 2006; McDermott et al., 2005). Further, loss of both GLI2 and GLI3 results in complete loss of HH signaling suggesting that GLI2 and GLI3 mediate most if not all of HH target genes transcription including upregulation of the third GLI family member, GLI1 (Buttitta et al., 2003b; Motoyama et al., 2015; Bai et al., 2004). These studies underscore an exciting example of evolutionary sub-functionalization where the once bipartite transcriptional function of the *Drosophila* GLI homolog, Ci, is now divided between all three mammalian GLI proteins that perform both overlapping and distinct functions in modulating HH transcriptional activity.

1.2.3 GLI protein processing and degradation: A complex process involving protein kinase A (PKA)

Post-translational modification of GLI proteins is a complex and highly regulated process that involves many different molecules. Even today, a complete understanding of the

mechanisms and molecules involved in regulating GLI protein function are not complete. As a result of the high level of HH pathway conservation between vertebrates and invertebrates, work in *Drosophila* has shaped our understanding and provided the groundwork for elucidating the mechanisms involved in vertebrate GLI protein processing and degradation. In particular, a study by Aza-Blanc and colleagues beautifully demonstrated that the *Drosophila* GLI homolog, Ci, is proteolytically cleaved into a repressor in the absence of HH ligand (Aza-Blanc et al., 1997). Shortly after this discovery, it was determined that extensive phosphorylation by several Ser/Thr kinases including protein kinase A (PKA), glycogen synthase kinase 3 (GSK3), and casein kinase I (CKI) family members leads to recruitment of the F-box containing protein Slimb/β-TrCP, a substrate-specific receptor of the SCF-type E3 ubiquitin ligase (Jia et al., 2005; Jiang and Struhl, 1998; Jia et al., 2002; Wang et al., 1999; Price and Kalderon, 2002; Smelkinson and Kalderon, 2006; Chen et al., 1999). A protein degradation domain (PDD) is further required for proper partial Ci processing by the proteasome **(**Figure 1.2**)**, a process that is inhibited in Ci mutants lacking the PDD (Tian et al., 2005; Méthot and Basler, 1999).

Roles for PKA in regulating vertebrate HH signaling have also been reported (Hammerschmidt et al., 1996; Epstein et al., 1996). Similar to Ci, GLI3 is phosphorylated by PKA at the first four PKA sites (P1-P4) in its C-terminus adjacent to the CK1 and GSK3 sites (black asterisks in Fig 1.2). Following these phosphorylation events full-length GLI3 is ubiquinated by the $SCF^{\beta TrCP}$ ubiquitin E3 ligase and subsequently processed by the proteasome into an N-terminal repressor (Wang et al., 2000a; Wang and Li, 2006; Tempé et al., 2006). Interestingly, GLI2 is also phosphorylated by PKA at the same sites as GLI3; in addition to a small fraction being processed into a N-terminal repressor, GLI2 is mostly destabilized resulting in degradation (Pan et al., 2009; 2006). Like Ci, both GLI2 and GLI3 contain a PDD that is

important for proteosomal degradation; however this domain is less potent in GLI2 (Pan and Wang, 2007). This destabilization of GLI2 in the absence of HH signaling partially explains why GLI3 functions as the major transcriptional repressor of the HH pathway, albeit GLI2 repressor activity is suggested to play minor roles in both neural tube and somite development (Buttitta et al., 2003b; Pan et al., 2009). In contrast, GLI1 lacks complete conservation of the conserved PKA phosphorylation residues, PDD, and is not processed in to a transcriptional repressor (Pan and Wang, 2007; Price and Kalderon, 2002) (Figure 1.2).

The role for PKA in initiation GLI2/3 repressor processing has been studied in great detail; however, positive regulation of GLI function by PKA has also been reported (Kaesler et al., 2000; Niewiadomski et al., 2013). In addition to the highly conserved PKA phosphorylation residues P1-P6 in GLI2 and GLI3 that are required for processing and degradation of GLI2 and GLI3, Niewiadomski et al. identified additional partial consensus PKA clusters, (Pc-g cluster, Figure 1.2) that are conserved between all vertebrate GLI proteins, as well as Ci, and are required for full activation of GLI2/3 transcriptional activators (Niewiadomski et al., 2014). In reporter assays, cells stably expressing versions of GLI2 where the Pc-g clusters are mutated to nonphosphorylatable or phosphomimetic residues showed 40% less and significantly more activity, respectively (Niewiadomski et al., 2014). In contrast to the P1-P6 residues, the Pc-g residues are completely conserved in GLI1, however their role in mediating GLI1 activation has not been tested. Interestingly, it is reported that additional residues within GLI1 are phosphorylated by PKA, and mutating these residues has both positive and negative functional consequences on GLI1 transcriptional activity (Kaesler et al., 2000). While more studies are necessary to fully understand the complex regulation of GLI proteins by PKA, it is clear that PKA controls both GLI processing and transcriptional activation.

In addition to $SCF^{\beta TrCP}$–mediated GLI processing and degradation, additional E3 ubiquitin ligases regulate the turnover of GLI proteins. For example, in *Drosophila*, levels of full-length Ci are controlled by the substrate-specific receptor for the Cul3-based E3 ubiquitin ligase Hib (Kent et al., 2006; Zhang et al., 2006). In flies, Loss of Hib leads to an accumulation of Ci, where as overexpression of Hib reduces Ci levels and inhibits HH signaling (Kent et al., 2006). Similar to Hib, the mammalian homolog, SPOP (speckle-type POZ protein), interacts with GLI2 and GLI3 to promote their ubiquitin-mediated processing and degradation (Chen et al., 2009; Zhang et al., 2009). In contrast, GLI1 is not a strong substrate for SPOP (Chen et al., 2009; Zhang et al., 2009), but instead is recruited to the E3 ubiquitin ligase, Itch, by the adaptor protein, Numb (Di Marcotullio et al., 2010). Together, these studies highlight several key protein components that regulate GLI protein processing and degradation, and further emphasize the complex regulation of GLI protein levels during embryonic development.

1.2.4 Suppressor of fused (Sufu): a vertebrate specific regulator of GLI protein function

In addition to PKA, suppressor of fused (SUFU) is another highly conserved HH pathway component that negatively regulates the HH signaling pathway (Preat, 1992). Loss-of-function mutations in *Sufu* suppress the phenotype in flies containing mutations in *Fu*, a serine-threonine kinase that is important for HH signaling downstream of Smo in *Drosophila* HH signaling (Preat et al., 1990; 1993; Thérond et al., 1993).Interestingly, while loss of SUFU is flies has no noticeable consequence in the absence of other mutations, *Sufu*$^{-/-}$ mice die in utero by E9.5 with severe developmental defects indicative of overactive HH signaling similar to those observed in *Ptch1*$^{-/-}$ mice that display constitutive HH pathway activation (Svärd et al., 2006). Like *Ptch1*$^{-/-}$ mice, *Sufu*$^{-/-}$ mice develop a ventralized neural tube and have deformed cephalic regions

including an open fore-, mid-, and hindbrains (Svärd et al., 2006). An earlier study identified an SYGH motif present in all mammalian GLI proteins that is required for SUFU binding– mutation of this motif in GLI1 results in constitutive GLI1 nuclear localization (Dunaeva et al., 2003)(Figure 1.2). Similarly, mouse embryonic fibroblasts (MEFs) lacking SUFU show increased nuclear localization of GLI1 (Svärd et al., 2006). A more mechanistic understanding of how of SUFU regulates GLI proteins came in a study by Humke et al. where they eloquently show that in the absence of HH signaling SUFU promotes GLI3 processing into its repressor form and that initiation of HH signaling promotes the dissociation of the SUFU-GLI3 complex and nuclear localization of full-length GLI3 (Humke et al., 2010). Interestingly, activation of PKA prevents the dissociation of the GLI3-SUFU complex, thus preventing nuclear localization and transcriptional activity of full-length GLI3 (Humke et al., 2010). SUFU also forms complexes with GLI2, and like SUFU-GLI3 complexes, HH signaling promotes the dissociation of SUFU from GLI2 (Humke et al., 2010).

Further studies showed that loss of SUFU results in destabilization of full-length but not C-terminally processed repressor versions of GLI2 and GLI3, where as overexpression of SUFU stabilizes both GLI2 and GLI3 (Wang et al., 2010). In this same study, Wang and colleagues demonstrated that knockdown of SPOP in *Sufu*$^{-/-}$ MEFS rescues full-length GLI2 and GLI3 levels, and consistent with this result, overexpression of SPOP promotes GLI2 and GLI3 processing and degradation (Wang et al., 2010). An earlier study demonstrated that SUFU interacts with GLI proteins through an additional C-terminal motif (Merchant et al., 2004)(Figure 1.2) and Wang and colleagues further showed that SUFU and SPOP compete for the same binding sites within the N- and C-termini of GLI3 and a C-terminal region of GLI2. Strikingly, expression of a constitutive GLI3 repressor in *Sufu*$^{-/-}$ mice mostly rescues the ventralized neural

tube, suggesting that C-terminally processed GLI3 repressor functions independently of SUFU (Wang et al., 2010).

Together, these studies demonstrate that SUFU is a negative regulator of HH signaling that interacts with full-length GLI proteins to promote their processing and degradation in addition to stabilizing and preventing their nuclear localization in a HH dependent manner. Further, dissociation of SUFU-GLI complexes is inhibited by PKA and depends on the presence of primary cilia, microtubule-based organelles that are implicated in regulating HH signaling (see below).

1.3 Regulation of GLI protein function by primary cilia

1.3.1 Link between vertebrate HH signaling and primary cilia

The discovery that vertebrate HH signaling requires primary cilia has drastically changed the dogma of HH signal transduction (Huangfu et al., 2003). Primary cilia are microtubule-based extensions of the cell surface that were once thought to be vestigial structures in vertebrates; however, now we know that these subcellular organelles regulate many important developmental processes including HH signaling (Goetz and Anderson, 2010). Intraflagellar transport (IFT) is a highly regulated process involving IFT particles (A and B) that are trafficked along a microtubule-based axoneme by anterograde (kinesin-2) and retrograde (dynein) motor proteins (Goetz and Anderson, 2010) (Figure 1.4). The first piece of evidence demonstrating that vertebrate HH signaling depends on primary cilia came from a forward-genetic screen in mice designed to identify mutations that disrupt embryonic development (Huangfu et al., 2003). Interestingly, many of the mutant embryos discovered in this screen had mutations in IFT

components, which resulted in phenotypes similar to those seen in HH mutants, in particular defects in HH-dependent neural patterning (Huangfu et al., 2003; Goetz and Anderson, 2010). In-depth investigations into the IFT mutants identified by Anderson and colleagues, initiated a large body of research dedicated to understanding how primary cilia regulate HH signaling and the subsequent discovery that several core HH pathway components localize to primary cilia both in the absence and presence of HH signaling, including the GLI proteins (Rohatgi et al., 2007; Corbit et al., 2005; Haycraft et al., 2005) (Figure 1.5). Mutations in several IFT components, including the anterograde motor (*Kif3a*), retrograde motor (*Dync2h1*), IFT A (*Ift122, Ift172,*), and IFT B (*Ift88*, *Ift27*, *Ift25*) complexes causes defects in GLI accumulation at the ciliary tip and correlates with defective HH signaling (Takeda et al., 1999; Ocbina et al., 2011; Huangfu and Anderson, 2005; Qin et al., 2011; Keady et al., 2012; Gorivodsky et al., 2009; Huangfu et al., 2003; Yang et al., 2015; Haycraft et al., 2005; Liu et al., 2005). In many cases these IFT mutations correlate with HH loss-of-function, in particular in the neural tube where defects in Gli activator function results in misspecification of ventral neuronal progenitor cells (Huangfu and Anderson, 2005; Huangfu et al., 2003). However, in some cases mutations in IFT components display apparent gain-of-function HH phenotypes, particularly in the mouse limb where defects in GLI3 repressor processing result in improper digit specification (Haycraft et al., 2005; Liu et al., 2005). While defects in IFT machinery perturb HH signaling and GLI function, how IFT components interact with and regulate GLI proteins is not well characterized.

1.3.2 Ciliary regulation of GLI protein processing and activation

All three mammalian GLI proteins localize to primary cilia, but not the proteolytically processed GLI3 repressor (Haycraft et al., 2005). GLI2 and GLI3 cycle through cilia at low levels in the absence of HH signaling, and within minutes after HH stimulation, both full-length GLI2 and GLI3 accumulate at the tips of primary cilia in a SMO and microtubule-dependent manner (Kim et al., 2009; Wen et al., 2010; Chen et al., 2009) (Figure 1.5). These studies confirmed that full length GLI2 and GLI3, but not their C-terminally truncated repressor versions, are enriched at ciliary tips. Further, defects in ciliogenesis disrupt GLI3 processing and full-length GLI2 activation which results in digit formation and neural tube defects (Haycraft et al., 2005; Liu et al., 2005). While these studies implicated primary cilia in regulating GLI processing and activation, whether GLI ciliary localization is required for this regulation and how the protein regulators of GLI transcriptional activity, namely SUFU and PKA, fit into the cilia-centric HH model had yet to be elucidated.

Insights into these mechanisms came with the finding that SUFU traffics in complex with GLI proteins through the primary cilia in a GLI-dependent manner (Haycraft et al., 2005; Zeng et al., 2010) (Figure 1.5). HH stimulation promotes the ciliary accumulation and subsequent dissociation of GLI2-SUFU and GLI3-SUFU complexes, a process dependent on primary cilia (Humke et al., 2010; Tukachinsky et al., 2010). However, constitutive activation of GLI proteins in the absence of SUFU is independent of primary cilia (Jia et al., 2009; Chen et al., 2009). Furthermore, PKA localizes near the basal body at the base of the cilium and loss of PKA causes an increase in GLI2 at the tips of primary cilia (Tuson et al., 2011; Barzi et al., 2009; Tukachinsky et al., 2010; Zeng et al., 2010) (Figure 1.5). Also, HH mediated dissociation of GLI-SUFU complexes is inhibited in cells lacking primary cilia or with overactive PKA, suggesting that GLI-SUFU complexes dissociate at the cilium in response to PKA inactivation

(Humke et al., 2010; Tukachinsky et al., 2010). In combination with the finding that cilia localization of GLI2 and GLI3 is not affected by loss of the conserved P1-4 PKA phosphorylation sites (Zeng et al., 2010), these data suggest that PKA modifies GLI proteins at the base of the cilium upon ciliary exit (Tuson et al., 2011). Together, these studies support a mechanism by which trafficking of the GLI-SUFU complexes within primary cilia controls the accessibility of these complexes to PKA phosphorylation upon ciliary exit. Since full-length, but not repressor versions of GLI2 and GLI3 are localized to the primary cilia (Wen et al., 2010; Haycraft et al., 2005), this further supports a model where in the absence of HH ligand, GLI2-SUFU and GLI3-SUFU complexes traffic through cilia at low levels where they are modified into a PKA substrate which results in GLI processing and degradation. HH pathway activation promotes ciliary dissociation of GLI2 and GLI3 from SUFU where they now avoid PKA mediated processing and degradation leading to activation of full-length transcriptional activators that can then localize to the nucleus and upregulate HH target gene transcription (Figure 1.5).

Many question still remain unresolved. For instance, the specific post-translational modifications that the GLI-SUFU complexes receive in the cilium, and whether these complexes dissociate within the primary cilia are still unresolved. In addition, HH pathway activation in the absence of PKA is dependent on primary cilia (Tuson et al., 2011), leaving open the possibility that additional cilium-dependent mechanisms exist downstream PKA inhibition that allow full activation of GLI proteins.

Interestingly, domains required for GLI2 cilia localization have been identified and deleting these domains prevents GLI2 cilia localization, separation form SUFU, and subsequent activation, supporting the model proposed above (Santos and Reiter, 2014; Liu et al., 2015).

Important to note, in the process of generating a mutant GLI2 allele lacking the cilia localization domain, Liu and colleagues additionally eliminate the conserved P1-P6 PKA residues and show that this GLI2 variant fails to activate Hh signaling (Liu et al., 2015). This is in contrast to a recent study that showed that stably expressing a version of GLI2 lacking the P1-P6 PKA sites highly activates HH signaling (Niewiadomski et al., 2014). These contrasting findings suggest that even a version of GLI2 insensitive to PKA phosphorylation that results in processing and degradation must traffic to the primary cilia to become fully active highlighting the possibility that primary cilia regulate GLI protein transcriptional activation through additional mechanisms.

Roles for primary cilia in negatively and positively regulating GLI protein function have been recently reported in human disease (Wong et al., 2009; Han et al., 2009). More specifically, Wong et al. demonstrate that tumors initiated by overactive Smo depend on primary cilia for facilitating positive signals through GLI activators and for suppressing negative signals through processing of GLI repressors (Wong et al., 2009). Future studies are required to fully understand how primary cilia regulate GLI protein activity and the importance of this regulation in HH-dependent tumorigenesis.

1.4 Kinesin motor regulation of GLI protein function

1.4.1 Complex regulation of GLI proteins by the kinesin-4 motor protein, KIF7

Despite the remarkably high level of pathway conservation shared between invertebrate and vertebrate HH signal transduction, *Drosophila* do not require primary cilia for proper HH signaling. This raises a fascinating question: Why does vertebrate HH signaling depend on primary cilia? A possible answer to this question may reside with the kinesin-4 motor family member, KIF7. Prior studies in *Drosophila* identified Costal 2 (Cos2) as a kinesin-like protein

that regulates HH signal transduction via direct interactions with the *Drosophila* GLI homolog Ci (Sisson et al., 1997; Robbins et al., 1997). Cos2 functions both positively and negatively to transduce the HH signal from the transmembrane receptors, Ptc and Smo, to the Gli transcription factor, Ci (Wang and Holmgren, 1999; Wang et al., 2000b; Wang and Jiang, 2004; Ruel et al., 2003). In the absence of Hh ligand, Cos2 scaffolds a complex containing the Fu kinase and Ci to microtubules resulting in recruitment of protein kinases and processing of Ci into a truncated repressor (Zhao et al., 2005). Upon Hh ligand stimulation, Cos2 no longer scaffolds Ci for processing, but instead forms a complex with Smo which allows predominance of full-length Ci activator and subsequent upregulation of HH target genes (Zhao et al., 2007; Ruel et al., 2003).

More recent studies in vertebrates identified a similar role for the Cos2 vertebrate homologue, KIF7, in the regulation of GLI protein function (Liem et al., 2009; Endoh-Yamagami et al., 2009; Cheung et al., 2009). In vertebrates, two Cos2 homologs exist, KIF7 and KIF27, both of which interact with GLI proteins (Endoh-Yamagami et al., 2009; Cheung et al., 2009; Maurya et al., 2013; Marks and Kalderon, 2011; Katoh and Katoh, 2004); however whether KIF27 regulates HH signaling and GLI protein activity is still unresolved. In contrast to KIF27, several studies have shown that mice lacking KIF7 display mild ectopic HH phenotypes due the dual role for KIF7 in both promoting and antagonizing GLI activity (Maurya et al., 2013; Hsu et al., 2011; Li et al., 2012). In fact, due to the mild ectopic HH phenotypes observed in mice lacking KIF7, an early report suggested that KIF7 is dispensable for vertebrate HH signaling (Varjosalo et al., 2006).

In *Drosophila*, point mutations in the motor domain of Cos2 disrupt its microtubule dependent motility thereby inhibiting its ability to repress HH signaling (Farzan et al., 2008; Ho et al., 2005). Similar results are observed in vertebrates where $Kif7^{maki}$ mice (harboring a L130P

mutation in the conserved motor domain) show mild ectopic activation of HH target genes (Liem et al., 2009). In this study, *Kif7*^{maki} mice display expanded motor neuron and NKX2.2+ domains, however, *Gli2 Kif7*^{maki} double mutants the motor neuron domain is not expanded dorsally and the floor plate and NKX2.2 domains are absent (Liem et al., 2009). This suggests that the expanded motor neuron and NKX2.2+ domains seen in the mutant mice are a result of increased GLI2 activity. In addition, *Kif7*^{maki} mice display preaxial polydactyly and defects in GLI3 processing likely contributing to the greater expansion of ventral progenitor domains seen in *Gli3 Kif7*^{maki} double mutants compared to *Gli3* mutants alone. Further, while *Smo* single mutants die by embryonic day 9.5 (E9.5) and fail to specify any ventral neuronal cell populations, *Smo;Kif7*^{maki} double mutants survive to E10.5 and partially specify both NKX2.2 and motor neuron cells, suggesting that the loss of *Kif7* function in *Smo* null mice partially rescues GLI activation. Along with a partial rescue in mice lacking the major HH signal transduction component SMO, *Ptch1;Kif7*^{maki} double mutants also partially rescue the severe phenotypes displayed by mice lacking the major Hh negative regulator, PTCH1 (Liem et al., 2009). Through a careful analysis, Anderson and colleagues showed that not only does KIF7 regulate HH signaling, but it does so by both positively and negatively regulating GLI activity through a mechanism that requires primary cilia (Liem et al., 2009). Together with other studies, the current paradigm is that, similar to Cos2, KIF7 promotes HH signaling through dissociation of SUFU-GLI complexes, but unique to vertebrates, controls the ciliary localization of GLI proteins in a tissue-specific manner (Hsu et al., 2011; Maurya et al., 2013; Endoh-Yamagami et al., 2009; Liem et al., 2009). While the KIF7-GLI interaction sites have not been precisely mapped, GLI proteins appear to interact with KIF7 via multiple domains, including an N-terminal motif (Marks and Kalderon, 2011).

KIF7 localizes to the tips of primary cilia in response to HH stimulation, and mutations that disrupt the motor domain of KIF7 perturb both KIF7 and GLI protein accumulation at the ciliary tip (Hsu et al., 2011; Liem et al., 2009). These experiments raised the possibility that KIF7 could act as an anterograde motor to directly traffic GLI-SUFU complexes. However, detailed investigation by Anderson and colleagues showed that KIF7 does not possess plus-end-directed microtubule motoring capabilities, but instead functions to organize the ciliary tip compartment through the regulation of microtubule dynamics (He et al., 2014). Further, the effects of KIF7 are controlled by PPFIA1- and PP2A-mediated regulation of KIF7 phosphorylation (Liu et al., 2014). These results suggest that either the loss of KIF7 (He et al., 2014), or altered KIF7 phosphorylation (Liu et al., 2014), affects the ciliary localization and activity of GLI proteins due to disorganization of the ciliary tip. This supports the idea that the ectopic activation of the HH pathway observed in mice defective in KIF7 function could result from ectopic GLI-SUFU complexes away from the ciliary tip, where they inappropriately dissociate in the absence of HH signaling.

Whether KIF7-mediated dissociation of the GLI-SUFU complexes requires the direct interaction of KIF7 for its negative and positive roles in regulating GLI activity requires further studies, but regardless, KIF7 shares at least some conserved functional roles in regulating HH signal transduction with its *Drosophila* homolog, Cos2. It is interesting to postulate that the intimate relationship between vertebrate HH signaling and primary cilia may be at least partly due to the evolutionary conserved role of KIF7 and Cos2 in sculpting microtubules. Lastly, the finding that KIF7 does not possess plus-end-directed microtubule motoring capabilities leaves a gap in our understanding of how GLI proteins are trafficked to the tips of primary cilia. A major

unresolved question remains: What motor proteins regulate plus-end-directed GLI trafficking within the primary cilia?

1.4.2 Role of kinesin-2 motors in the regulation of HH signaling

The kinesin-2 motors are a functionally diverse subgroup of the kinesin superfamily that mediate plus-end-directed trafficking events both within and outside of primary cilia (Scholey, 2013). Within the kinesin-2 family, three motor complexes exist: (1) a heterotrimeric KIF3A/KIF3B/KAP3 complex, (2) a heterotrimeric KIF3A/KIF3C/KAP3 complex, and (3) a homodimeric KIF17 complex (Figure 1.6). Multiple roles for kinesin-2 motor proteins in regulating cell processes and embryonic development have been reported, including intraflagellar transport and cilium assembly, opsin transport in photoreceptor development, and axonal and cytoplasmic organelle transport (Scholey, 2013; Hirokawa, 2000).

The heterotrimeric KIF3A/KIF3B/KAP3 is the most studied member of the kinesin-2 motor family and is known for its roles in intraflagellar transport and cilia assembly (Scholey, 2013; Hirokawa et al., 2009; Hirokawa, 2000; Nonaka et al., 1998; Takeda et al., 2000). In fact, mice with mutations in *Kif3A*, *Kif3B*, or the kinesin-associated protein, *Kap3* (*Kifap3*) (Yamazaki et al., 1996), die by mid-gestation due to defects in left-asymmetry as a result of defects in ciliogenesis (Takeda et al., 1999; Nonaka et al., 1998; Hirokawa, 2000; Teng et al., 2005). Similar to KIF3B, KIF3C forms an additional complex with KIF3A and KAP3 (Figure 1.6); however KIF3C is dispensable for normal embryonic development and functions in distinct tissues (Yang and Goldstein, 1998; Muresan et al., 1998). Interestingly, KIF3C also forms a distinct complex from KIF3A and KAP3 (Muresan et al., 1998), but how this heterotrimeric

KIF3A/KIF3C/KAP3 complex regulates plus-end-directed microtubule trafficking requires more studies.

Initial investigations into the mechanisms that regulate heterotrimeric kinesin-2 complex assembly and function in vertebrates suggested that KIF3A and KIF3B interact with cargo via the armadillo repeats of KAP3 (Takeda et al., 2000; Yamazaki et al., 1996; Gindhart and Goldstein, 1996), yet examples also exist where KIF3A interacts with cargo independently of KAP3 (Huang et al., 2011; Tanuma et al., 2008; Phang et al., 2014). For example, the TRIM protein RNF33 interacts with KIF3A and KIF3B in mouse testis in the absence of KAP3 (Huang et al., 2011). Further, two isoforms of KAP3 exist, KAP3A and KAP3B, but how these isoforms differ in both their interactions with KIF3A, KIF3B and protein cargos is unknown (Yamazaki et al., 1996). While it is clear that the heterotrimeric KIF3A/KIF3B/KAP3 complex regulates important cellular processes, the mechanism by which this complex interacts with and regulates cargo trafficking requires additional experiments.

Interestingly, mice lacking KIF3A and KIF3B display phenotypes indicative of disrupted HH signaling, including craniofacial abnormalities, loss of ventral progenitor cells in the developing neural tube, and excessive bone and cartilage formation during mouse skeletogenesis (Takeda et al., 1999; Huangfu et al., 2003; Nonaka et al., 1998; Koyama et al., 2007). These findings suggest that members of the heterotrimeric kinesin-2 complex play important roles in HH-dependent tissue patterning, but whether this regulation is through direct interactions and trafficking of HH components remains unclear. Unfortunately, teasing apart a functional role for KIF3A, KIF3B, and KAP3 in directly regulating HH signaling is complicated by the fact that genetic manipulation of either complex member causes defects in ciliogenesis.

In contrast to the heterotrimeric KIF3A/KIF3B/KAP3 kinesin-2 complex, the homodimeric KIF17 complex is dispensable for normal ciliogenesis and has not been implicated in HH signaling (Wong-Riley and Besharse, 2012). While mice lacking KIF17 are viable and appear anatomically normal, loss of KIF17 leads to neuronal dysfunction in mice and is associated with schizophrenia in humans (Yin et al., 2011; Wong-Riley and Besharse, 2012; Tarabeux et al., 2010; Setou et al., 2000). Furthermore, recent studies have revealed that KIF17 functions in a diverse range of distinct cell processes, including dendritic transport of neurotransmitters and mRNA, intraflagellar transport in the specialized vertebrate photoreceptor and olfactory sensory cilia, and stabilization of microtubule polarity (Guillaud et al., 2003; Jaulin and Kreitzer, 2010; Yin et al., 2012; Setou et al., 2000; Yin et al., 2011; Insinna et al., 2008; 2009; Takano et al., 2007; Jenkins et al., 2006). Further, structure-function experiments discovered that KIF17 contains a sequence within the C-terminal tail that mediates both its nuclear and ciliary entry (Dishinger et al., 2010). Interestingly, KIF17 interacts with and regulates the delivery of signaling molecules to primary cilia (Jenkins et al., 2006). For example, KIF17 delivers cyclic nucleotide-gated channels to the ciliary membrane in MDCK kidney epithelial cells (Jenkins et al., 2006). Similar to KIF17, KAP3 also shuttles between the nuclear and ciliary compartments in sea urchin embryos (Morris et al., 2004); however, whether KAP3 localizes to the nucleus in vertebrates requires further investigation. Together these studies suggest that, similar to GLI proteins, members of both the heterotrimeric and homodimeric kinesin-2 complexes localize to both cilia and nuclear compartments.

Both the heterotrimeric KIF3A/KIF3B/KAP3 and the homodimeric KIF17 motor complex are expressed in multiple neuronal tissues where they play indispensible roles in regulating plus-end-directed microtubule cargo transport. GLI proteins, like the kinesin-2

complexes, are also highly expressed in many different neuronal tissues where they function to transduce HH signaling during embryonic and postnatal neurological processes (Ruiz i Altaba et al., 2002). Although kinesin-2 motors have been implicated as regulators of HH signaling for over a decade, whether these motors directly regulate HH signaling through interactions with GLI proteins, or other HH components, has not been assessed.

1.5 Conclusion

Vertebrate GLI proteins undergo extensive regulation both in the presence and absence of HH signaling to ensure that HH target genes are properly regulated. In *Drosophila*, the GLI homolog Ci functions as both a transcriptional activator and repressor, whereas these duties have been split between three mammalian GLI proteins, GLI1, GLI2 and GLI3. Processing and activation of GLI proteins is a highly regulated process that requires modifications by and interactions with many different proteins, including SUFU, PKA, and KIF7. Recent studies indicate that the interactions between SUFU, PKA, and KIF7 and GLIs are further modulated by their localization to primary cilia. Despite the large body of evidence that suggest GLI trafficking to cilia is required for proper transcriptional activity, the mechanisms that regulate these trafficking events remain unknown.

Like GLI proteins, kinesin-2 protein complexes, namely the heterotrimeric KIF3A/KIF3B/KAP3 and homodimeric KIF17 complex, localize to multiple subcellular compartments where they regulate plus-end-directed microtubule trafficking. This in combination with the finding that KIF7 lacks plus-end-directed motoring capabilities makes kinesin-2 motor complexes presumptive candidates for regulating GLI subcellular trafficking; thus I dedicated my doctoral research to assessing a role for both the heterotrimeric

KIF3A/KIF3B/KAP3 and the homodimeric KIF17 complexes in regulating GLI protein trafficking and function.

A difficult problem still remains: How do you assess a role for the KIF3A/KIF3B/KAP3 complex in regulating Gli proteins away from its function in ciliogenesis? In Chapter II, I tackle this problem by performing a series of structure-function analyses to define novel, specific interactions between GLI proteins and components of the heterotrimeric complex. Using a combination of cell signaling assays and chicken *in ovo* electroporations, I test the significance of these interactions on GLI transcriptional activity. In Chapter III, I investigate a role for the homodimeric KIF17 complex in regulating GLI protein activity. Here, I take a biochemical approach to assess physicals interactions between KIF17 and each of mammalian GLI proteins. Further, I examine a functional role for KIF17 in regulating GLI protein function and subcellular localization in cells expressing a version of KIF17 that lacks the conserved motor domain. Lastly, I take advantage of the viability of *Kif17*$^{-/-}$ mice and thoroughly assess both the expression of KIF17 during HH-dependent cerebellar development and the consequences of cerebellar proliferation in the absence of KIF17.

1.6 Figures

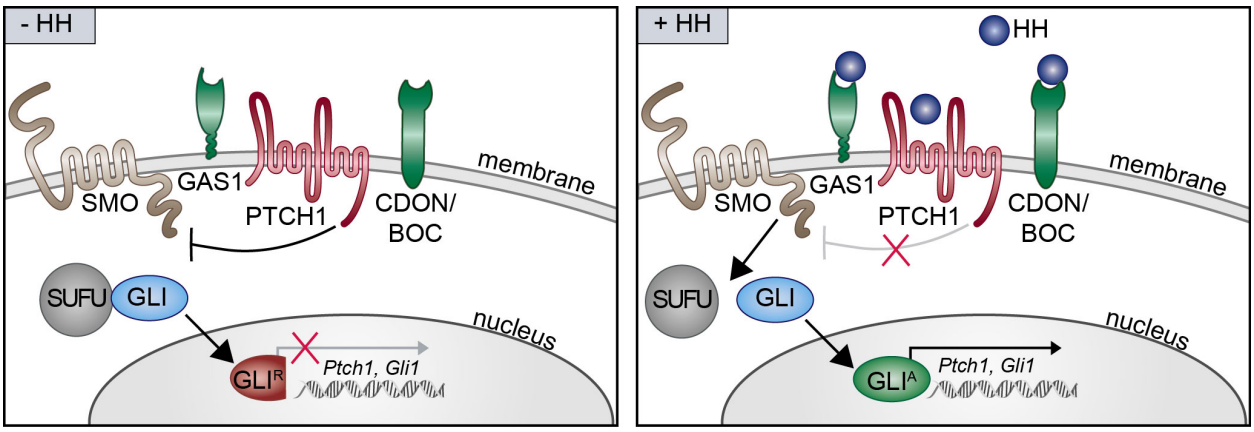

Figure 1.1. Schematic of the vertebrate Hedgehog (HH) signaling pathway.
(Left) In the absence of HH signaling, PTCH1 constitutively inhibits the activity of SMO, a key transducer of the HH signaling pathway. This leads to processing of GLI transcription factors into transcriptional repressors that restrict HH target gene expression, including *Ptch1* and *Gli1*. (Right) HH ligand binding to PTCH1 and the co-receptors, GAS1, CDON, and BOC relieves PTCH1 inhibition of SMO leading to processing of GLI transcription factors into transcriptional activators that bind DNA and activate HH target gene transcription.

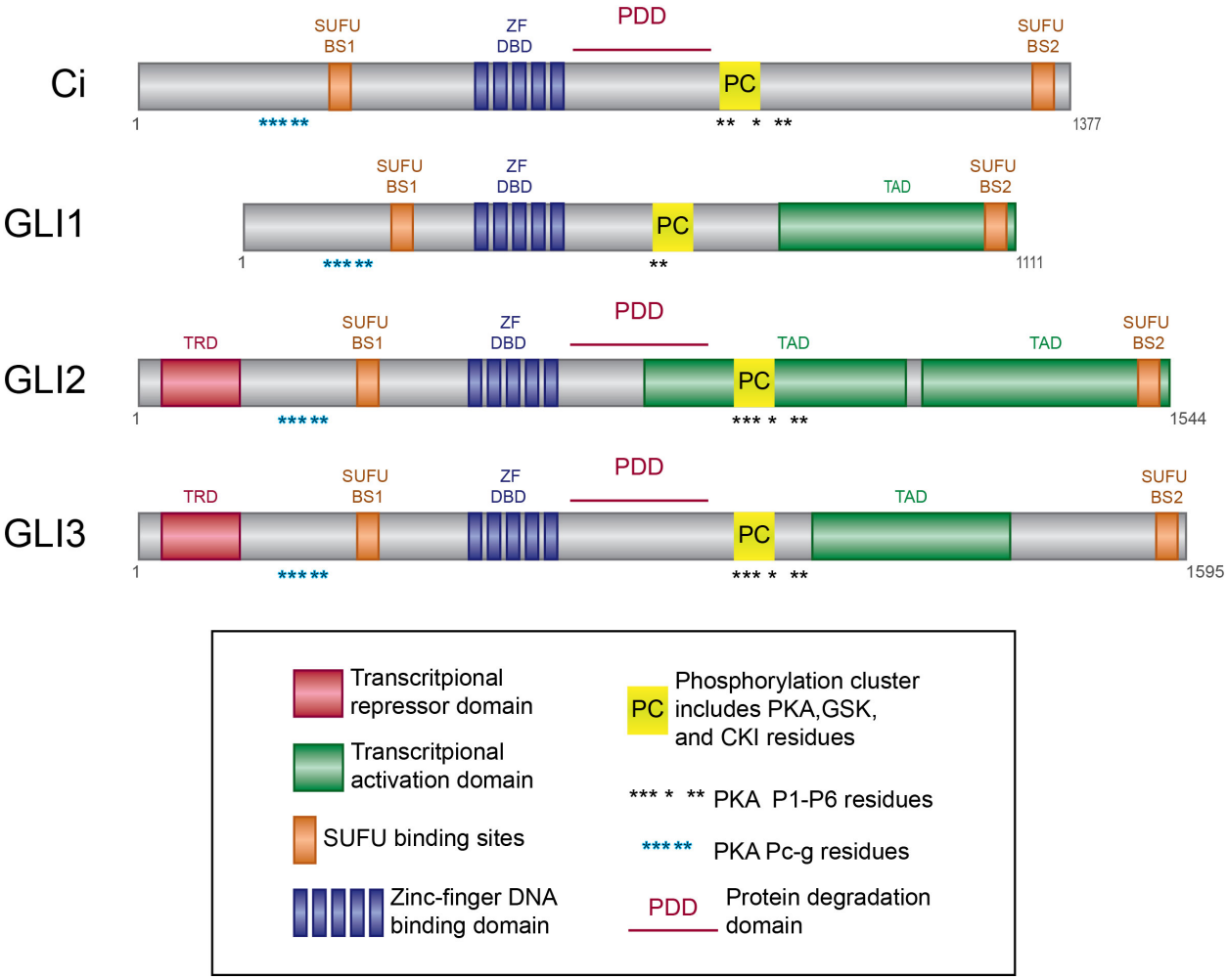

Figure 1.2. Schematic representation of domains and motifs in GLI proteins.
Structural domains and modification sites within *Drosophila* GLI protein, Cubitus interruptus (Ci) and mouse GLI1, GLI2, and GLI3 are represented. Figure adapted from (Hui and Angers, 2011)

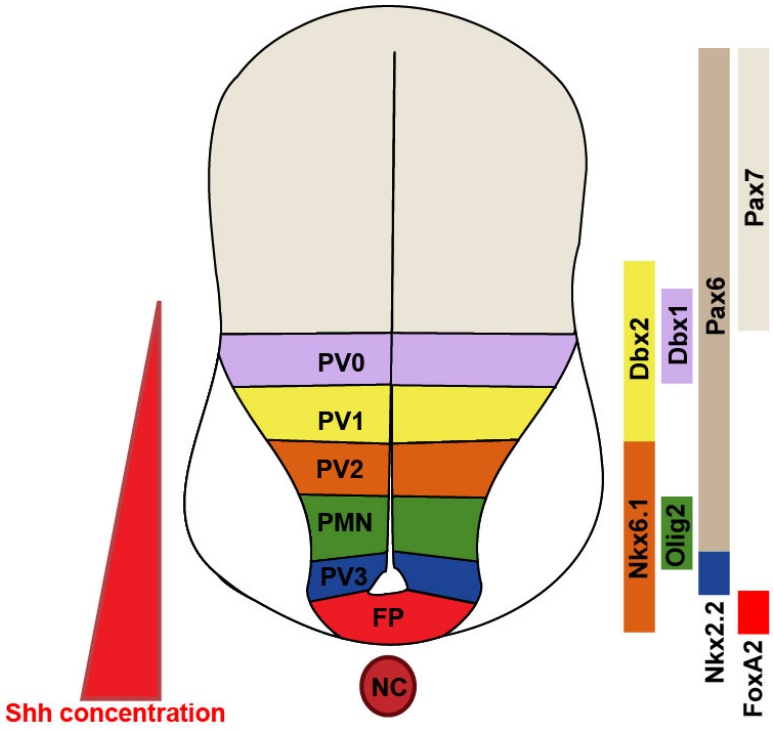

Figure 1.3. A gradient of SHH signaling specifies distinct neuronal progenitor domains in the ventral neural tube. In the developing spinal cord, SHH secreted from the notochord and later the floor plate establishes a gradient of HH ligand within the ventral neural tube. This gradient induces (Class II; *Nkx6.1, Olig2, Nkx2.2, FoxA2, Dbx1, Dbx2*) and represses (Class I; *Pax7, Pax3*) HH target genes in a concentration-dependent manner. Combinatorial expression of these transcription factors along the dorsal-ventral axis specifies 5 distinct ventral neuronal progenitor domains.

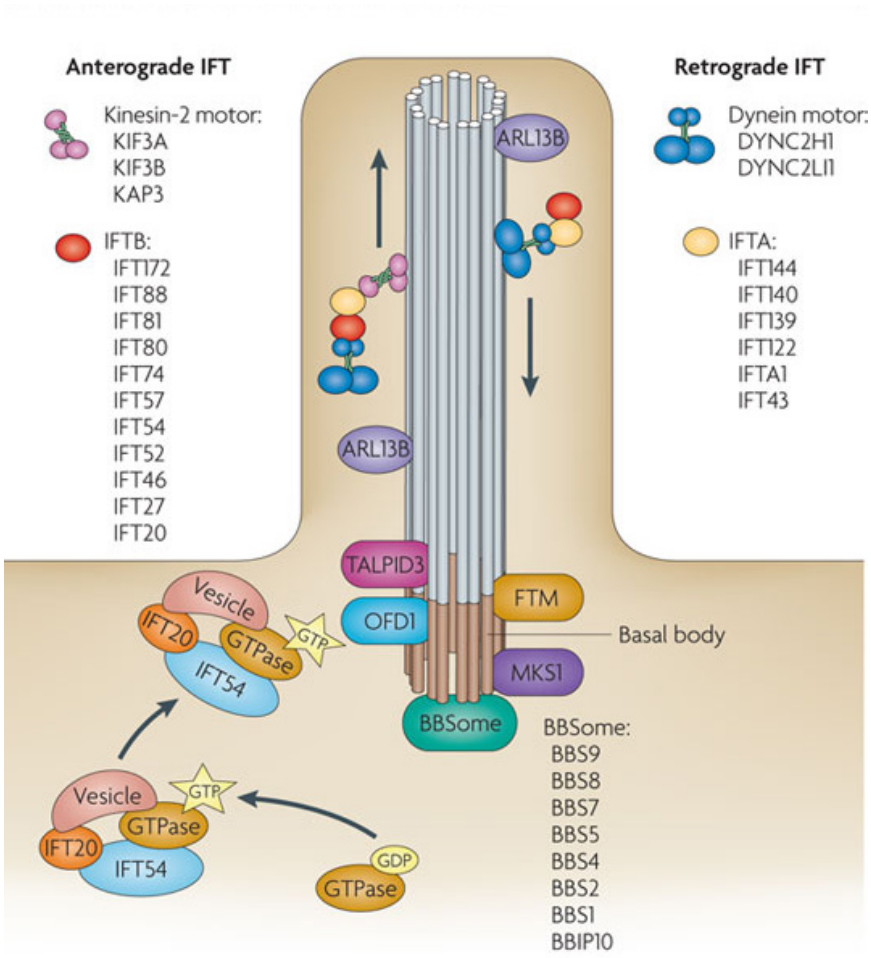

Figure 1.4. Intraflagellar trafficking in primary cilia.
Cargo is transported from the base to the tip of primary (anterograde trafficking) along the microtubule axoneme by kinesin-2 motor proteins along with intraflagellar transport A (IFT A) and IFT B complexes. The dynein motor (which consist of cytoplasmic dynein 2 heavy chain 1 (DYNC2H1) and cytoplasmic dynein 2 light chain 1 (DYNC2LI1)) mediates the return of IFT complexes to the base of primary cilia (retrograde trafficking) complexes. Figure adapted from (Goetz and Anderson, 2010).

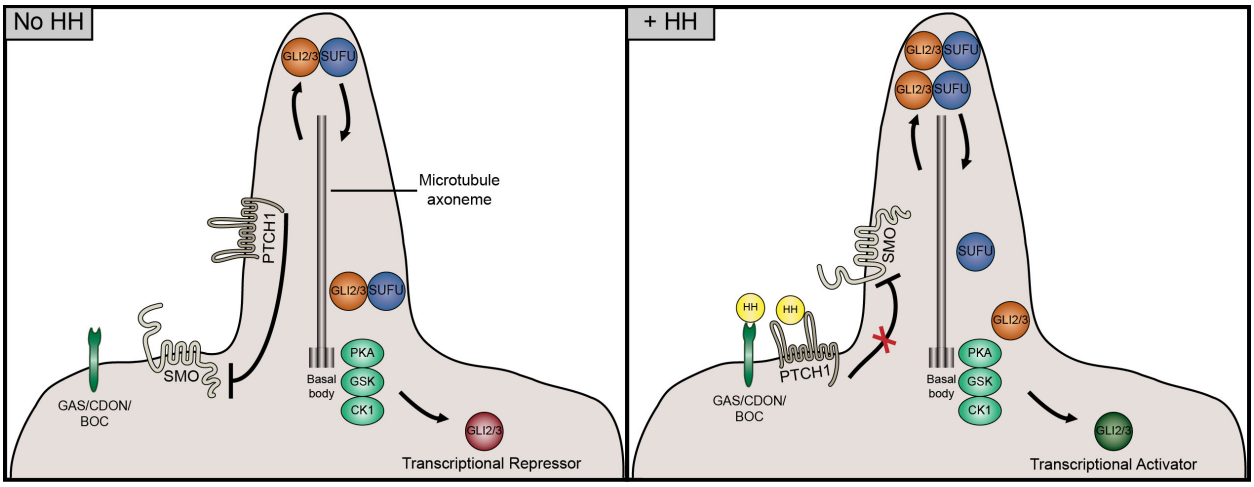

Figure 1.5. Ciliary trafficking of vertebrate HH signaling pathway components. (Left) In the absence of HH signaling, GLI2 and GLI3 cycle through cilia at low levels and are subsequently phosphorylated by PKA, CKI and GSK3β upon ciliary exit. This leads to their proteolytic cleavage to generate the repressor forms, GLI2R and GLI3R, respectively. (Right) In the presence of HH signaling, SMO is activated and accumulates in primary cilia. The activation of SMO results in increased ciliary accumulation of SUFU-GLI2 and SUFU-GLI3 complexes, dissociation of the GLI–SUFU complex, and the transport of full-length, activated GLI2 and GLI3 proteins from the cilia to the nucleus bypassing proteolytic processing.

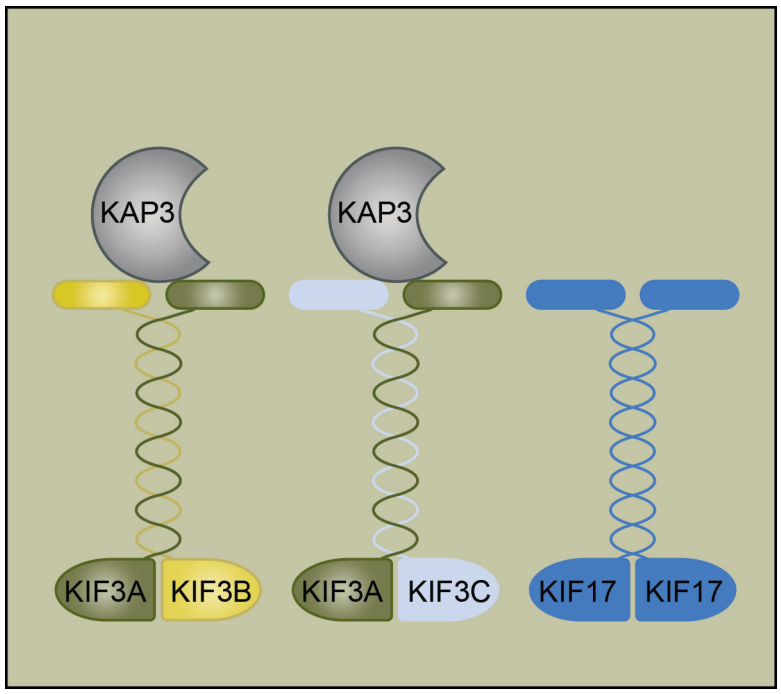

Figure 1.6. Kinesin-2 motor protein complexes.
Schematic representation of the three kinesin-2 motor protein complexes: (1) heterotrimeric KIF3A/KIF3B/KAP3, (2) heterotrimeric KIF3A/KIF3C/KAP3, and (3) the homodimeric KIF17 complex. Figure adapted from (Verhey and Hammond, 2009).

1.7 References

Alexandre, C., A. Jacinto, and P.W. Ingham. 1996. Transcriptional activation of hedgehog target genes in Drosophila is mediated directly by the cubitus interruptus protein, a member of the GLI family of zinc finger DNA-binding proteins. *Genes & Development*. 10:2003–2013.

Allen, B.L., J.Y. Song, L. Izzi, I.W. Althaus, J.-S. Kang, F. Charron, R.S. Krauss, and A.P. McMahon. 2011. Overlapping Roles and Collective Requirement for the Coreceptors GAS1, CDO, and BOC in SHH Pathway Function. *Developmental Cell*. 20:775–787. doi:10.1016/j.devcel.2011.04.018.

Altaba, A.R.I. 1998. Combinatorial Gli gene function in floor plate and neuronal inductions by Sonic hedgehog.

Aza-Blanc, P., F.A. Ramírez-Weber, M.P. Laget, C. Schwartz, and T.B. Kornberg. 1997. Proteolysis that is inhibited by hedgehog targets Cubitus interruptus protein to the nucleus and converts it to a repressor. *Cell*. 89:1043–1053.

Bai, C.B., D. Stephen, and A.L. Joyner. 2004. All mouse ventral spinal cord patterning by hedgehog is Gli dependent and involves an activator function of Gli3. *Developmental Cell*. 6:103–115.

Bai, C.B., W. Auerbach, J.S. Lee, D. Stephen, and A.L. Joyner. 2002. Gli2, but not Gli1, is required for initial Shh signaling and ectopic activation of the Shh pathway. *Development*.

Barzi, M., J. Berenguer, A. Menendez, R. Alvarez-Rodriguez, and S. Pons. 2009. Sonic-hedgehog-mediated proliferation requires the localization of PKA to the cilium base. *J. Cell. Sci.* 123:62–69. doi:10.1242/jcs.060020.

Buttitta, L., R. Mo, C.-C. Hui, and C.-M. Fan. 2003a. Interplays of Gli2 and Gli3 and their requirement in mediating Shh-dependent sclerotome induction. *Development*. 130:6233–6243. doi:10.1242/dev.00851.

Buttitta, L., R. Mo, C.-C. Hui, and C.-M. Fan. 2003b. Interplays of Gli2 and Gli3 and their requirement in mediating Shh-dependent sclerotome induction. *Development*. 130:6233–6243. doi:10.1242/dev.00851.

Büscher, D., B. Bosse, J. Heymer, and U. Rüther. 1997. Evidence for genetic control of Sonic hedgehog by Gli3 in mouse limb development. *Mech. Dev.* 62:175–182.

Chen, M.-H., C.W. Wilson, Y.-J. Li, K.K.L. Law, C.-S. Lu, R. Gacayan, X. Zhang, C.-C. Hui, and P.-T. Chuang. 2009. Cilium-independent regulation of Gli protein function by Sufu in Hedgehog signaling is evolutionarily conserved. *Genes & Development*. 23:1910–1928. doi:10.1101/gad.1794109.

Chen, Y., J.R. Cardinaux, R.H. Goodman, and S.M. Smolik. 1999. Mutants of cubitus interruptus that are independent of PKA regulation are independent of hedgehog signaling. *Development*. 126:3607–3616.

Cheung, H.O.-L., X. Zhang, A. Ribeiro, R. Mo, S. Makino, V. Puviindran, K.K.L. Law, J. Briscoe, and C.-C. Hui. 2009. The Kinesin Protein Kif7 Is a Critical Regulator of Gli Transcription Factors in Mammalian Hedgehog Signaling. *Sci Signal*. 2:ra29. doi:10.1126/scisignal.2000405.

Corbit, K.C., P. Aanstad, V. Singla, A.R. Norman, D.Y.R. Stainier, and J.F. Reiter. 2005. Vertebrate Smoothened functions at the primary cilium. *Nature*. 437:1018–1021. doi:10.1038/nature04117.

Dai, P., H. Akimaru, Y. Tanaka, T. Maekawa, M. Nakafuku, and S. Ishii. 1999. Sonic Hedgehog-induced activation of the Gli1 promoter is mediated by GLI3. *J. Biol. Chem.* 274:8143–8152.

Di Marcotullio, L., A. Greco, D. Mazzà, G. Canettieri, L. Pietrosanti, P. Infante, S. Coni, M. Moretti, E. De Smaele, E. Ferretti, I. Screpanti, and A. Gulino. 2010. Numb activates the E3 ligase Itch to control Gli1 function through a novel degradation signal. *Oncogene*. 30:65–76. doi:10.1038/onc.2010.394.

Ding, Q., J. Motoyama, S. Gasca, R. Mo, H. Sasaki, J. Rossant, and C.C. Hui. 1998. Diminished Sonic hedgehog signaling and lack of floor plate differentiation in Gli2 mutant mice.

Dishinger, J.F., H.L. Kee, P.M. Jenkins, S. Fan, T.W. Hurd, J.W. Hammond, Y.N.-T. Truong, B. Margolis, J.R. Martens, and K.J. Verhey. 2010. Ciliary entry of the kinesin-2 motor KIF17 is regulated by importin-beta2 and RanGTP. *Nat. Cell Biol.* 12:703–710. doi:10.1038/ncb2073.

Domínguez, M., M. Brunner, E. Hafen, and K. Basler. 1996. Sending and receiving the hedgehog signal: control by the Drosophila Gli protein Cubitus interruptus. *Science*. 272:1621–1625.

Dunaeva, M., P. Michelson, P. Kogerman, and R. Toftgard. 2003. Characterization of the physical interaction of Gli proteins with SUFU proteins. *J. Biol. Chem.* 278:5116–5122. doi:10.1074/jbc.M209492200.

Echelard, Y., D.J. Epstein, B. St-Jacques, L. Shen, J. Mohler, J.A. McMahon, and A.P. McMahon. 1993. Sonic hedgehog, a member of a family of putative signaling molecules, is implicated in the regulation of CNS polarity. *Cell*. 75:1417–1430.

Endoh-Yamagami, S., M. Evangelista, D. Wilson, X. Wen, J.-W. Theunissen, K. Phamluong, M. Davis, S.J. Scales, M.J. Solloway, F.J. de Sauvage, and A.S. Peterson. 2009. The Mammalian Cos2 Homolog Kif7 Plays an Essential Role in Modulating Hh Signal Transduction during Development. *Current Biology*. 19:1320–1326. doi:10.1016/j.cub.2009.06.046.

Epstein, D.J., E. Martí, M.P. Scott, and A.P. McMahon. 1996. Antagonizing cAMP-dependent protein kinase A in the dorsal CNS activates a conserved Sonic hedgehog signaling pathway.

Farzan, S.F., M. Ascano, S.K. Ogden, M. Sanial, A. Brigui, A. Plessis, and D.J. Robbins. 2008. Costal2 functions as a kinesin-like protein in the hedgehog signal transduction pathway.

Curr. Biol. 18:1215–1220. doi:10.1016/j.cub.2008.07.026.

Gindhart, J.G., and L.S. Goldstein. 1996. Armadillo repeats in the SpKAP115 subunit of kinesin-II. *Trends Cell Biol.* 6:415–416.

Goetz, S.C., and K.V. Anderson. 2010. The primary cilium: a signalling centre during vertebrate development. *Nat. Rev. Genet.* 11:331–344. doi:10.1038/nrg2774.

Gorivodsky, M., M. Mukhopadhyay, M. Wilsch-Braeuninger, M. Phillips, A. Teufel, C. Kim, N. Malik, W. Huttner, and H. Westphal. 2009. Intraflagellar transport protein 172 is essential for primary cilia formation and plays a vital role in patterning the mammalian brain. *Dev. Biol.* 325:24–32. doi:10.1016/j.ydbio.2008.09.019.

Guillaud, L., M. Setou, and N. Hirokawa. 2003. KIF17 dynamics and regulation of NR2B trafficking in hippocampal neurons. *J. Neurosci.* 23:131–140.

Hammerschmidt, M., M.J. Bitgood, and A.P. McMahon. 1996. Protein kinase A is a common negative regulator of Hedgehog signaling in the vertebrate embryo. *Genes & Development*. 10:647–658.

Han, Y.-G., H.J. Kim, A.A. Dlugosz, D.W. Ellison, R.J. Gilbertson, and A. Alvarez-Buylla. 2009. Dual and opposing roles of primary cilia in medulloblastoma development. *Nat. Med.* 15:1062–1065. doi:10.1038/nm.2020.

Haycraft, C.J., B. Banizs, Y. Aydin-Son, Q. Zhang, E.J. Michaud, and B.K. Yoder. 2005. Gli2 and Gli3 localize to cilia and require the intraflagellar transport protein polaris for processing and function. *PLoS Genet.* 1:e53. doi:10.1371/journal.pgen.0010053.

He, M., R. Subramanian, F. Bangs, T. Omelchenko, K.F. Liem Jr, T.M. Kapoor, and K.V. Anderson. 2014. The kinesin-4 protein Kif7 regulates mammalian Hedgehog signalling by organizing the cilium tip compartment. *Nat. Cell Biol.* 16:663–672. doi:doi:10.1038/ncb2988.

Hepker, J., Q.T. Wang, C.K. Motzny, R. Holmgren, and T.V. Orenic. 1997. Drosophila cubitus interruptus forms a negative feedback loop with patched and regulates expression of Hedgehog target genes. *Development*. 124:549–558.

Hirokawa, N. 2000. Stirring up Development with the Heterotrimeric Kinesin KIF3. *Traffic*. 1:29–34. doi:10.1034/j.1600-0854.2000.010105.x.

Hirokawa, N., Y. Noda, Y. Tanaka, and S. Niwa. 2009. Kinesin superfamily motor proteins and intracellular transport. *Nat Rev Mol Cell Biol*. 10:682–696. doi:10.1038/nrm2774.

Ho, K.S., K. Suyama, M. Fish, and M.P. Scott. 2005. Differential regulation of Hedgehog target gene transcription by Costal2 and Suppressor of Fused. *Development*. 132:1401–1412. doi:10.1242/dev.01689.

Hsu, S.-H.C., X. Zhang, C. Yu, Z.J. Li, J.S. Wunder, C.-C. Hui, and B.A. Alman. 2011. Kif7

promotes hedgehog signaling in growth plate chondrocytes by restricting the inhibitory function of Sufu. *Development*. 138:3791–3801. doi:10.1242/dev.069492.

Huang, C.-J., C.-C. Huang, and C.-C. Chang. 2011. Association of the testis-specific TRIM/RBCC protein RNF33/TRIM60 with the cytoplasmic motor proteins KIF3A and KIF3B. *Mol Cell Biochem*. 360:121–131. doi:10.1007/s11010-011-1050-8.

Huangfu, D., A. Liu, A.S. Rakeman, N.S. Murcia, L. Niswander, and K.V. Anderson. 2003. Hedgehog signalling in the mouse requires intraflagellar transport proteins. *Nature*. 426:83–87. doi:10.1038/nature02061.

Huangfu, D., and K.V. Anderson. 2005. Cilia and Hedgehog responsiveness in the mouse. *Proc. Natl. Acad. Sci. U.S.A.* 102:11325–11330. doi:10.1073/pnas.0505328102.

Hui, C.-C., and S. Angers. 2011. Gli Proteins in Development and Disease. *Annu. Rev. Cell Dev. Biol.* 27:513–537. doi:10.1146/annurev-cellbio-092910-154048.

Hui, C.-C., D. Slusarski, K.A. Platt, R. Holmgren, and A.L. Joyner. 1994. Expression of Three Mouse Homologs of the Drosophila Segment Polarity Gene cubitus interruptus, Gli, Gli-2, and Gli-3, in Ectoderm- and Mesoderm-Derived Tissues Suggests Multiple Roles during Postimplantation Development. *Dev. Biol.* 162:402–413. doi:10.1006/dbio.1994.1097.

Hui, C.C., and A.L. Joyner. 1993. A mouse model of greig cephalopolysyndactyly syndrome: the extra-toesJ mutation contains an intragenic deletion of the Gli3 gene. *Nat Genet*. 3:241–246. doi:10.1038/ng0393-241.

Humke, E.W., K.V. Dorn, L. Milenkovic, M.P. Scott, and R. Rohatgi. 2010. The output of Hedgehog signaling is controlled by the dynamic association between Suppressor of Fused and the Gli proteins. *Genes & Development*. 24:670–682. doi:10.1101/gad.1902910.

Hynes, M., D.M. Stone, M. Dowd, S. Pitts-Meek, A. Goddard, A. Gurney, and A. Rosenthal. 1997. Control of Cell Pattern in the Neural Tube by the Zinc Finger Transcription Factor and Oncogene Gli-1. *Neuron*. 19:15–26. doi:10.1016/S0896-6273(00)80344-X.

Ingham, P.W. 1998. Transducing Hedgehog: the story so far. *The EMBO Journal*. 17:3505–3511. doi:10.1093/emboj/17.13.3505.

Insinna, C., M. Humby, T. Sedmak, U. Wolfrum, and J.C. Besharse. 2009. Different roles for KIF17 and kinesin II in photoreceptor development and maintenance. *Dev. Dyn.* 238:2211–2222. doi:10.1002/dvdy.21956.

Insinna, C., N. Pathak, B. Perkins, and I. Drummond. 2008. The homodimeric kinesin, Kif17, is essential for vertebrate photoreceptor sensory outer segment development. *Developmental …*.

J M Ruppert, K.W.K.A.J.W.S.H.B.F.T.K.M.L.L.H.N.S.S.J.O.B.V. 1988. The GLI-Kruppel family of human genes. *Molecular and Cellular Biology*. 8:3104.

Jaulin, F., and G. Kreitzer. 2010. KIF17 stabilizes microtubules and contributes to epithelial morphogenesis by acting at MT plus ends with EB1 and APC. *J. Cell Biol.* 190:443–460. doi:10.1083/jcb.201006044.

Jenkins, P.M., T.W. Hurd, L. Zhang, D.P. McEwen, R.L. Brown, B. Margolis, K.J. Verhey, and J.R. Martens. 2006. Ciliary targeting of olfactory CNG channels requires the CNGB1b subunit and the kinesin-2 motor protein, KIF17. *Curr. Biol.* 16:1211–1216. doi:10.1016/j.cub.2006.04.034.

Jia, J., A. Kolterud, H. Zeng, A. Hoover, S. Teglund, R. Toftgard, and A. Liu. 2009. Suppressor of Fused inhibits mammalian Hedgehog signaling in the absence of cilia. *Dev. Biol.* 330:452–460. doi:10.1016/j.ydbio.2009.04.009.

Jia, J., K. Amanai, G. Wang, J. Tang, B. Wang, and J. Jiang. 2002. Shaggy/GSK3 antagonizes Hedgehog signalling by regulating Cubitus interruptus. *Nature*. 416:548–552. doi:10.1038/nature733.

Jia, J., L. Zhang, Q. Zhang, C. Tong, B. Wang, F. Hou, K. Amanai, and J. Jiang. 2005. Phosphorylation by double-time/CKIepsilon and CKIalpha targets cubitus interruptus for Slimb/beta-TRCP-mediated proteolytic processing. *Developmental Cell*. 9:819–830. doi:10.1016/j.devcel.2005.10.006.

Jiang, J., and G. Struhl. 1998. Regulation of the Hedgehog and Wingless signalling pathways by the F-box/WD40-repeat protein Slimb : Abstract : Nature. *Nature*.

Kaesler, S., B. Lüscher, and U. Rüther. 2000. Transcriptional activity of GLI1 is negatively regulated by protein kinase A. *Biol. Chem.* 381:545–551. doi:10.1515/BC.2000.070.

Katoh, Y., and M. Katoh. 2004. KIF27 is one of orthologs for Drosophila Costal-2. *Int. J. Oncol.* 25:1875–1880.

Keady, B.T., R. Samtani, K. Tobita, M. Tsuchya, J.T. San Agustin, J.A. Follit, J.A. Jonassen, R. Subramanian, C.W. Lo, and G.J. Pazour. 2012. IFT25 Links the Signal-Dependent Movement of Hedgehog Components to Intraflagellar Transport. *Developmental Cell*. 22:940–951. doi:10.1016/j.devcel.2012.04.009.

Kent, D., E.W. Bush, and J.E. Hooper. 2006. Roadkill attenuates Hedgehog responses through degradation of Cubitus interruptus.

Kim, J., M. Kato, and P.A. Beachy. 2009. Gli2 trafficking links Hedgehog-dependent activation of Smoothened in the primary cilium to transcriptional activation in the nucleus. *Proc. Natl. Acad. Sci. U.S.A.* 106:21666–21671. doi:10.1073/pnas.0912180106.

Kinzler, K.W., and B. Vogelstein. 1990. The GLI gene encodes a nuclear protein which binds specific sequences in the human genome. *Molecular and Cellular Biology*. 10:634–642.

Kinzler, K.W., J.M. Ruppert, S.H. Bigner, and B. Vogelstein. 1988. The GLI gene is a member of the Kruppel family of zinc finger proteins. *Nature*. 332:371–374. doi:10.1038/332371a0.

Kinzler, K.W., S.H. Bigner, D.D. Bigner, J.M. Trent, M.L. Law, S.J. O'Brien, A.J. Wong, and B. Vogelstein. 1987. Identification of an amplified, highly expressed gene in a human glioma. *Science*. 236:70–73.

Koyama, E., B. Young, M. Nagayama, Y. Shibukawa, M. Enomoto-Iwamoto, M. Iwamoto, Y. Maeda, B. Lanske, B. Song, R. Serra, and M. Pacifici. 2007. Conditional Kif3a ablation causes abnormal hedgehog signaling topography, growth plate dysfunction, and excessive bone and cartilage formation during mouse skeletogenesis. *Development*. 134:2159–2169. doi:10.1242/dev.001586.

Krauss, S., J.P. Concordet, and P.W. Ingham. 1993. A functionally conserved homolog of the Drosophila segment polarity gene hh is expressed in tissues with polarizing activity in zebrafish embryos. *Cell*. 75:1431–1444.

Lee, J., K.A. Platt, P. Censullo, and A. Ruiz i Altaba. 1997. Gli1 is a target of Sonic hedgehog that induces ventral neural tube development. *Development*. 124:2537–2552.

Lee, J.J., D.P. von Kessler, S. Parks, and P.A. Beachy. 1992. Secretion and localized transcription suggest a role in positional signaling for products of the segmentation gene hedgehog. *Cell*.

Li, Z.J., E. Nieuwenhuis, W. Nien, X. Zhang, J. Zhang, V. Puviindran, B.J. Wainwright, P.C.W. Kim, and C.-C. Hui. 2012. Kif7 regulates Gli2 through Sufu-dependent and -independent functions during skin development and tumorigenesis. *Development*. 139:4152–4161. doi:10.1242/dev.081190.

Liem, K.F., M. He, P.J.R. Ocbina, and K.V. Anderson. 2009. Mouse Kif7/Costal2 is a cilia-associated protein that regulates Sonic hedgehog signaling. *Proc. Natl. Acad. Sci. U.S.A.* 106:13377–13382. doi:10.1073/pnas.0906944106.

Liu, A., B. Wang, and L.A. Niswander. 2005. Mouse intraflagellar transport proteins regulate both the activator and repressor functions of Gli transcription factors. *Development*. 132:3103–3111. doi:10.1242/dev.01894.

Liu, J., H. Zeng, and A. Liu. 2015. The loss of Hh responsiveness by a non-ciliary Gli2 variant. *Development*. 142:1651–1660. doi:10.1242/dev.119669.

Liu, Y.C., A.L. Couzens, A.R. Deshwar, L.D. B McBroom-Cerajewski, X. Zhang, V. Puviindran, I.C. Scott, A.-C. Gingras, C.-C. Hui, and S. Angers. 2014. The PPFIA1-PP2A protein complex promotes trafficking of Kif7 to the ciliary tip and Hedgehog signaling. *Sci Signal*. 7:ra117. doi:10.1126/scisignal.2005608.

Marigo, V., R.A. Davey, Y. Zuo, and J.M. Cunningham. 1996a. Biochemical evidence that patched is the Hedgehog receptor. ....

Marigo, V., R.L. Johnson, A. Vortkamp, and C.J. Tabin. 1996b. Sonic hedgehog differentially regulates expression of GLI and GLI3 during limb development. *Dev. Biol.* 180:273–283. doi:10.1006/dbio.1996.0300.

Marks, S.A., and D. Kalderon. 2011. Regulation of mammalian Gli proteins by Costal 2 and PKA in Drosophila reveals Hedgehog pathway conservation. *Development*. 138:2533–2542. doi:10.1242/dev.063479.

Masuya, H., T. Sagai, K. Moriwaki, and T. Shiroishi. 1997. Multigenic control of the localization of the zone of polarizing activity in limb morphogenesis in the mouse. *Dev. Biol.* 182:42–51. doi:10.1006/dbio.1996.8457.

Maurya, A.K., J. Ben, Z. Zhao, R.T.H. Lee, W. Niah, A.S.M. Ng, A. Iyu, W. Yu, S. Elworthy, F.J.M. van Eeden, and P.W. Ingham. 2013. Positive and Negative Regulation of Gli Activity by Kif7 in the Zebrafish Embryo. *PLoS Genet.* 9:e1003955. doi:10.1371/journal.pgen.1003955.

McDermott, A., M. Gustafsson, T. Elsam, C.-C. Hui, C.P. Emerson, and A.-G. Borycki. 2005. Gli2 and Gli3 have redundant and context-dependent function in skeletal muscle formation. *Development*. 132:345–357. doi:10.1242/dev.01537.

Merchant, M., F.F. Vajdos, M. Ultsch, H.R. Maun, U. Wendt, J. Cannon, W. Desmarais, R.A. Lazarus, A.M. de Vos, and F.J. de Sauvage. 2004. Suppressor of fused regulates Gli activity through a dual binding mechanism. *Molecular and Cellular Biology*. 24:8627–8641. doi:10.1128/MCB.24.19.8627-8641.2004.

Méthot, N., and K. Basler. 1999. Hedgehog controls limb development by regulating the activities of distinct transcriptional activator and repressor forms of Cubitus interruptus. *Cell*. 96:819–831.

Mo, R., A.M. Freer, D.L. Zinyk, M.A. Crackower, J. Michaud, H.H. Heng, K.W. Chik, X.M. Shi, L.C. Tsui, S.H. Cheng, A.L. Joyner, and C. Hui. 1997. Specific and redundant functions of Gli2 and Gli3 zinc finger genes in skeletal patterning and development.

Mohler, J., and K. Vani. 1992. Molecular organization and embryonic expression of the hedgehog gene involved in cell-cell communication in segmental patterning of Drosophila. *Development*. 115:957–971.

Morris, R.L., C.N. English, J.E. Lou, and F.J. Dufort. 2004. Redistribution of the kinesin-II subunit KAP from cilia to nuclei during the mitotic and ciliogenic cycles in sea urchin embryos. *Developmental …*.

Motoyama, J., J. Liu, R. Mo, Q. Ding, M. Post, and C.C. Hui. 1998. Essential function of Gli2 and Gli3 in the formation of lung, trachea and oesophagus. *Nat Genet*. 20:54–57. doi:10.1038/1711.

Motoyama, J., L. Milenkovic, M. Iwama, Y. Shikata, M.P. Scott, and C.-C. Hui. 2015. Efficient live fluorescence imaging of intraflagellar transport in mammalian primary cilia. *In* proxy.lib.umich.edu. Elsevier. 189–201.

Muresan, V., T. Abramson, A. Lyass, D. Winter, E. Porro, F. Hong, N.L. Chamberlin, and B.J. Schnapp. 1998. KIF3C and KIF3A form a novel neuronal heteromeric kinesin that associates

with membrane vesicles. *Mol. Biol. Cell*. 9:637–652.

Niewiadomski, P., A. Zhujiang, M. Youssef, and J.A. Waschek. 2013. Interaction of PACAP with Sonic hedgehog reveals complex regulation of the hedgehog pathway by PKA. *Cell. Signal.* 25:2222–2230. doi:10.1016/j.cellsig.2013.07.012.

Niewiadomski, P., J.H. Kong, R. Ahrends, Y. Ma, E.W. Humke, S. Khan, M.N. Teruel, B.G. Novitch, and R. Rohatgi. 2014. Gli protein activity is controlled by multisite phosphorylation in vertebrate hedgehog signaling. *Cell Rep*. 6:168–181. doi:10.1016/j.celrep.2013.12.003.

Nonaka, S., Y. Tanaka, Y. Okada, S. Takeda, A. Harada, Y. Kanai, M. Kido, and N. Hirokawa. 1998. Randomization of left-right asymmetry due to loss of nodal cilia generating leftward flow of extraembryonic fluid in mice lacking KIF3B motor protein. *Cell*. 95:829–837.

Nüsslein-Volhard, C., and E. Wieschaus. 1980. Mutations affecting segment number and polarity in Drosophila. *Nature*. 287:795–801.

Ocbina, P.J.R., J.T. Eggenschwiler, I. Moskowitz, and K.V. Anderson. 2011. Complex interactions between genes controlling trafficking in primary cilia. *Nat Genet*. doi:10.1038/ng.832.

Orenic, T.V., D.C. Slusarski, K.L. Kroll, and R.A. Holmgren. 1990. Cloning and characterization of the segment polarity gene cubitus interruptus Dominant of Drosophila. *Genes & Development*. 4:1053–1067.

Pan, Y., and B. Wang. 2007. A novel protein-processing domain in Gli2 and Gli3 differentially blocks complete protein degradation by the proteasome. *J. Biol. Chem.* 282:10846–10852. doi:10.1074/jbc.M608599200.

Pan, Y., C. Wang, and B. Wang. 2009. Phosphorylation of Gli2 by protein kinase A is required for Gli2 processing and degradation and the Sonic Hedgehog-regulated mouse development. *Dev. Biol.* 326:177–189. doi:10.1016/j.ydbio.2008.11.009.

Pan, Y., C.B. Bai, A.L. Joyner, and B. Wang. 2006. Sonic hedgehog signaling regulates Gli2 transcriptional activity by suppressing its processing and degradation. *Molecular and Cellular Biology*. 26:3365–3377. doi:10.1128/MCB.26.9.3365-3377.2006.

Park, H.L., C. Bai, K.A. Platt, M.P. Matise, A. Beeghly, C.C. Hui, M. Nakashima, and A.L. Joyner. 2000. Mouse Gli1 mutants are viable but have defects in SHH signaling in combination with a Gli2 mutation. *Development*. 127:1593–1605.

Persson, M., D. Stamataki, P. te Welscher, E. Andersson, J. Böse, U. Rüther, J. Ericson, and J. Briscoe. 2002. Dorsal-ventral patterning of the spinal cord requires Gli3 transcriptional repressor activity. *Genes & Development*. 16:2865–2878. doi:10.1101/gad.243402.

Phang, H.-Q., J.-L. Hoon, S.-K. Lai, Y. Zeng, K.-H. Chiam, H.-Y. Li, and C.-G. Koh. 2014. POPX2 phosphatase regulates the KIF3 kinesin motor complex. *J. Cell. Sci.* 127:727–739. doi:10.1242/jcs.126482.

Platt, K.A., J. Michaud, and A.L. Joyner. 1997. Expression of the mouse Gli and Ptc genes is adjacent to embryonic sources of hedgehog signals suggesting a conservation of pathways between flies and mice. *Mech. Dev.* 62:121–135.

Preat, T. 1992. Characterization of Suppressor of fused, a complete suppressor of the fused segment polarity gene of Drosophila melanogaster.

Preat, T., P. Thérond, B. Limbourg-Bouchon, A. Pham, H. Tricoire, D. Busson, and C. Lamour-Isnard. 1993. Segmental polarity in Drosophila melanogaster: genetic dissection of fused in a Suppressor of fused background reveals interaction with costal-2. *Genetics*. 135:1047–1062.

Preat, T., P. Thérond, C. Lamour-Isnard, B. Limbourg-Bouchon, H. Tricoire, I. Erk, M.C. Mariol, and D. Busson. 1990. A putative serine/threonine protein kinase encoded by the segment-polarity fused gene of Drosophila. *Nature*. 347:87–89. doi:10.1038/347087a0.

Price, M.A., and D. Kalderon. 2002. Proteolysis of the Hedgehog signaling effector Cubitus interruptus requires phosphorylation by Glycogen Synthase Kinase 3 and Casein Kinase 1. *Cell*.

Qin, J., Y. Lin, R.X. Norman, H.W. Ko, and J.T. Eggenschwiler. 2011. Intraflagellar transport protein 122 antagonizes Sonic Hedgehog signaling and controls ciliary localization of pathway components. *Proceedings of the …*.

Riddle, R.D., R.L. Johnson, E. Laufer, and C. Tabin. 1993. Sonic hedgehog mediates the polarizing activity of the ZPA. *Cell*. 75:1401–1416.

Robbins, D.J., K.E. Nybakken, R. Kobayashi, and J.C. Sisson. 1997. Hedgehog elicits signal transduction by means of a large complex containing the kinesin-related protein costal2. *Cell*.

Roelink, H., A. Augsburger, J. Heemskerk, V. Korzh, S. Norlin, A. Ruiz i Altaba, Y. Tanabe, M. Placzek, T. Edlund, and T.M. Jessell. 1994. Floor plate and motor neuron induction by vhh-1, a vertebrate homolog of hedgehog expressed by the notochord. *Cell*. 76:761–775.

Rohatgi, R., L. Milenkovic, and M.P. Scott. 2007. Patched1 regulates hedgehog signaling at the primary cilium. *Science*. 317:372–376. doi:10.1126/science.1139740.

Ruel, L., R. Rodriguez, A. Gallet, L. Lavenant-Staccini, and P.P. Thérond. 2003. Stability and association of Smoothened, Costal2 and Fused with Cubitus interruptus are regulated by Hedgehog. *Nat. Cell Biol.* 5:907–913. doi:10.1038/ncb1052.

Ruiz i Altaba, A., V. Palma, and N. Dahmane. 2002. Hedgehog-Gli signalling and the growth of the brain. *Nat. Rev. Neurosci.* 3:24–33. doi:10.1038/nrn704.

Santos, N., and J.F. Reiter. 2014. A central region of Gli2 regulates its localization to the primary cilium and transcriptional activity. *J. Cell. Sci.* 127:1500–1510. doi:10.1242/jcs.139253.

Sasaki, H., C. Hui, M. Nakafuku, and H. Kondoh. 1997. A binding site for Gli proteins is

essential for HNF-3beta floor plate enhancer activity in transgenics and can respond to Shh in vitro. *Development*.

Sasaki, H., Y. Nishizaki, C. Hui, M. Nakafuku, and H. Kondoh. 1999. Regulation of Gli2 and Gli3 activities by an amino-terminal repression domain: implication of Gli2 and Gli3 as primary mediators of Shh signaling. *Development*. 126:3915–3924.

Scholey, J.M. 2013. Kinesin-2: A Family of Heterotrimeric and Homodimeric Motors with Diverse Intracellular Transport Functions. *Annu. Rev. Cell Dev. Biol.*

Setou, M., T. Nakagawa, D.H. Seog, and N. Hirokawa. 2000. Kinesin superfamily motor protein KIF17 and mLin-10 in NMDA receptor-containing vesicle transport. *Science*. 288:1796–1802.

Sisson, J.C., K.S. Ho, K. Suyama, and M.P. Scott. 1997. Costal2, a novel kinesin-related protein in the Hedgehog signaling pathway. *Cell*.

Slusarski, D.C., C.K. Motzny, and R. Holmgren. 1995. Mutations that alter the timing and pattern of cubitus interruptus gene expression in Drosophila melanogaster. *Genetics*.

Smelkinson, M.G., and D. Kalderon. 2006. Processing of the Drosophila hedgehog signaling effector Ci-155 to the repressor Ci-75 is mediated by direct binding to the SCF component Slimb. *Curr. Biol.* 16:110–116. doi:10.1016/j.cub.2005.12.012.

Stone, D.M., M. Hynes, M. Armanini, T.A. Swanson, and Q. Gu. 1996. The tumour-suppressor gene patched encodes a candidate receptor for Sonic hedgehog. *Nature*.

Svärd, J., K.H. Henricson, M. Persson-Lek, and B. Rozell. 2006. Genetic elimination of Suppressor of fused reveals an essential repressor function in the mammalian Hedgehog signaling pathway. *Developmental Cell*.

Tabata, T., S. Eaton, and T.B. Kornberg. 1992. The Drosophila hedgehog gene is expressed specifically in posterior compartment cells and is a target of engrailed regulation. *Genes & Development*. 6:2635–2645.

Takano, K., T. Miki, J. Katahira, and Y. Yoneda. 2007. NXF2 is involved in cytoplasmic mRNA dynamics through interactions with motor proteins. *Nucleic Acids Res.* 35:2513–2521. doi:10.1093/nar/gkm125.

Takeda, S., H. Yamazaki, D.H. Seog, Y. Kanai, S. Terada, and N. Hirokawa. 2000. Kinesin superfamily protein 3 (KIF3) motor transports fodrin-associating vesicles important for neurite building. *J. Cell Biol.* 148:1255–1265.

Takeda, S., Y. Yonekawa, Y. Tanaka, Y. Okada, S. Nonaka, and N. Hirokawa. 1999. Left-right asymmetry and kinesin superfamily protein KIF3A: new insights in determination of laterality and mesoderm induction by kif3A-/- mice analysis. *J. Cell Biol.* 145:825–836.

Tanuma, N., M. Nomura, M. Ikeda, I. Kasugai, Y. Tsubaki, K. Takagaki, T. Kawamura, Y.

Yamashita, I. Sato, M. Sato, R. Katakura, K. Kikuchi, and H. Shima. 2008. Protein phosphatase Dusp26 associates with KIF3 motor and promotes N-cadherin-mediated cell–cell adhesion. *Oncogene*. 28:752–761. doi:10.1038/onc.2008.431.

Tarabeux, J., N. Champagne, E. Brustein, F.F. Hamdan, J. Gauthier, M. Lapointe, C. Maios, A. Piton, D. Spiegelman, É. Henrion, B. Millet, J.L. Rapoport, L.E. DeLisi, R. Joober, F. Fathalli, É. Fombonne, L. Mottron, N. Forget-Dubois, M. Boivin, J.L. Michaud, R.G. Lafrenière, P. Drapeau, M.-O. Krebs, and G.A. Rouleau. 2010. De Novo Truncating Mutation in Kinesin 17 Associated with Schizophrenia. *Biological Psychiatry*. 68:649–656. doi:10.1016/j.biopsych.2010.04.018.

Tempé, D., M. Casas, S. Karaz, M.-F. Blanchet-Tournier, and J.-P. Concordet. 2006. Multisite protein kinase A and glycogen synthase kinase 3beta phosphorylation leads to Gli3 ubiquitination by SCFbetaTrCP. *Molecular and Cellular Biology*. 26:4316–4326. doi:10.1128/MCB.02183-05.

Teng, J., T. Rai, Y. Tanaka, Y. Takei, T. Nakata, M. Hirasawa, A.B. Kulkarni, and N. Hirokawa. 2005. The KIF3 motor transports N-cadherin and organizes the developing neuroepithelium. *Nat. Cell Biol.* 7:474–482. doi:10.1038/ncb1249.

Thérond, P., D. Busson, E. Guillemet, B. Limbourg-Bouchon, T. Preat, R. Terracol, H. Tricoire, and C. Lamour-Isnard. 1993. Molecular organisation and expression pattern of the segment polarity gene fused of Drosophila melanogaster. *Mech. Dev.* 44:65–80.

Tian, L., R.A. Holmgren, and A. Matouschek. 2005. A conserved processing mechanism regulates the activity of transcription factors Cubitus interruptus and NF-[kappa]B - Nature Structural & Molecular Biology. *Nature structural & molecular ….*

Tukachinsky, H., L.V. Lopez, and A. Salic. 2010. A mechanism for vertebrate Hedgehog signaling: recruitment to cilia and dissociation of SuFu-Gli protein complexes. *J. Cell Biol.* 191:415–428. doi:10.1083/jcb.201004108.

Tuson, M., M. He, and K.V. Anderson. 2011. Protein kinase A acts at the basal body of the primary cilium to prevent Gli2 activation and ventralization of the mouse neural tube. *Development*. 138:4921–4930. doi:10.1242/dev.070805.

Varjosalo, M., S.-P. Li, and J. Taipale. 2006. Divergence of hedgehog signal transduction mechanism between Drosophila and mammals. *Developmental Cell*. 10:177–186. doi:10.1016/j.devcel.2005.12.014.

Verhey, K.J., and J.W. Hammond. 2009. Traffic control: regulation of kinesin motors. *Nat Rev Mol Cell Biol*. 10:765–777. doi:10.1038/nrm2782.

Vortkamp, A., M. Gessler, and K.H. Grzeschik. 1991. GLI3 zinc-finger gene interrupted by translocations in Greig syndrome families. *Nature*. 352:539–540. doi:10.1038/352539a0.

Wang, B., and Y. Li. 2006. Evidence for the direct involvement of {beta}TrCP in Gli3 protein processing. *Proc. Natl. Acad. Sci. U.S.A.* 103:33–38. doi:10.1073/pnas.0509927103.

Wang, B., J.F. Fallon, and P.A. Beachy. 2000a. Hedgehog-regulated processing of Gli3 produces an anterior/posterior repressor gradient in the developing vertebrate limb. *Cell*. 100:423–434.

Wang, C., Y. Pan, and B. Wang. 2010. Suppressor of fused and Spop regulate the stability, processing and function of Gli2 and Gli3 full-length activators but not their repressors.

Wang, G., and J. Jiang. 2004. Multiple Cos2/Ci interactions regulate Ci subcellular localization through microtubule dependent and independent mechanisms. *Dev. Biol.* 268:493–505. doi:10.1016/j.ydbio.2004.01.008.

Wang, G., B. Wang, and J. Jiang. 1999. Protein kinase A antagonizes Hedgehog signaling by regulating both the activator and repressor forms of Cubitus interruptus. *Genes & Development*. 13:2828–2837.

Wang, G., K. Amanai, B. Wang, and J. Jiang. 2000b. Interactions with Costal2 and suppressor of fused regulate nuclear translocation and activity of cubitus interruptus. *Genes & Development*. 14:2893–2905.

Wang, Q.T., and R.A. Holmgren. 1999. The subcellular localization and activity of Drosophila cubitus interruptus are regulated at multiple levels. *Development*. 126:5097–5106.

Wen, X., C.K. Lai, M. Evangelista, J.A. Hongo, F.J. de Sauvage, and S.J. Scales. 2010. Kinetics of Hedgehog-Dependent Full-Length Gli3 Accumulation in Primary Cilia and Subsequent Degradation. *Molecular and Cellular Biology*. 30:1910–1922. doi:10.1128/MCB.01089-09.

Wong, S.Y., A.D. Seol, P.-L. So, A.N. Ermilov, C.K. Bichakjian, E.H. Epstein, A.A. Dlugosz, and J.F. Reiter. 2009. Primary cilia can both mediate and suppress Hedgehog pathway-dependent tumorigenesis. *Nat. Med.* 15:1055–1061. doi:10.1038/nm.2011.

Wong-Riley, M.T.T., and J.C. Besharse. 2012. The kinesin superfamily protein KIF17: one protein with many functions. *Biomol Concepts*. 3:267–282. doi:10.1515/bmc-2011-0064.

Yamazaki, H., T. Nakata, Y. Okada, and N. Hirokawa. 1996. Cloning and characterization of KAP3: a novel kinesin superfamily-associated protein of KIF3A/3B. *Proc. Natl. Acad. Sci. U.S.A.* 93:8443–8448.

Yang, N., L. Li, T. Eguether, J.P. Sundberg, G.J. Pazour, and J. Chen. 2015. Intraflagellar transport 27 is essential for hedgehog signaling but dispensable for ciliogenesis during hair follicle morphogenesis. *Development*. 142:2860–2860. doi:10.1242/dev.128751.

Yang, Z., and L.S. Goldstein. 1998. Characterization of the KIF3C neural kinesin-like motor from mouse. *Mol. Biol. Cell*. 9:249–261.

Yin, X., X. Feng, Y. Takei, and N. Hirokawa. 2012. Regulation of NMDA receptor transport: a KIF17-cargo binding/releasing underlies synaptic plasticity and memory in vivo. *J. Neurosci.* 32:5486–5499. doi:10.1523/JNEUROSCI.0718-12.2012.

Yin, X., Y. Takei, M.A. Kido, and N. Hirokawa. 2011. Molecular Motor KIF17 Is Fundamental

for Memory and Learning via Differential Support of Synaptic NR2A/2B Levels. *Neuron*. 70:310–325. doi:10.1016/j.neuron.2011.02.049.

Zeng, H., J. Jia, and A. Liu. 2010. Coordinated translocation of mammalian Gli proteins and suppressor of fused to the primary cilium. *PLoS ONE*. 5:e15900. doi:10.1371/journal.pone.0015900.

Zhang, Q., L. Zhang, B. Wang, C.Y. Ou, C.T. Chien, and J. Jiang. 2006. A hedgehog-induced BTB protein modulates hedgehog signaling by degrading Ci/Gli transcription factor. *Developmental Cell*.

Zhang, Q., Q. Shi, Y. Chen, T. Yue, S. Li, B. Wang, and J. Jiang. 2009. Multiple Ser/Thr-rich degrons mediate the degradation of Ci/Gli by the Cul3-HIB/SPOP E3 ubiquitin ligase. *Proceedings of the National Academy of Sciences*. 106:21191–21196. doi:10.1073/pnas.0912008106.

Zhao, Y., C. Tong, and J. Jiang. 2007. Hedgehog regulates smoothened activity by inducing a conformational switch. *Nature*. 450:252–258. doi:10.1038/nature06225.

Zhao, Y., C. Tong, G. Wang, B. Wang, J. Jia, and J. Jiang. 2005. Hedgehog-regulated Costal2-kinase complexes control phosphorylation and proteolytic processing of Cubitus interruptus. *Developmental Cell*.

CHAPTER II:

The Heterotrimeric Kinesin-2 Complex Interacts with and Regulates GLI Protein Function

2.1 Abstract

GLI transport to the primary cilium and nucleus is required for proper HH signaling; however, the mechanisms that mediate these trafficking events are poorly understood. Kinesin-2 motor proteins regulate ciliary transport of cargo, yet their role in GLI protein function remains unexplored. To examine a role for the heterotrimeric KIF3A/KIF3B/KAP3 kinesin-2 motor complex in regulating GLI activity, we performed a series of structure-function analyses using biochemical, cell signaling and in vivo approaches that define novel, specific interactions between GLI proteins and two components of this complex, KAP3 and KIF3A. We find that all three mammalian GLI proteins interact with KAP3 and map specific interaction sites in both proteins. Further, we find that GLI proteins interact selectively with KIF3A, but not KIF3B and that GLI interacts synergistically with KAP3 and KIF3A. Using a combination of cell signaling assays and chicken in ovo electroporations, we demonstrate that KAP3 interactions restrict GLI activator, but not GLI repressor function. These data suggest that GLI interactions with KIF3A/KIF3B/KAP3 complexes are essential for proper GLI transcriptional activity.

2.2 Introduction

Hedgehog (HH) signaling is an evolutionarily conserved pathway that is indispensible for embryonic development and functions in adult tissue homeostasis, renewal, and regeneration (reviewed in (McMahon et al., 2003; Briscoe and Thérond, 2013). Vertebrate HH signaling initiates when secreted HH ligands bind to the twelve-pass transmembrane receptor Patched (PTCH1) (Stone et al., 1996; Marigo et al., 1996) and to the co-receptors GAS1, CDON, and BOC (Allen et al., 2011); this relieves inhibition of Smoothened (SMO), a seven-pass transmembrane GPCR-like protein that initiates a signal transduction cascade culminating in modulation of the GLI family of zinc-finger transcription factors (GLI1-3) (Hui and Angers, 2011). As effector molecules of the HH pathway, GLI proteins act in the nucleus to both activate and repress HH target gene expression (Ruiz i Altaba, 2011; Sasaki et al., 1999; Stamataki, 2005; Vokes et al., 2007).

There are three mammalian GLI proteins– GLI1, which functions exclusively as a transcriptional activator and is dispensable for mammalian development (Bai et al., 2002), GLI2, the main transcriptional activator of the HH pathway (Ding et al., 1998; Bai et al., 2002), and GLI3, which acts primarily as a transcriptional repressor (Altaba, 1999; Bai et al., 2004). GLI2 and GLI3 both contain N-terminal repressor and C-terminal activation domains that regulate their function (Sasaki et al., 1999; Aza-Blanc et al., 2000; Stamataki, 2005). In the absence of HH signaling, GLI2 and GLI3 are proteolytically processed into N-terminal repressors that inhibit HH target gene transcription (Wang et al., 2000). Conversely, HH ligand stimulation promotes the accumulation of full-length GLI2 and GLI3 that activate HH target gene transcription (Pan et al., 2006).

Recent studies indicate a significant role for primary cilia in the regulation of GLI protein processing and function (reviewed by Nozawa et al., 2013). GLI2 and GLI3 constitutively traffic through primary cilia at low levels (Haycraft et al., 2005; Norman et al., 2009) while HH pathway activation promotes GLI2 and GLI3 accumulation at the tips of primary cilia (Endoh-Yamagami et al., 2009; Wen et al., 2010); this correlates with the accumulation of full-length GLI proteins that activate HH target gene transcription. Notably, all mammalian GLI proteins traffic to primary cilia (Haycraft et al., 2005), and disruption of ciliogenesis affects both processing and function of GLI2 and GLI3, which results in digit formation and neural tube patterning defects (Haycraft et al., 2005; Liu et al., 2005). Despite their implication in GLI protein regulation, the mechanisms by which primary cilia regulate GLI activity and processing are not well understood.

Intraflagellar transport (IFT) complexes are responsible for cilia formation, maintenance, and trafficking of cargo within primary cilia (reviewed by Pedersen and Rosenbaum, 2008). These complexes consist of IFT particles (A and B) that are trafficked along microtubule-based axonemes by anterograde (kinesin-2) and retrograde (dynein) motor proteins (reviewed by Goetz and Anderson, 2010). Roles for these various IFT components in GLI protein ciliary trafficking are starting to emerge. For example, mutations in genes that encode for components of retrograde motors (*Dync2h1*), IFT A complexes (*Ift122*), or IFT B complexes (*Ift25*) cause GLI protein mislocalization at ciliary tips that correlates with aberrant HH signaling (Ocbina et al., 2011; Qin et al., 2011; Keady et al., 2012). While these studies indicate a role for IFT particles and retrograde motors in GLI processing and function, the mechanisms of how GLI proteins are trafficked within and between subcellular compartments remains largely unexplored.

One outstanding question is: what regulates the intracellular trafficking of GLI proteins between the cytoplasm, nucleus, and primary cilium? The KIF3A/KIF3B/KAP3 heterotrimeric complex is an evolutionarily conserved kinesin-2 motor that mediates plus-end-directed protein transport along microtubules and plays important functional roles in both ciliary and intracellular transport (reviewed by Scholey, 2013; Cole et al., 1993; Wedaman, 1996). Mutations in *Kif3a*, *Kif3b*, or the non-motor component, kinesin-associated protein (*Kifap3*; referred to hereafter as *Kap3*) cause ciliary defects that lead to mid-gestation lethality and randomization in left-right asymmetry (Takeda et al., 1999; Hirokawa, 2000; Nonaka et al., 1998). Mice lacking KIF3A also display aberrant neural tube patterning similar to phenotypes seen in mice containing mutations that prevent HH pathway activation (Huangfu et al., 2003). Previous work in vertebrates identified KAP3 as an armadillo repeat-containing protein that forms a heterotrimeric complex with KIF3A and KIF3B and scaffolds cargo to the motors (Yamazaki et al., 1995; 1996). Similar to *Kif3a* and *Kif3b* mutant mice, *Kap3* mutant mice die during mid-gestation (Teng et al., 2005) due to the central role of the heterotrimeric kinesin-2 complex in ciliogenesis (reviewed in (Scholey, 2013). Further, it is this critical role for KIF3A, KIF3B, and KAP3 in ciliogenesis that complicates the use of genetics to address their role in HH signaling and explains why a role for these molecules in regulating GLI protein activity has remained elusive.

In order to dissect the role of the KIF3A/KIF3B/KAP3 complex in directly regulating GLI protein trafficking and function independent of its role in ciliogenesis, we employed a combination of biochemical, cell signaling, and in vivo approaches to define novel interactions between GLI proteins and members of the kinesin-2 motor complex. Specifically we demonstrate that both KAP3 and KIF3A, but not KIF3B interact with GLI proteins and map the site of these interactions between all three proteins. Further, using cell signaling assays and

chicken in ovo electroporations we find that KAP3 restricts GLI activator, but not GLI repressor function. Together, these data identify novel, selective physical interactions between kinesin-2 motor complex components that specifically regulate GLI protein function.

2.3 Results

KAP3 localizes with GLI2 and GLI3 in different subcellular compartments

To determine whether the heterotrimeric KIF3A/KIF3B/KAP3 complex co-localizes with GLI proteins, we initially compared the distribution of endogenous GLI2 and GLI3 with endogenous KAP3 in mouse embryonic fibroblasts (MEFs) (Figure 2.1). In wildtype MEFs, both GLI2 and GLI3 localize to multiple subcellular compartments including the nucleus, cytoplasm, and the tips of primary cilia (Figure 2.1A and Figure 2.1B, top rows). Similar to GLI2 and GLI3, KAP3 localizes to multiple subcellular compartments and co-localizes with GLI2 and GLI3 within the tips of primary cilia (Figure 2.1A and Figure 2.1B, top rows, white arrows). While GLI2 and GLI3 co-localize with KAP3 largely at the tips of primary cilia in wildtype MEFs, co-localization is observed along the entire length of the cilium in *Dync2h1* mutant MEFs that are defective in retrograde ciliary trafficking (Figure 2.1A, middle row and Figure 2.1B, bottom row;(Ocbina et al., 2011). Further, KAP3 localizes to primary cilia in *Gli2*$^{-/-}$*;Gli3*$^{-/-}$ MEFs suggesting that endogenous KAP3 ciliary localization is independent of GLI2 and GLI3 (Figure 2.1A, bottom row).

In addition to assessing endogenous co-localization, we also compared the distribution of endogenous GLI2 and GLI3 with epitope-tagged KAP3A (KAP3A::HA) in HH-responsive NIH/3T3 fibroblasts (Figure 2.1; Figure 2.2). Similar to what we observe in MEFs, endogenous GLI2 and GLI3 localize to multiple subcellular compartments including the cytoplasm, nucleus,

and primary cilium (Figure 2.1A and Figure 2.2A, top row). Similarly, KAP3A::HA localizes to multiple subcellular compartments and co-localizes with endogenous GLI2 and GLI3 in primary cilia (Figure2.1A and Figure 2.2A, white arrows). More importantly, KAP3A::HA distribution is similar to endogenous KAP3 confirming that KAP3A::HA localizes to the same subcellular compartments as endogenous KAP3 (Compare Figure 2.1A and Figure 2.2A).

To confirm the specificity of the endogenous GLI2 and GLI3 antibodies in NIH/3T3 cells and to assess whether KAP3A::HA ciliary localization requires GLI2 and/or GLI3, we examined KAP3A::HA localization in *Gli2*$^{-/-}$*;Gli3*$^{-/-}$ MEFs (Figure 2.3A and Figure 2.2A, bottom rows). In *Gli2*$^{-/-}$*;Gli3*$^{-/-}$ MEFs, no GLI2 or GLI3 antibody signal is detected however KAP3A::HA still localizes to primary cilia (Figure 2.3A and Figure 2.2A, bottom rows). These data indicate that like endogenous KAP3, KAP3A::HA localizes to primary cilia independently of GLI2 and GLI3.

To further assess GLI2/KAP3A co-localization, we expressed an epitope-tagged version of GLI2 (MYC::GLI2) in NIH/3T3 cells (Figure 2.2B). MYC::GLI2 localizes to both the nucleus and cytoplasm and co-localizes with KAP3A::HA in these subcellular compartments (Figure 2.2B). These data suggest that in addition to primary cilia, GLI2 can co-localize with KAP3 in the cytoplasm and nucleus when expressed at similar levels.

KAP3A and KAP3B specifically interact with all full-length mammalian GLI proteins

To investigate whether KAP3 proteins physically interact with GLI2, we performed co-immunoprecipitation experiments in COS-7 cells. Two isoforms of mammalian KAP3 exist– KAP3A and KAP3B (Yamazaki et al., 1996). KAP3A is a 792 amino acid protein containing nine armadillo repeats (Yamazaki et al., 1996). KAP3B is an alternatively spliced isoform of KAP3A that contains a 66 base pair insertion immediately downstream of the codon for amino

acid 757, generating a truncated 772 amino acid protein (Yamazaki et al., 1996). COS-7 cells were co-transfected with MYC::GLI2 and either KAP3A::HA or KAP3B:HA followed by immunoprecipitation and western blot analysis (Figure 2.3, B and C). We find that both KAP3A::HA and KAP3B::HA co-precipitate with MYC::GLI2 (Figure 2.3B). Similarly, immunoprecipitation of either KAP3A::HA or KAP3B::HA also co-precipitates MYC::GLI2 (Figure 2.3C). Notably, both KAP3A::HA and KAP3B::HA appear to be stabilized in the presence of GLI2 (Figure 2.3, B and C, cf. KAP3 expression in lysates from cells transfected with KAP3 alone and lysates co-transfected with KAP3 and GLI2). In contrast, KAP3A and KAP3B do not interact significantly with the structurally related, zinc finger containing transcription factor, ZIC1 (Figure 2.4A). Overall, these data suggest that GLI2 specifically interacts with both isoforms of KAP3.

The physical association of GLI2 with KAP3A and KAP3B prompted us to ask whether KAP3A and KAP3B also interact with the other full-length mammalian GLI proteins, namely GLI1 and GLI3. Similarly to GLI2, we find that KAP3A co-precipitates with either GLI1 or GLI3 (Figure 2.3D, top panels) and that immunoprecipitation of KAP3A also co-precipitates GLI1 and GLI3 (Figure 2.3D, middle panels). We also find that KAP3B co-precipitates with GLI1 and GLI3 (Figure 2.3E). Taken together, these data indicate that KAP3A and KAP3B physically interact specifically with all three mammalian GLI proteins.

To determine whether the interaction between GLI and KAP3 proteins is direct, we purified FLAG-tagged GLI1 and FLAG-tagged KAP3A from cell lysates (Figure 2.3F) and performed immunoprecipitation experiments using an antibody directed against endogenous KAP3 (Figure 2.3G). We find that purified FLAG::GLI1 co-precipitates with purified KAP3A::FLAG (Figure 2.3G). In contrast, purified GFP::FLAG does not co-precipitate with

KAP3A (Figure 2.3G). These results suggest that GLI proteins interact directly and specifically with KAP3.

GLI2 selectively interacts with kinesin-2 motors and synergistically binds KIF3A and KAP3A

The mechanism by which KAP3 facilitates cargo binding as part of the KIF3A/KIF3B motor complex is not well understood, and whether this complex is involved in transport of the GLI proteins has yet to be addressed. Previous work indicates that KIF3A/KIF3B can exist as a separate heterodimeric complex that can bind cargo in the absence of KAP3 (Huang et al., 2011; Yamazaki et al., 1995; 1996), suggesting that kinesin-2 motors may use multiple mechanisms to associate with cargo. To test whether KIF3A and KIF3B themselves can interact with GLI proteins, we performed immunoprecipitation studies in COS-7 cells transfected with MYC::GLI2 and either KIF3A::HA or KIF3B::HA (Figure 2.5A). As a control, we performed similar experiments in COS-7 cells expressing KAP3A::FLAG and either KIF3A::HA or KIF3B::HA (Figure 2.5A).

Surprisingly, immunoprecipitation of GLI2 co-precipitates KIF3A, but not KIF3B (Figure 2.5A, top panels). In contrast, both KIF3A and KIF3B co-precipitate with KAP3 (Figure 2.5A, middle panels). Importantly, KIF3A and KIF3B are expressed at equal levels in cell lysates, indicating that protein expression is not an explanation for this discrepancy (Figure 2.5A, lower panels). Quantitation of these interactions over three separate experiments indicates that nearly 25 times as much KIF3A precipitates with GLI2 compared to KIF3B (Figure 2.5B), while relatively equal amounts of KIF3A and KIF3B interact with KAP3 (KIF3A:KIF3B ~1; Figure 2.5B). Together these data suggest that GLI2 can interact with kinesin-2 motors, and that GLI2 preferentially interacts with KIF3A.

Since the majority of KAP3 in the cell associates with KIF3A/KIF3B (Yamazaki et al., 1995; Yamazaki et al., 1996), we examined whether the co-expression of KAP3A with KIF3A or KIF3B would promote interactions with GLI2. We immunoprecipitated MYC::GLI2 from COS-7 cells expressing KAP3A::FLAG and either KIF3A::HA (Figure 2.5C) or KIF3B::HA (Figure 3D). Strikingly, co-expression of KAP3A and KIF3A results in significantly more co-precipitation of both proteins with GLI2 compared to expression of either protein individually (Figure 2.5C; top panel, cf. lane 5 and lane 8; second panel, cf. lane 6 and lane 8). In stark contrast, co-expression of KAP3A and KIF3B does not enhance the amount of KIF3B (Figure 2.5D; top panel, cf. lane 5 and lane 8) or KAP3A (Figure 2.5D; second panel, cf. lane 6 and lane 8) that co-precipitates with GLI2. Taken together, these data suggest that GLI2 preferentially interacts with KIF3A compared to KIF3B and that co-expression of KIF3A and KAP3A promotes synergistic interactions of both proteins with GLI2.

The armadillo repeats in KAP3 mediate interactions with GLI2

We next performed a complementary set of biochemical experiments to determine the regions within KAP3A and KIF3A that are required to interact with GLI proteins. Previous work indicates that KAP3A interacts with cargo proteins via its armadillo repeats (Gindhart and Goldstein, 1996; Jimbo et al., 2002; Morris et al., 2004; Brown et al., 2005); however, whether KAP3A interacts with GLI proteins in a similar manner is unclear. To test this, we generated two epitope-tagged, truncated versions of KAP3A (KAP3AΔC::HA and KAP3AΔN::HA; Figure 2.5E). These constructs alternately delete over 100 amino acids C-terminal (KAP3ΔC) or N-terminal (KAP3ΔN) of the centrally-located armadillo repeats of KAP3. Immunoprecipitation of GLI2 co-precipitates full-length KAP3A, KAP3AΔC, and KAP3AΔN (Figure 2.5F). These data

are consistent with the notion that the armadillo repeats in KAP3A mediate interactions with GLI2. Attempts to identify specific armadillo repeats in KAP3 that are required to interact with GLI proteins were hindered by poor expression of these constructs, thus precluding further analysis (data not shown).

The N-terminal motor domain of KIF3A is dispensable for interactions with GLI2

To map the domain within KIF3A that mediates interactions with GLI proteins, we immunoprecipitated MYC::GLI2 from cells expressing either KIF3A::HA or a version of KIF3A that lacks the conserved N-terminal motor domain, DNKIF3A::HA (Figure 2.5G). KIF3A and DNKIF3A both co-precipitate with GLI2, albeit less strongly when compared to KAP3A (Figure 2.5H, top panels). Notably DNKIF3A is expressed at lower levels than full-length KIF3A, which may explain the quantitative difference in GLI2 association (Figure 2.5H, bottom panels). Regardless, these data indicate that the motor domain of KIF3A is dispensable for interactions with GLI2.

KAP3A interacts with constitutive GLI repressor, but not constitutive GLI activator

Given that GLI1-3 interact with KAP3, we sought to identify the domains within the GLI proteins that mediate binding to KAP3. Specifically, we examined the requirements for the N- and C-termini of the GLI proteins in KAP3 interactions (Figure 2.6). Here we took advantage of the high degree of sequence conservation shared between mammalian GLI2 and GLI3 proteins. GLI2 and GLI3 contain a conserved amino-terminal transcriptional repressor domain, and a carboxy–terminal transcriptional activation domain (Sasaki et al., 1999). We generated two construct: one that encodes an epitope-tagged, C-terminal truncated GLI3 (MYC::GLI3R) that

functions as a constitutive transcriptional repressor (Meyer and Roelink, 2003) and a second that encodes an epitope-tagged, N-terminal truncated, constitutively active GLI2 (MYC::GLI2ΔN; (Roessler et al., 2005); Figure 2.6A).

To confirm the activity of these constructs, we tested their function in a cell-based HH reporter assay. Consistent with previous reports, full-length GLI2 induces an approximately a 12-fold increase in HH-dependent luciferase expression in NIH/3T3 fibroblasts compared to no treatment (Kim et al., 2009); Figure 2.6B). This is similar to the level of induction observed when cells are exposed to NSHH-conditioned medium (Figure 2.6B). Importantly, we observed a synergistic induction of luciferase activity (~ 40-fold induction) when *Gli2*-transfected cells were also treated with NSHH-conditioned medium (Figure 2.6B). These results confirm that MYC::GLI2 functions to activate HH-dependent transcription in NIH/3T3 cells.

In contrast to full-length GLI2, expression of constitutively active MYC::GLI2ΔN results in approximately 90-fold induction of luciferase activity (Figure 2.6C). These results support previous studies (Roessler et al., 2005; Sasaki et al., 1999) and confirm that MYC::GLI2ΔN functions to activate HH signaling at high levels in mammalian cells. To determine the requirement for the N-terminal domain of GLI2 in mediating KAP3 binding, we performed additional co-immunoprecipitation studies (Figure 2.6D). Surprisingly, while full-length GLI2 and GLI2ΔN are expressed at similar levels in cell lysates and are precipitated equivalently, KAP3A only co-precipitates with full-length GLI2 and does not significantly interact with GLI2ΔN (Figure 2.6D). These data suggest that the amino-terminal domain of GLI2 is required to interact with KAP3 proteins.

We next tested MYC::GLI3R activity in luciferase assays and compared its function to full-length MYC::GLI3 (Figure 2.6F). Unlike GLI2, full-length GLI3 does not induce significant

HH pathway activity in the absence of ligand treatment (Figure 2.6F). Further, treatment of cells expressing full-length GLI3 with NSHH-conditioned medium does not significantly induce luciferase activity beyond that observed with NSHH treatment alone (Figure 2.6F). These data are consistent with the current paradigm that GLI3 functions mainly as a transcriptional repressor in vivo (Wang et al., 2000). In contrast, MYC::GLI3R induces a small, but significant decrease in luciferase induction when compared to no treatment in the absence of HH ligand treatment (Figure 2.6F). Similarly, MYC::GLI3R significantly decreases NSHH-mediated luciferase induction (Figure 2.6F). These data confirm that MYC::GLI3R functions as a transcriptional repressor in cell signaling assays.

We performed immunoprecipitation studies with full-length GLI3 and GLI3R to assess interactions with KAP3A (Figure 2.6G). Similarly to Figure 2, KAP3A co-precipitates with full-length GLI3. Importantly, KAP3A also co-precipitates with GLI3R (Figure 2.6G). These data suggest that the N-terminus of GLI3 is sufficient to mediate physical interactions with KAP3A. Notably, immunofluorescence localization data demonstrate that GLI3R is localized exclusively to the nucleus (Figure 2.7). Taken together, these results further suggest that there is a common N-terminal domain in GLI2 and GLI3 that promotes interactions with KAP3.

The N-terminus of GLI2 interacts with KAP3A

To more precisely map the domains within the GLI proteins that interact with KAP3A, we generated a series of epitope-tagged, N-terminal truncated versions of GLI2 (Figure 2.8A). GLI2ΔN, which fails to appreciably interact with KAP3A (Figure 2.6D), lacks the amino-terminal 328 amino acids of GLI2 (Roessler et al., 2005). Therefore, we generated MYC::GLI2$^{154\text{-}1586}$ to determine if amino acids 154 to 328 mediate KAP3 binding. Similar to

GLI2ΔN, and in contrast to full-length GLI2, immunoprecipitation of MYC::GLI2$^{154\text{-}1586}$ fails to co-precipitate KAP3A (Figure 2.8B). We employed this strategy iteratively, generating MYC::GLI2$^{61\text{-}1586}$ to assess whether amino acids 61 to 153 mediate GLI2 interactions with KAP3A. Importantly, GLI2$^{61\text{-}1586}$ does co-precipitate similar amounts of KAP3A as compared to full-length GLI2 (Figure 2.8B). These data suggest that GLI2 interacts with KAP3A via an N-terminal motif that lies between amino acids 61 and 153.

To test the functional significance of this interaction, we again utilized luciferase reporter assays in HH-responsive NIH/3T3 cells (Figure 2.8C). While expression of full-length GLI2 promotes a small but significant increase in luciferase activity, GLI2$^{154\text{-}1586}$ induces an approximately 70-fold increase in luciferase activity, similar to the induction observed with GLI2ΔN (cf. Figure 2.6C and 2.8C). In contrast GLI2$^{61\text{-}1586}$ promotes much lower levels of signaling (approximately 12-fold) which is similar to the induction observed with full-length GLI2 (Figure 2.8C). These data correlate GLI binding to KAP3 with reduced HH pathway activity.

Having narrowed the KAP3-binding domain in GLI2 to less than 100 amino acids, we generated two additional constructs to more finely map this interaction. We first generated GLI2$^{108\text{-}1586}$, and similar to GLI2ΔN, GLI2$^{108\text{-}1586}$ does not co-precipitate KAP3A as effectively as full-length GLI2 or GLI2$^{61\text{-}1586}$ (Figure 2.8D). These data suggest that amino acids 61 to 108 are necessary to interact with KAP3A. Therefore, we also deleted these amino acids from full-length GLI2 (GLI2$^{\Delta 61\text{-}108}$; Figure 2.8A). GLI2$^{\Delta 61\text{-}108}$ does not effectively co-precipitate KAP3A compared to full-length GLI2 (Figure 2.8D), confirming that amino acids 61-108 are essential for GLI2 interactions with KAP3.

To further test the correlation between GLI-KAP3 interactions and reduced HH pathway activity (Figure 2.8C), we examined whether deletion of the domain responsible for KAP3 binding might result in higher GLI activity. Indeed, GLI2$^{\Delta 61\text{-}108}$ promotes approximately three-fold greater luciferase induction than full-length GLI2 in cell signaling assays (Figure 2.8E). Together, these data identify an interaction between GLI2 and KAP3A that is mediated by 47 amino acids within the N-terminus of GLI2 that acts to restrict GLI2 activity.

KAP3A interactions with GLI3 do not alter GLI repressor function

To test whether the KAP3-binding domain identified in GLI2 could also mediate interactions between GLI3 and KAP3A, we generated a MYC::GLI3R$^{\Delta 134\text{-}182}$ construct that deletes the analogous motif in GLI3 (Figure 2.9A). Similar to GLI2$^{\Delta 61\text{-}108}$ (Figure 2.8D), GLI3R$^{\Delta 134\text{-}182}$ does not effectively co-precipitate KAP3A compared to full-length GLI3 and GLI3R (Figure 2.9B), demonstrating that the 47 amino acid KAP3-binding domain is conserved between GLI2 and GLI3.

We also compared the repressor function of GLI3R to GLI3R$^{\Delta 134\text{-}182}$ in the presence of NSHH-mediated luciferase induction (Figure 2.9C). Surprisingly, and in stark contrast to the transcriptional activation data obtained with GLI2, GLI3R and GLI3R$^{\Delta 134\text{-}182}$ are equally effective in repressing HH pathway activation (from approximately 4.5 fold to 1.5 fold) suggesting that perturbing the interaction between GLI3R and KAP3 does not alter GLI3 repressor activity (Figure 2.9C). Taken together, these data indicate that the KAP3-binding domain is conserved between GLI2 and GLI3, and that KAP3-binding selectively restricts GLI activator, but not GLI repressor function.

KAP3 interactions with GLI2 restrict HH pathway activation in vivo

To extend the observation that KAP3-GLI interactions selectively restrict GLI activator but not GLI repressor function, we utilized chicken in ovo neural tube electroporations (Figure 2.10). Here, we can assess the consequences of GLI function on the expression of endogenous HH targets to readout different levels of HH pathway activation, including those targets (e.g. NKX2.2) that exclusively require GLI activator function for their expression (Bai et al., 2004; Bai and Joyner, 2001; Bai et al., 2002; Oosterveen et al., 2012; Peterson et al., 2012).

Electroporation of empty vector (*pCIG*) does not alter expression of the low level HH pathway target, NKX6.1 (Figure 2.10A). In contrast, electroporation of *Gli2* promotes cell autonomous, ectopic NKX6.1 expression, as does electroporation of a KAP-binding deficient *Gli2* construct ($Gli2^{\Delta 61\text{-}108}$) and constitutively active $Gli2^{\Delta N}$ (Figure 2.10A). Strikingly, GLI2 is not sufficient to promote ectopic NKX2.2 expression in the developing neural tube, while expression of a KAP3-binding deficient GLI2 (GLI2Δ61-108) does induce cell autonomous NKX2.2 expression, similar to what is observed with expression of constitutively active GLI2ΔN (Figure 2.10B). Notably, ectopic NKX2.2+ cells are detected even in the dorsal most aspect of the chicken neural tube (Figure 2.10B, arrows).

To test whether KAP3-binding deficient GLI3R (GLI3RΔ134-182) is sufficient to repress endogenous HH target genes in the developing chicken neural tube, we electroporated GLI3R and GLI3RΔ134-182 and assessed PAX7 expression (Figure 2.11). While HH signaling normally restricts PAX7 expression to the dorsal neural tube, electroporation of GLI3R results in ventral expansion of PAX7 even in the ventral most aspect of the neural tube (Figure 2.11A, top row, white arrows). Similar to GLI3R, the KAP3-binding deficient GLI3R (GLI3RΔ134-182) induces ectopic PAX7 expression throughout the ventral neural tube (Figure 2.11A, bottom row,

white arrows). Together, these data support the notion that KAP3-binding restricts the activator, but not repressor function of the GLI proteins.

2.4 Discussion

GLI proteins physically interact with the heterotrimeric kinesin-2 motor complex

Tightly regulated trafficking and processing of GLI proteins are vital for proper HH signaling (Haycraft et al., 2005; Kim et al., 2009). However, the mechanisms that regulate GLI protein function remain poorly understood. Here we present evidence that the heterotrimeric KIF3A/KIF3B/KAP3 kinesin-2 motor complex selectively regulates GLI activator function through multiple physical interactions (Figure 2.12A). Specifically, we find that all three mammalian GLI proteins physically interact with the kinesin-associated protein, KAP3. Further, we demonstrate that GLI2 and GLI3 interact with KAP3 via a conserved N-terminal 47 amino acid domain that restricts GLI activator, but not GLI repressor function. We also map the GLI binding site in KAP3 to the conserved armadillo repeats that mediate interactions with other KAP3 cargo proteins (Gindhart and Goldstein, 1996; Jimbo et al., 2002; Phang et al., 2014). In addition, we find that GLI proteins selectively interact with the KIF3A kinesin-2 motor component, but not appreciably with KIF3B. Strikingly, GLI proteins interact synergistically with KIF3A and KAP3, forming a robust complex that suggests GLI protein function is regulated by multiple interactions with the kinesin-2 motor complex. To our knowledge, this study provides the first evidence that GLI proteins physically interact with plus-end-directed kinesin-2 motor proteins, despite their implication in HH signaling for over a decade (Takeda et al., 1999; Huangfu et al., 2003). These results are of particular significance given that ciliary transport of cargo is currently believed to be largely mediated by interactions with IFT particles

(Scholey, 2003; Bhogaraju et al., 2013; Qin et al., 2004). However, our data suggest a novel paradigm where direct interactions of kinesin-2 motors with GLI protein cargo can regulate their trafficking and function. Notably, these results are consistent with recent work suggesting that kinesin-2 motors also mediate the anterograde trafficking of dynein proteins independently of IFT particles (Hao et al., 2011). Further studies are needed to elucidate whether ciliary trafficking of GLI proteins occurs independently of IFT and BBSome protein interactions.

Complex regulation of GLI protein processing and activity

Multiple proteins modulate GLI transcriptional activity to control the output of HH signaling. Suppressor of Fused (SUFU) represses HH signaling by binding GLI proteins and preventing their nuclear transport (Kogerman et al., 1999; Barnfield et al., 2005). SUFU-GLI complexes traffic to primary cilia in response to HH stimulation, a process necessary for dissociation of the complex and subsequent nuclear translocation of GLI proteins (Tukachinsky et al., 2010), but the mechanisms that control complex assembly/disassembly are unclear. Here we show that KAP3 interacts with GLI2 and GLI3 and co-localizes with these proteins in primary cilia. KAP3 may control GLI activity through effects on SUFU-GLI complex formation. However, interactions between KAP3 and the constitutively nuclear localized GLI3R also suggest a role for KAP3 at the level of nuclear trafficking. It is plausible that the KIF3A/KIF3B/KAP3 complex controls both the nuclear and ciliary trafficking of GLI proteins, but further experiments are required to elucidate these mechanisms. It will be of particular interest to test whether KAP3 affects SUFU-GLI interactions and the requirement for cilia in this process.

KAP3 interactions with GLI proteins specifically regulate GLI activator function

We demonstrate that a conserved 47 amino acid domain in GLI2 and GLI3 mediates KAP3 interactions, and that deletion of this domain from GLI2 results in increased transcriptional activity. Notably this motif encompasses a portion of a previously identified N-terminal repressor domain (Sasaki et al., 1999). As a result, one possibility is that the increase in GLI2 activity is simply due to loss of this poorly defined repressor domain. However, two key findings argue against this notion. First, elimination of the analogous domain in GLI3 does not alter GLI3 repressor function, suggesting that this domain does not possess general repressive activity. Second, electroporation of a KAP-binding deficient *Gli2* construct in the developing chicken neural tube induces ectopic NKX2.2 expression, which requires GLI activator function and cannot be induced simply by the loss of GLI repression (Matise et al., 1998; Bai et al., 2004). Together, these data support a novel paradigm where GLI-KAP3 interactions selectively restrict the activator, but not the repressor function of GLI proteins.

These observations are similar to SUFU regulation of GLI proteins, where GLI3 repressor can function independently of SUFU (Wang et al., 2010). In these studies, SUFU interacts with both GLI2 and GLI3, however GLI3 repressor is able to rescue the ventralized neural tube phenotype in *Sufu*$^{-/-}$ embryos (Wang et al., 2010). It is interesting to speculate that, similar to SUFU, KAP3 may regulate GLI activator proteins during transit to the nucleus, although the nature of GLI, KAP3 and SUFU interplay will require further study.

Regulation of GLI function by kinesin proteins

Initial studies in *Drosophila* identified Cos2 as a kinesin-related protein that controls HH signaling through interactions with Ci, the *Drosophila* homologue of GLI (Sisson et al., 1997;

Robbins et al., 1997). More recent studies in vertebrates identified a similar role for the *Cos2* homologue, *Kif7*, in the regulation of GLI protein function (Liem et al., 2009; Endoh-Yamagami et al., 2009; Cheung et al., 2009). In particular, KIF7, and the structurally related kinesin KIF27, both interact with GLI proteins (Endoh-Yamagami et al., 2009; Cheung et al., 2009; Maurya et al., 2013; Marks and Kalderon, 2011), while KIF7 specifically functions to both promote and antagonize GLI activity (Maurya et al., 2013; Hsu et al., 2011; Li et al., 2012). KIF7 promotes HH signaling through dissociation of SUFU-GLI complexes, and controls the ciliary localization of GLI proteins in a tissue-specific manner (Hsu et al., 2011; Maurya et al., 2013; Endoh-Yamagami et al., 2009). While the KIF7-GLI interaction sites have not been precisely mapped, GLI proteins appear to interact with KIF7 via multiple domains, including an N-terminal motif (Marks and Kalderon, 2011). One hypothesis is that KAP3 competes for KIF7 binding to GLI proteins, thus limiting dissociation of GLI-SUFU complexes and restricting GLI protein function. Interestingly, KIF7 functions to organize the ciliary tip compartment through the regulation of microtubule dynamics (He et al., 2014). Further, the effects of KIF7 are controlled by PPFIA1- and PP2A-mediated regulation of KIF7 phosphorylation (Liu et al., 2014).These results suggest that either the loss of KIF7 (He et al., 2014), or altered KIF7 phosphorylation (Liu et al., 2014), affects the ciliary localization and activity of GLI proteins. However, given that KIF7 does not possess plus-end-directed microtubule motor activity (He et al., 2014), one possibility is that KAP3-GLI protein interactions are disrupted in *Kif7* mutant cells due to the disorganized ciliary tip compartments. It will be particularly important to test these interactions in cells with different KIF7 expression levels and phosphorylation states, and to assess the role of KIF7 in mediating kinesin-2 interactions with GLI proteins.

Our data indicate that, in addition to KIF7 and KIF27, GLI proteins also interact with KIF3A, suggesting that multiple kinesin proteins control GLI function. That KIF3A interacts with GLI proteins independently of KAP3 has precedence in the literature. For example, the TRIM protein RNF33 interacts with KIF3A and KIF3B in mouse testis (Huang et al., 2011). Additionally, the protein phosphatases DUSP26 and POPX2 interact with both KIF3 and KAP3 proteins (Tanuma et al., 2008; Phang et al., 2014). These data also raise the question of whether GLI proteins interact with yet additional kinesin proteins. Our results indicate that GLI2 preferentially interacts with KIF3A, but not KIF3B, analogous to earlier data demonstrating selective interactions of GLI2 with KIF7 and KIF27 (Cheung et al., 2009). Future studies will be required to determine whether GLI proteins interact with: 1) additional kinesin-2 motors, including KIF3C and KIF17 (Yang et al., 2001; Yang and Goldstein, 1998; Insinna et al., 2008; Snow et al., 2004), 2) other kinesin motors implicated in ciliary trafficking (Morsci and Barr, 2011), and 3) non-ciliary kinesin motors (Hirokawa et al., 2009).

In addition to kinesin-2 motors and their adaptor proteins, intraflagellar transport (IFT) particles, such as IFT25 and IFT122, also regulate GLI ciliary localization (Qin et al., 2011; Keady et al., 2012). However, whether this is mediated by physical interactions between GLI and IFT particles remains unexplored, and whether KAP3 interacts directly with these IFT particles has not been tested. One possibility is that, along with KAP3, IFT particles interact with GLI proteins to mediate ciliary GLI trafficking. In addition to their role in ciliary trafficking, IFT particles also function in trafficking outside of the primary cilium (reviewed by Baldari and Rosenbaum, 2010). For example, IFT particles traffic T-cell receptors to the immune synapse (Finetti et al., 2009). Future studies will determine whether IFT particles interact with GLI proteins and the consequences of these interactions on GLI processing and activity.

In summary, despite the indirect role of KIF3A/KIF3B/KAP3 in HH signaling due to their role in ciliogenesis, our knowledge of whether these motors control HH signaling directly through interactions with HH pathway components has remained unexplored. Here we identify GLI proteins as novel cargo of the heterotrimeric kinesin-2 motor complex that physically interact with KAP3 and selectively interact with KIF3A, but not KIF3B. Based on our data we propose a model (Figure 2.12B) where GLI proteins interact with kinesin-2 motors via synergisitic interactions with KAP3 and KIF3A that selectively restrict GLI activator, but not GLI repressor function. We postulate that kinesin-2 motors may regulate: 1) anterograde GLI trafficking to ciliary tips, 2) GLI trafficking to the nucleus following ciliary transport, or 3) GLI transport to other cellular compartments (Figure 2.12B). While the precise molecular mechanism awaits elucidation, our findings identify a direct role for the kinesin-2 motor protein complex in HH signaling through physical interactions with GLI proteins that selectively regulate GLI transcriptional activity.

2.5 Materials and Methods

DNA Constructs

To generate 6X MYC-tagged constructs m*Gli1*, h*Gli2*, h*Gli2ΔN*, h$Gli2^{280\text{-}1586}$, h$Gli2^{262\text{-}1586}$, h$Gli2^{218\text{-}1586}$, h$Gli2^{154\text{-}1586}$, h$Gli2^{108\text{-}1586}$, h$Gli2^{61\text{-}1586}$, h*Gli3*, and h*Gli3R* cDNAs were cloned into pCDNA3 using standard molecular biology techniques. To generate a version of hGLI2 lacking amino acids 61-108 (h$Gli2\Delta^{61\text{-}108}$), we amplified h*Gli2* using forward (5'-TCTTGCCACCATTCCATGCGGCTGGCCCTGGGGAGTCCCC- 3') and reverse (5'-GGGGACTCCCCAGGGCCAGCCGCATGGAATGGTGGCAAGA-3') mutagenesis primers. To generate a version of hGLI3R lacking amino acids 134-182 (h$GLI3R^{\Delta 134\text{-}182}$) we amplified

h*GLI3R* using forward (5'-TTTTCCCTGCCTTCCATCCTACTGCTGCTTCCGAGTCTCC-3') and reverse (5'-GGAGACTCGGAAGCAGCAGTAGGATGGAAGGCAGGGAAAA- 3') mutagenesis primers. Hemagglutinin (HA)-tagged h*Kap3a*, h*Kap3b*, h*Kif3a*, h*DNkif3a*, m*Kif3b,* Flag (FLAG)-tagged h*Kap3a,* HA-tagged h*Gli2*Δ*N* and 6X MYC-tagged h*Gli2* and h*Gli2*$^{\Delta 61\text{-}108}$ cDNAs were cloned into pCIG (Megason and McMahon, 2002).

Immunoprecipitation and Western Blot Analysis

COS-7 cells were transiently transfected with the relevant DNA constructs using Lipofectamine 2000 (Invitrogen, Cat. #11668). The cells were lysed 48 hr after transfection in HEPES lysis buffer (25mM HEPES pH 7.4, 115mM KOAc, 5mM NaOAc, 5mM $MgCl_2$, 0.5mM EGTA, and 1% TX-100) containing protease inhibitor (Roche, Cat. #11836153001). Cell lysates were then subjected to centrifugation at 14,000 x *g* for 15 min to remove the insoluble fraction and protein concentrations were determined using a BCA Assay Kit (Pierce, Cat. #23225). Cell lysates (1mg) were then pre-cleared with Protein G agarose beads (Roche, Cat. #11719416001) for 1 hr at 4°C. MYC- or HA-tagged proteins were immunoprecipitated from pre-cleared lysates using either anti-MYC (1:150; Santa Cruz, Cat. #sc-40) or anti-HA (1:300; Covance, Cat. #MMS-101) antibodies for 2 hr at 4°C. Following immunoprecipitation, the lysates were incubated with Protein G agarose beads for 1 hr at 4°C. The Protein G agarose beads were washed 5 x 8 min in HEPES lysis buffer and re-suspended in 30 µl of 1x PBS and 6x Laemmli buffer. The samples were boiled for 10 minutes and proteins were separated using SDS-PAGE and analyzed by western blotting. Anti-MYC (1:1000) and anti-HA (1:1000) primary antibodies, peroxidase-conjugated AffiniPure goat anti-mouse light chain secondary antibody (1:50,000; Jackson ImmunoResearch, Cat. # 115-035-174), and a Konica Minolta SRX-101A medical film

processor were used to visualize tagged proteins. Western blots were quantified using ImageJ software.

Purification and immunoprecipitation of FLAG-tagged proteins

For purification of GFP::FLAG, KAP3A::FLAG, and FLAG::GLI1, COS-7 cells were transfected with the appropriate DNA expression constructs. At 48 hr post-transfection, cells were harvested via lysis in a solution containing 50mM HEPES (pH 7.5), 150 mM NaCl, 1% Triton X-100, and a protease inhibitor cocktail. Lysates were centrifuged at 16,000 x g for 15 min. The resulting supernatant was mixed with anti-FLAG M2 agarose beads (Sigma-Aldrich) and incubated for 2 hr at 4°C. After extensive washes in lysis buffer, bound proteins were eluted from the beads with two 20 min incubations with 300 μg/ml of 3X FLAG peptide (ApexBio) at 25°C. Post elution lysates were subjected to SDS-PAGE and analyzed by Gel Code Blue staining (Thermo Scientific). Equal amounts of the eluted FLAG-tagged proteins were combined and KAP3A-FLAG was immunoprecipitated from lysates using mouse anti-KAP3 (BD Biosciences) and the same immunoprecipitation methods described above. A mouse Anti-FLAG antibody (1:1000, Sigma-Aldrich), peroxidase-conjugated AffiniPure goat anti-mouse light chain secondary antibody (1:50,000; Jackson ImmunoResearch), and a Konica Minolta SRX-101A medical film processor were used to visualize tagged proteins.

Cell Culture and Luciferase Assays

NIH/3T3 cells were cultured at 37°C, 5% CO_2, 95% humidity in Dulbecco's modified eagle medium (DMEM; Gibco, Cat. #11965-092) containing 10% bovine calf serum (ATCC; Cat. #30-2030) and penicillin/streptomycin/glutamine (Gibco, Cat. #10378-016). Luciferase

assays were performed by plating 2.5 x 10^4 cells/well in 24 well plates. The next day cells were co-transfected using Lipofectamine 2000 with the DNA constructs indicated in each experiment in addition to *Ptc*Δ136-GL3 (Chen et al., 1999; Nybakken et al., 2005) and pSV-Beta-galactosidase (Promega) constructs to report HH pathway activation and normalize transfections, respectively. Cells were changed to low-serum media (DMEM supplemented with 0.5% bovine calf serum and penicillin/streptomycin/glutamine) 48 hr after transfection and cultured at 37°C in 5%$C0_2$ for an additional 48 hr. NSHH-conditioned medium was added immediately after low-serum change where relevant to activate the HH pathway. Cells were harvested and luciferase and beta-galactosidase activities were measured using Luciferase Assay System (Promega Cat. # E1501) and BetaFluor β-gal assay kit (Novagen, Cat. #70979-3). Multiple assays were performed and each sample was assayed in triplicate.

Immunofluorescence staining

NIH/3T3 fibroblasts were seeded at a density of 1.5 x 10^5 cells/well in 6 well plates. Cells were transfected 24 hr later with either empty vector (pCIG) or with a DNA construct encoding KAP3::HA using Lipofectamine 2000. Cells were grown in low-serum media starting 8 hr after transfection, fixed 48 hr post-transfection in 4% paraformaldehyde for 10 min at room temperature, and permeabilized with a 5 min incubation in 0.2% Triton X-100 in PBS. Immunostaining was performed using the following primary antibodies: mouse anti-acetylated tubulin (1:2500; Sigma), rabbit anti-gamma tubulin (1:2500; Sigma), mouse anti-KAP3 (1:500; BD Biosciences), rabbit anti-ARL13B (1:500; Proteintech), mouse anti-HA (1:1000; Covance), guinea pig anti-GLI2 (1:300; a gift from Dr. J.T. Eggenschwiler, University of Georgia), mouse anti-GLI3 (1:1000; obtained from Dr. S.J. Scales, Genentech). The following secondary

antibodies were used at a dilution of 1:500: Alexa 488 goat anti-guinea pig IgG, Alexa 488 goat anti-mouse IgG2b, Alexa 555 goat anti-mouse IgG1, Alexa 633 goat anti-rabbit IgG. To visualize nuclei, DAPI (Invitrogen) was incubated for 5 min at a dilution of 1:30,000. Cells were imaged using a Leica Upright SP5X White Light Laser Confocal Microscope. Images were processed using Adobe Photoshop and Illustrator.

Chick in ovo neural tube electroporations and immunostaining

Electroporations were performed as previously described (Allen et al., 2011). In brief, DNA (1.0 μg/μl) was injected into the neural tubes of Hamburger-Hamilton stage 10-12 chicken embryos with 50 ng/μl Fast Green. Embryos were dissected after 48 hours and fixed in 4% PFA for immunofluorescent analysis. The following antibodies were used for neural tube immunostaining: mouse IgG1 anti-NKX6.1 [1:20, Developmental Studies Hybridoma Bank (DSHB)], mouse IgG1 anti-PAX7 (1:20, DSHB), mouse IgG2b anti-NKX2.2 (1:20, DSHB). Nuclei were visualized using DAPI (1:30,000, Molecular Probes). Alexa 555 secondary antibodies (1:500, Molecular Probes) were visualized on a Leica Upright SP5X Light Laser Confocal Microscope. Images were processed using Adobe Photoshop and Illustrator.

2.6 Acknowledgements

This chapter has been published in *Journal of Cell Science* (See citation below) and has been included in this dissertation with permission from the journal editors.

Brandon S. Carpenter, Renee L. Barry, Kristen J. Verhey, and Benjamin L. Allen. 2015. The Heterotrimeric Kinesin-2 Complex Interacts with and Regulates GLI Protein Function. *Journal of Cell Science*. 128:1034-1050. doi:10.1242/jcs.162552.

We thank Drs. S. Scales (Genentech) and J. Eggenschwiler (University of Georgia) for sharing anti-GLI3 and anti-GLI2 antibodies, respectively. We are grateful to Drs. B. Yoder (University of Alabama-Birmingham) and A. Dlugosz (University of Michigan) for the full-length *Gli* constructs. We also thank Dr. K. Barald (University of Michigan) for providing the *Zic1* construct. We are especially grateful to Dr. B. Tsai and members of his lab for critical technical assistance. We thank members of the Allen lab for insightful comments and helpful suggestions. The NKX2.2 and NKX6.1 antibodies were obtained from the Developmental Studies Hybridoma Bank developed under the auspices of the NICHD and maintained by The University of Iowa, Department of Biological Sciences, Iowa City, IA. Confocal microscopy was performed in the Microscopy and Image Analysis Laboratory at the University of Michigan. This work was supported by The University of Michigan Center for Organogenesis, an American Heart Association scientist development grant (11SDG6380000) and by NIH grants (R21 CA167122 and R01 DC014428) to B.L.A.

2.7 Author contributions

B.S.C. and B.L.A. conceived and designed the experiments. B.S.C. executed the experiments and collected the data. R.L.B. assisted in executing the immunoprecipitation experiments involving KAP3B. B.S.C. and B.L.A. analyzed and interpreted the data. K.J.V. provided kinesin-2 and KAP3 constructs, as well as technical advice, experimental suggestions and aided with manuscript preparation and editing. B.S.C. and B.L.A. wrote and edited the manuscript.

2.8 Figures

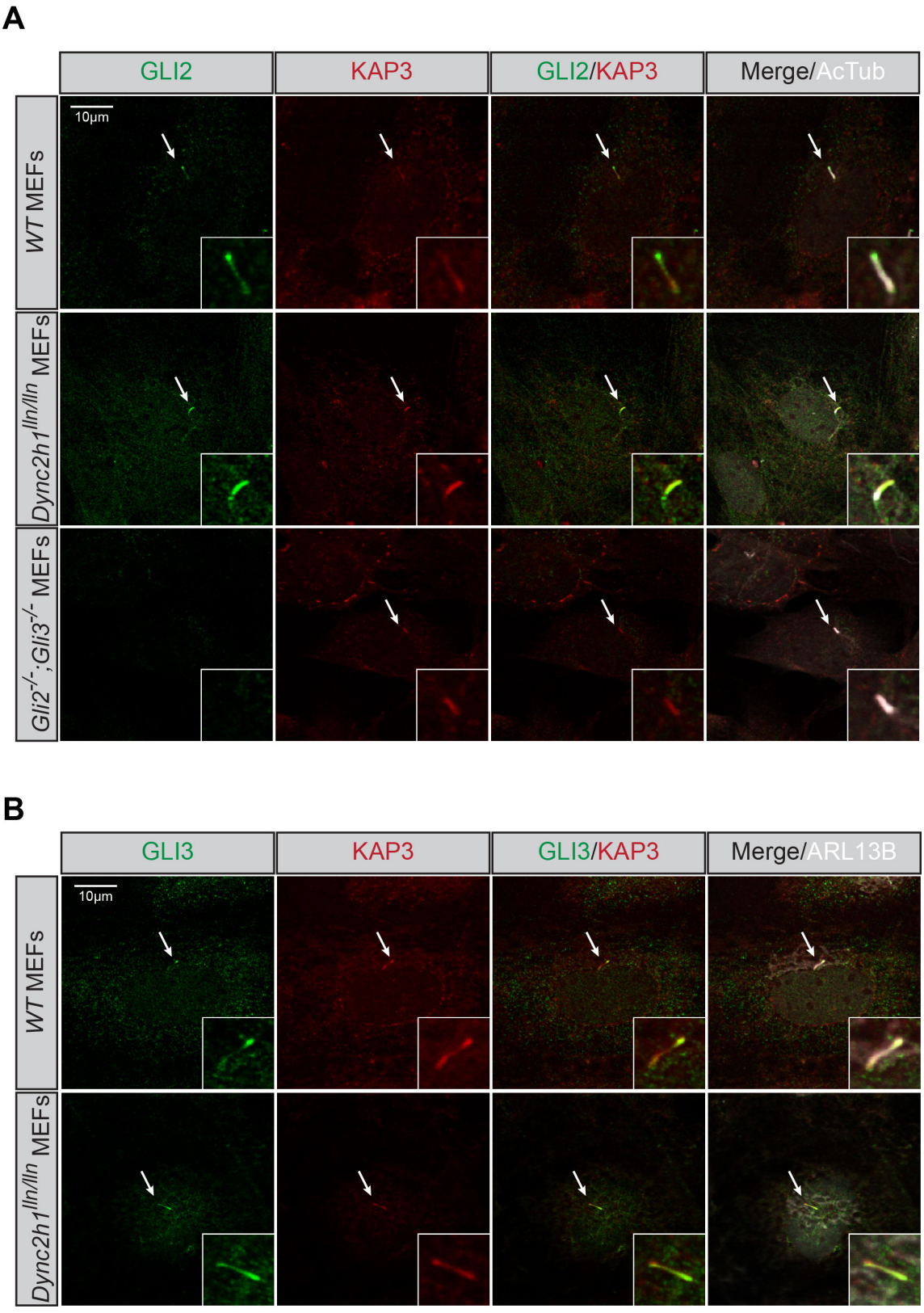
A
GLI2
KAP3
GLI2/KAP3
Merge/AcTub
10μm
WT MEFs
Dync2h1lln/lln MEFs
Gli2-/-;Gli3-/- MEFs
B
GLI3
KAP3
GLI3/KAP3
Merge/ARL13B
10μm
WT MEFs
Dync2h1lln/lln MEFs

Figure 2.1. Endogenous KAP3 and GLI proteins localize to primary cilia.
(A) Antibody detection of endogenous GLI2 (green) and KAP3 (red) in wild-type (top row), *Dync2h1*$^{lln/lln}$ (middle row), or *Gli2*$^{-/-}$;*Gli3*$^{-/-}$ MEFs (bottom row). Primary cilia are identified with antibodies against acetylated tubulin (AcTub; grey). (B) Antibody detection of endogenous GLI3 (green) and KAP3 (red) in wild-type (top row) and *Dync2h1*$^{lln/lln}$ (middle row) MEFs (bottom row). Primary cilia are identified with antibodies against ARL13B (ARL13B; grey). Scale bar, 10 μm. Arrows denote localization of KAP3A and GLI2 or GLI3 in primary cilia.

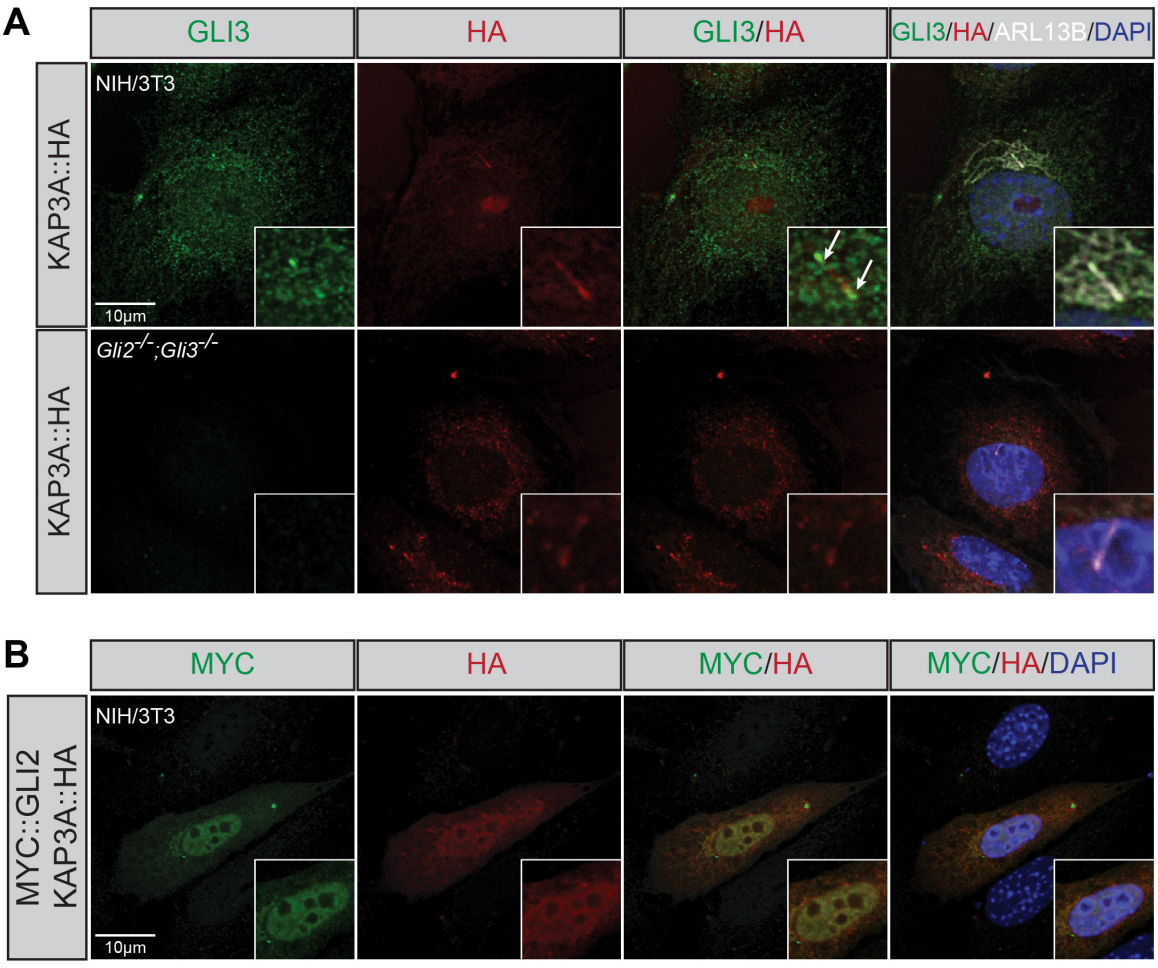

Figure 2.2. KAP3A co-localizes with mammalian GLI proteins.
(A) Antibody detection of endogenous GLI3 in NIH/3T3 cells (top row; green) or Gli2-/-;Gli3-/- MEFs (bottom row; green) expressing HA-tagged KAP3A (KAP3::HA). Primary cilia are identified using antibodies directed against ARL13B (ARL13B; grey). DAPI denotes nuclei (blue). Insets represent high magnification images of primary cilia. Scale bar, 10μm. (B) Antibody detection of MYC::GLI2 (green) and KAP3A::HA (red) in NIH/3T3 cells. DAPI (blue) identifies nuclei. Scale bar, 10μm.

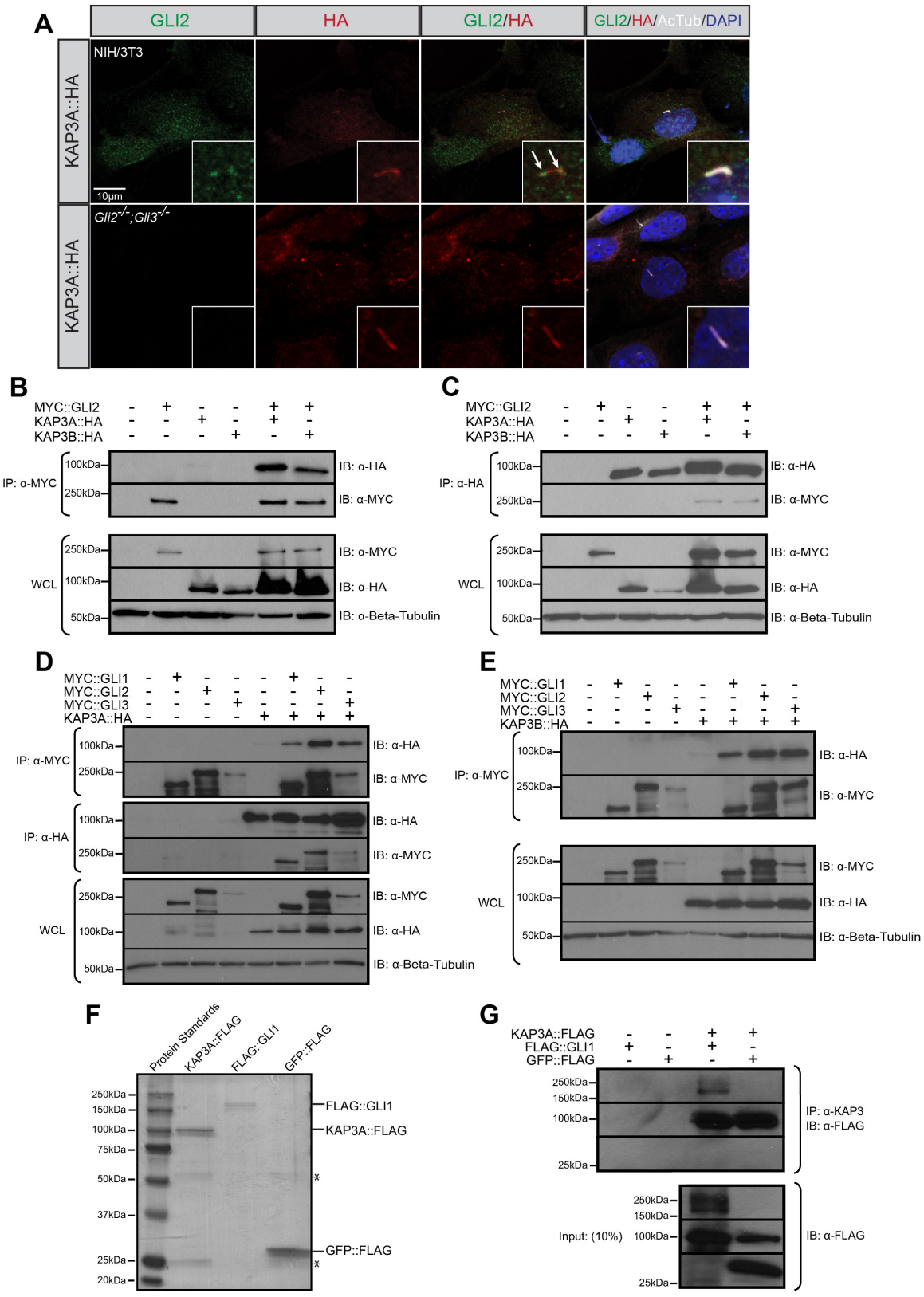
A
GLI2
HA
GLI2/HA
GLI2/HA/AcTub/DAPI
KAP3A::HA
NIH/3T3
10μm
Gli2-/-;Gli3-/-
B
MYC::GLI2
KAP3A::HA
KAP3B::HA
IP: α-MYC
IB: α-HA
IB: α-MYC
WCL
IB: α-Beta-Tubulin
C
IP: α-HA
D
MYC::GLI1
MYC::GLI2
MYC::GLI3
E
F
Protein Standards
KAP3A::FLAG
FLAG::GLI1
GFP::FLAG
FLAG::GLI1
KAP3A::FLAG
GFP::FLAG
G
IP: α-KAP3
IB: α-FLAG
Input: (10%)

Figure 2.3. KAP3 localizes and interacts with mammalian GLI proteins.
(A) Antibody detection of endogenous GLI2 in NIH/3T3 cells (top row; green) or *Gli2*$^{-/-}$;*Gli3*$^{-/-}$ MEFs (bottom row; green) expressing HA-tagged KAP3A (KAP3::HA; red). Primary cilia are identified using antibodies directed against acetylated tubulin (AcTub; grey). DAPI denotes nuclei (blue). Insets represent high magnification images of primary cilia. Scale bar, 10 μm. Arrows denote co-localization of KAP3A and GLI2 in primary cilia. (B) Immunoprecipitation of MYC-tagged GLI2 (MYC::GLI2) from COS-7 cells expressing either HA-tagged KAP3A (KAP3A::HA) or KAP3B (KAP3B::HA). (C) Immunoprecipitation of KAP3A::HA or KAP3B::HA from COS-7 cells co-expressing MYC::GLI2. (D) Immunoprecipitation of MYC::GLI1-3 or KAP3A::HA from COS-7 cells co-expressing MYC::GLI1-3 and/or KAP3A::HA. (E) Immunoprecipitation of MYC::GLI1-3 from COS-7 cells co-expressing MYC::GLI1-3, and/or KAP3B::HA. Immunoprecipitates (IP) and whole cell lysates (WCL) were subjected to SDS-PAGE and western blot analysis (IB) using antibodies directed against MYC (α-MYC) and HA (α-HA). Antibody detection of Beta-Tubulin (α-Beta-Tubulin) was used to confirm equal loading across lanes. (F) Gel Code Blue detection of affinity purified KAP3A::FLAG, FLAG::GLI1, and GFP::FLAG from COS-7 cell lysates. Asterisks (*) denote FLAG antibody heavy and light chains eluted from the FLAG agarose beads. (G) Immunoprecipitation (top blots) of purified KAP3A::FLAG using an endogenous KAP3 antibody (IP: α-KAP3) followed by western blot analysis with anti-FLAG antibody (IB: α-FLAG) to detect KAP3A::FLAG, FLAG::GLI1 or GFP::FLAG. 10% of the inputs (bottom blots) were visualized by western blot analysis to confirm equal protein levels. The molecular weights (in kDa) of protein standards are indicated at the left of each blot.

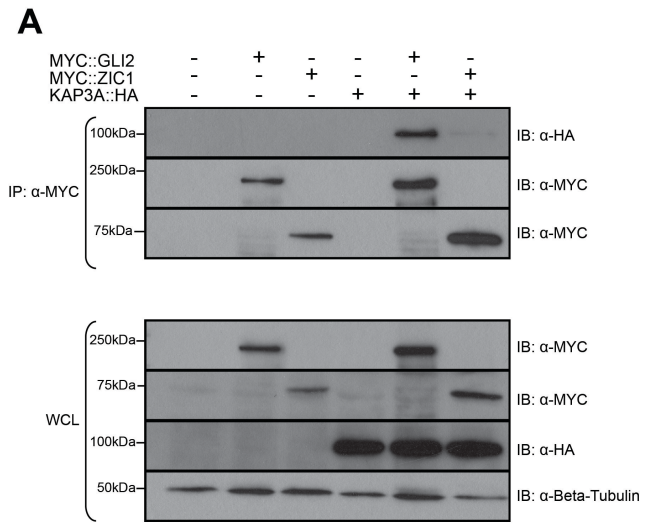

Figure 2.4. KAP3A does not interact with ZIC1.
(A) Immunoprecipitation of MYC-tagged GLI2 (MYC::GLI2) or MYC-tagged ZIC1 (MYC::ZIC1) from COS-7 cells expressing HA-tagged KAP3A (KAP3A::HA). Immunoprecipitates (IP) and whole cell lysates (WCL) were subjected to SDS-PAGE and western blot analysis (IB) using antibodies directed against MYC (α-MYC) and HA (α-HA).

Antibody detection of Beta-Tubulin (α-Beta-Tubulin) was used to confirm equal loading across lanes. The molecular weights (in kDa) of protein standards are indicated at the left of each blot.

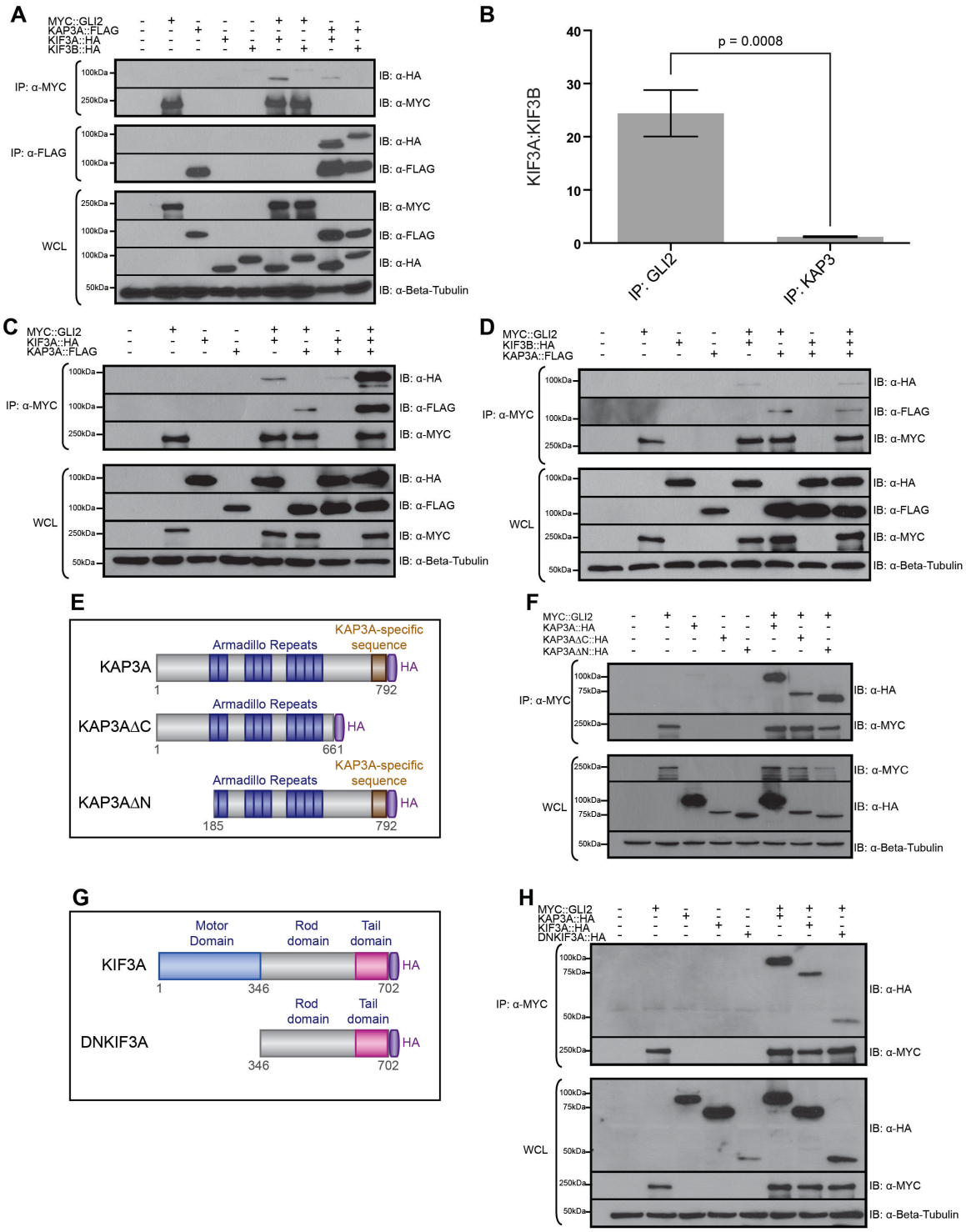

Figure 2.5. GLI2 selectively interacts with kinesin-2 motors and synergistically binds the tail domain of KIF3A and the armadillo repeats of KAP3A. (A) Immunoprecipitation of MYC::GLI2 or KAP3A::FLAG from COS-7 cells expressing KIF3A::HA or KIF3B::HA. (B) Quantitation of the ratio of KIF3A:KIF3B that co-precipitates with either MYC::GLI2 or KAP3A::FLAG. Error bars represent the mean +/- S.D. of the band densities from three separate experiments; a p-value of 0.0008 indicates a significant difference in the KIF3A:KIF3B ratio that co-precipitates with MYC::GLI2 compared to KAP3A::FLAG (Student's unpaired t-test). (C) Immunoprecipitation of MYC::GLI2 from COS-7cells expressing KIF3A::HA and/or KAP3A::FLAG. (D) Immunoprecipitation of MYC::GLI2 from COS-7 cells expressing KIF3B::HA and/or KAP3A::FLAG. Immunoprecipitates (IP) and whole cell lysates (WCL) were subjected to SDS-PAGE and western blot analysis (IB) using antibodies directed against MYC (α-MYC) and HA (α-HA). Antibody detection of Beta-Tubulin (α-Beta-Tubulin) was used to confirm equal loading across lanes. (E) Graphic representation of full-length and truncated human KAP3A proteins. KAP3A contains highly conserved armadillo repeats (dark blue), a KAP3A-specific sequence (gold), and an HA-tag at the C-terminus (purple). (F) Immunoprecipitation of MYC::GLI2 from COS-7 cells expressing KAP3A::HA, KAP3AΔC::HA, or KAP3AΔN::HA. (G) Graphic representation of full-length and truncated human KIF3A proteins. KIF3A contains a highly conserved motor domain (blue), a rod domain (grey), a cargo-binding tail domain (pink), and an HA-tag at the C-terminus (purple). (H) Immunoprecipitation of MYC::GLI2 from COS-7 cells expressing KAP3A::HA, KIF3A::HA, or DNKIF3A::HA. Immunoprecipitates (IP) and whole cell lysates (WCL) were subjected to SDS-PAGE and western blot analysis (IB) using antibodies directed against MYC (α-MYC) and HA (α-HA). Antibody detection of Beta-Tubulin (α-Beta-Tubulin) was used to confirm equal loading across lanes. The molecular weights (in kDa) of protein standards are indicated at the left of each blot.

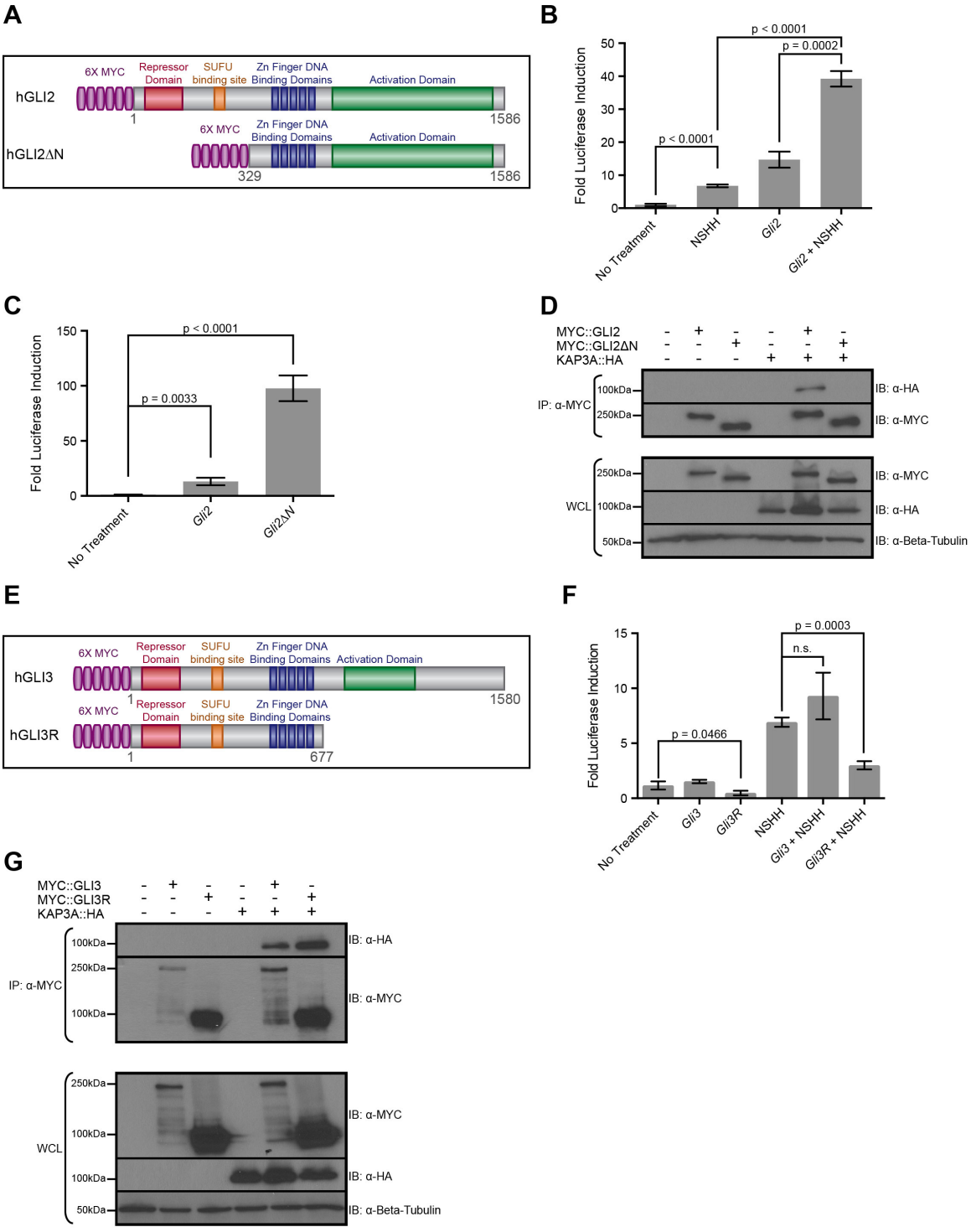

Figure 2.6. The N-termini of GLI2 and GLI3 interact with KAP3A.
(A) Graphic representation of full-length and truncated human GLI2 proteins. A 6X MYC epitope tag (purple) is present at the N-terminus of each GLI2 protein. Highly conserved GLI2 protein sequences include a transcriptional repressor domain (red, absent from hGLI2ΔN), SUFU binding site (orange, absent from hGLI2ΔN), five zinc-finger DNA binding domains (dark blue), phosphorylation cluster (light blue) and a transcriptional activation domain (green). (B)

Luciferase activity readout of HH signaling following treatment of NIH/3T3 fibroblasts with NSHH after transfection with either empty vector (No Treatment) or *Gli2*-pCDNA3 (*Gli2*). HH pathway activity is measured as fold luciferase induction. Error bars represent the mean +/- S.D. for triplicate samples from a single experiment and are representative of three independent experiments; p-values are indicated above the relevant treatment groups (Student's unpaired *t*-test). (C) Comparison of HH pathway activity in NIH/3T3 cells expressing hGLI2 or hGLI2ΔN. (D) Immunoprecipitation of MYC::GLI2 or MYC::GLI2ΔN from COS-7 cells co-expressing KAP3A::HA. Immunoprecipitates (IP) and whole cell lysates (WCL) were subjected to SDS-PAGE and western blot analysis (IB) using antibodies directed against MYC (α-MYC) and HA (α-HA). Antibody detection of Beta-Tubulin (α-Beta-Tubulin) was used to confirm equal loading across lanes. The molecular weights (in kDa) of protein standards are indicated at the left of each blot. (E) Graphic representation of full-length and truncated human GLI3 proteins. (F) Luciferase activity readout of HH signaling following treatment of NIH/3T3 fibroblasts with NSHH after transfection with either empty vector (No Treatment), *Gli3*-pCDNA3 (*Gli3*), or *Gli3R*-pCDNA3 (*Gli3R*). HH pathway activity is measured as fold luciferase induction. Error bars represent the mean +/- S.D. for triplicate samples in a single experiment and are representative of three independent experiments; p-values are indicated above the relevant treatment groups (Student's unpaired *t*-test). n.s., not significant ($p>0.05$). (G) Immunoprecipitation of MYC::GLI3 or MYC::GLI3R from COS-7 cells co-expressing KAP3A::HA.

A

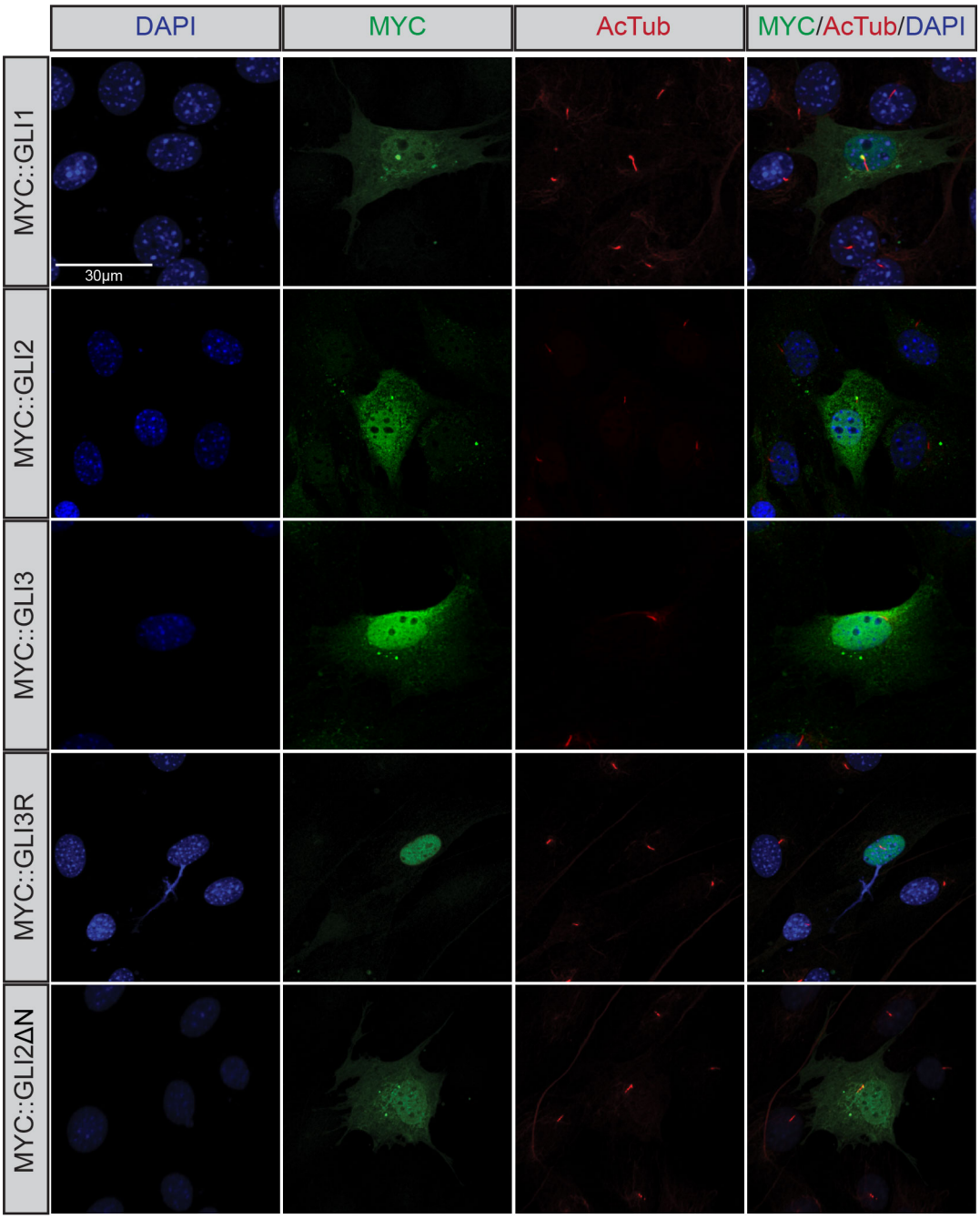

B

	Nuclear	Cytoplasm	Cilia
GLI1	17/20	20/20	12/20
GLI2	18/20	17/20	11/20
GLI3	20/20	11/20	2/20
GLI3R	20/20	1/20	0/20
GLI2ΔN	20/20	20/20	9/20

Figure 2.7. Subcellular localization of MYC-tagged GLI constructs in NIH/3T3 cells.
(A) Localization of MYC::GLI1, MYC::GLI2, MYC::GLI3, MYC::GLI3R, and MYC::GLI2ΔN in NIH/3T3 cells (green). Primary cilia are identified using antibodies directed against acetylated tubulin (AcTub; grey). DAPI denotes nuclei (blue). (B) Summary of subcellular localization of MYC-tagged GLI constructs (N=20 cells). Scale bar, 30μm.

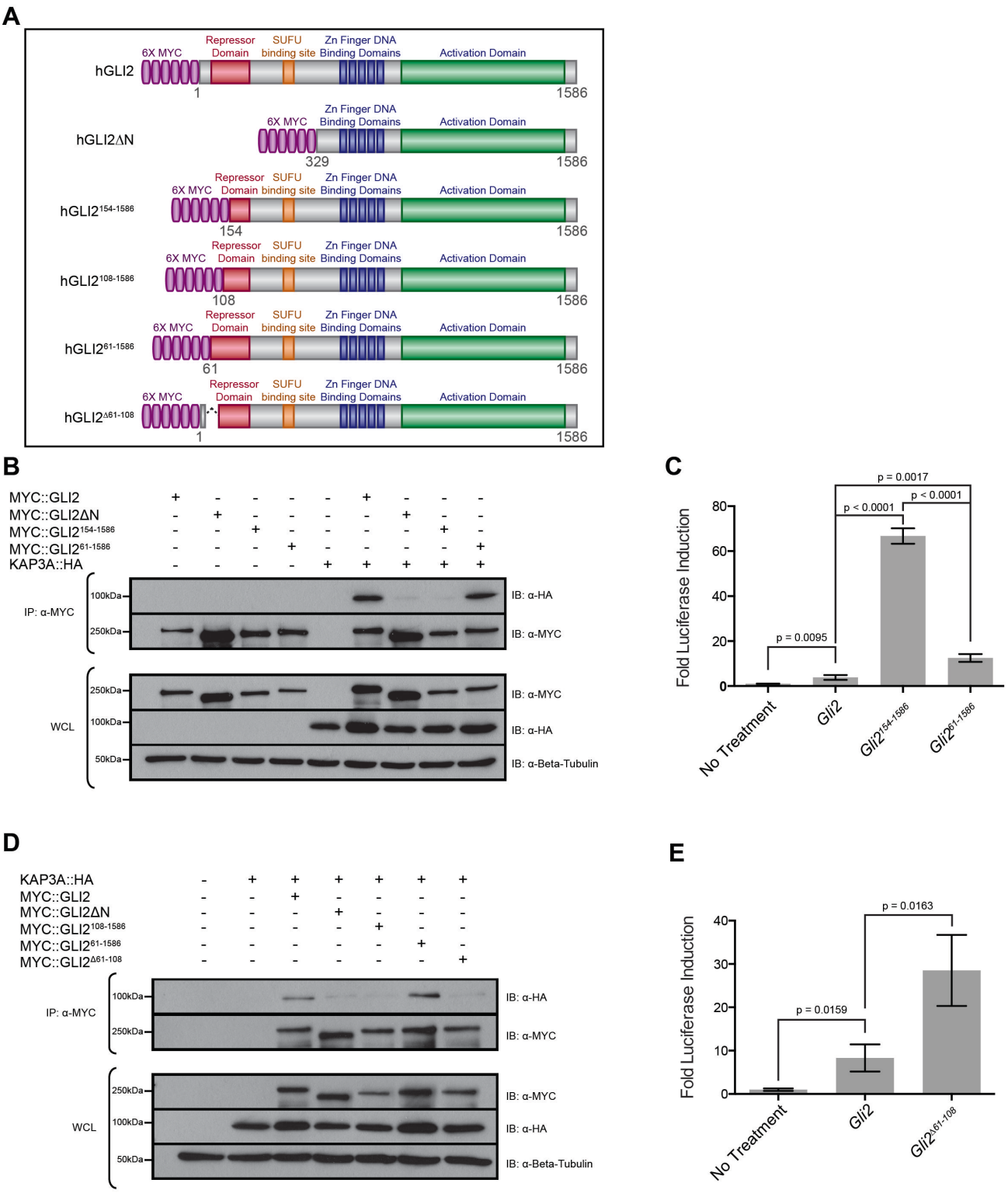
A
6X MYC
Repressor Domain
SUFU binding site
Zn Finger DNA Binding Domains
Activation Domain
hGLI2
1
1586
hGLI2ΔN
329
hGLI2154-1586
154
hGLI2108-1586
108
hGLI261-1586
61
hGLI2Δ61-108
B
MYC::GLI2
MYC::GLI2ΔN
MYC::GLI2154-1586
MYC::GLI261-1586
KAP3A::HA
IP: α-MYC
100kDa
250kDa
IB: α-HA
IB: α-MYC
WCL
50kDa
IB: α-Beta-Tubulin
C
Fold Luciferase Induction
p = 0.0017
p < 0.0001
p < 0.0001
p = 0.0095
No Treatment
Gli2
Gli2154-1586
Gli261-1586
D
KAP3A::HA
MYC::GLI2
MYC::GLI2ΔN
MYC::GLI2108-1586
MYC::GLI261-1586
MYC::GLI2Δ61-108
E
Fold Luciferase Induction
p = 0.0163
p = 0.0159
No Treatment
Gli2
Gli2Δ61-108

Figure 2.8. GLI2 interacts with KAP3A via an N-terminal domain that restricts GLI2 function.(A) Graphic representation of full-length and truncated human GLI2 proteins. (B) Immunoprecipitation of MYC::GLI2, MYC::GLI2ΔN, MYC::GLI2$^{154\text{-}1586}$ or MYC::GLI2$^{61\text{-}1586}$ from COS-7 cells expressing KAP3A::HA. (C) Luciferase activity readout of HH signaling after transfection with either empty vector (No Treatment), *Gli2*, *Gli2*$^{154\text{-}1586}$ or *Gli2*$^{61\text{-}1586}$. HH pathway activity is measured as fold luciferase induction. Error bars represent the mean +/- S.D. for triplicate samples in a single experiment and are representative of three independent experiments; p-values are indicated above the relevant treatment groups (Student's unpaired *t*-test). (D) Immunoprecipitation of MYC::GLI2, MYC::GLI2ΔN, MYC::GLI2$^{108\text{-}1586}$, MYC::GLI2$^{61\text{-}1586}$, or GLI2 $^{\Delta\ 61\text{-}108}$ from COS-7 cells expressing KAP3A::HA. Immunoprecipitates (IP) and whole cell lysates (WCL) were subjected to SDS-PAGE and western blot analysis (IB) using antibodies directed against MYC (α-MYC) and HA (α-HA). Antibody detection of Beta-Tubulin (α-Beta-Tubulin) was used to confirm equal loading across lanes. The molecular weights (in kDa) of protein standards are indicated at the left of each blot. (E) Comparison of full-length GLI2 and GLI2$^{\Delta 61\text{-}108}$ activity in HH-responsive NIH/3T3 cells.

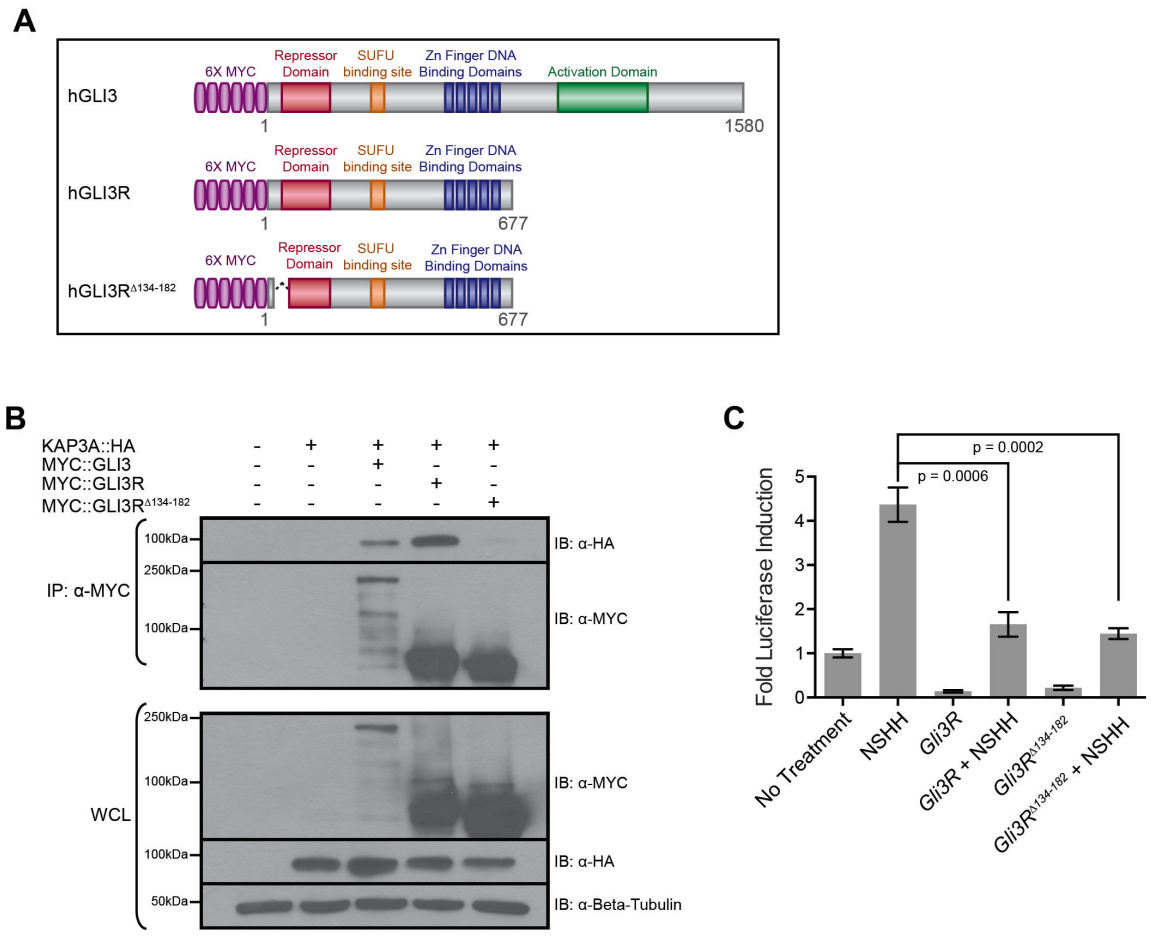

Figure 2.9. KAP3A interacts with an N-terminal GLI3 domain that does not alter GLI repressor function. (A) Graphic representation of full-length and truncated human GLI3 proteins. (B) Immunoprecipitation of MYC::GLI3, MYC::GLI3R, or MYC::GLI3RΔ134-182 from COS-7 cells expressing KAP3A::HA. (C) Luciferase activity readout of HH signaling after transfection with either empty vector (No Treatment), *Gli3R* or $Gli3^{\Delta 134\text{-}182}$. HH pathway activity is measured as fold luciferase induction. Error bars represent the mean +/- S.D. for triplicate samples in a single experiment and are representative of three independent experiments; p-values are indicated above the relevant treatment groups (Student's unpaired t-test).

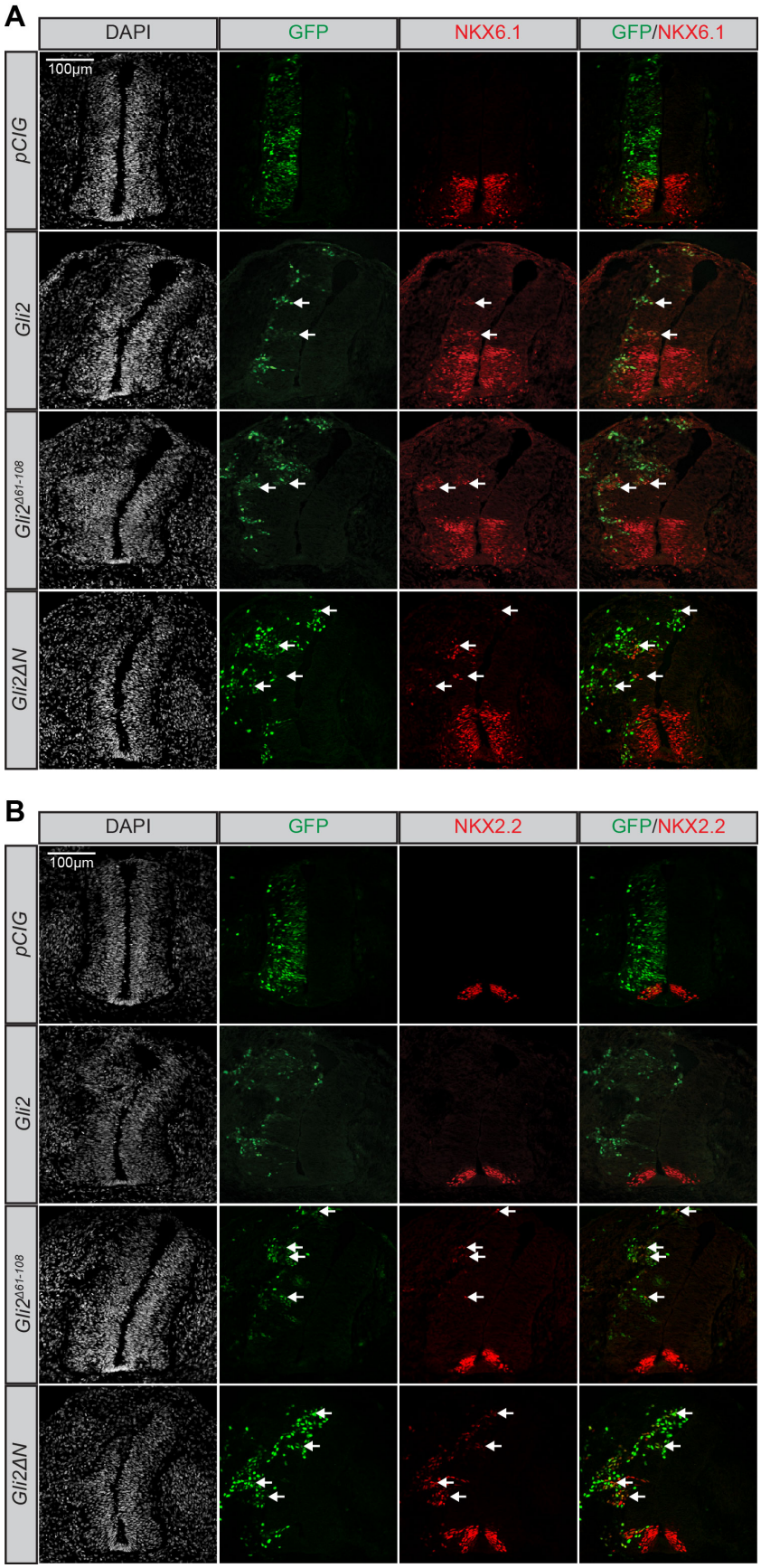
A
DAPI
GFP
NKX6.1
GFP/NKX6.1
100μm
pCIG
Gli2
Gli2Δ61-108
Gli2ΔN
B
DAPI
GFP
NKX2.2
GFP/NKX2.2
100μm
pCIG
Gli2
Gli2Δ61-108
Gli2ΔN

Figure 2.10. KAP3 binding restricts GLI2 activity in vivo.
(A) Transverse sections of Hamburger-Hamilton stage 21-22 chicken neural tubes electroporated with *pCIG* (top row), *Gli2* (upper row), *Gli2Δ61-108* (lower row), or *Gli2ΔN* (bottom row) were stained with antibodies raised against NKX6.1 (red). GFP expressing cells (green) denote electroporated cells. DAPI marks nuclei. Arrows indicate ectopic expression of NKX6.1. (B) Transverse sections of Hamburger-Hamilton stage 21-22 chicken neural tubes stained with antibodies raised against NKX2.2 (red). GFP expressing cells (green) denote electroporated cells. DAPI marks nuclei. Arrows indicate ectopic NKX2.2 expression. Scale bar, 100μm

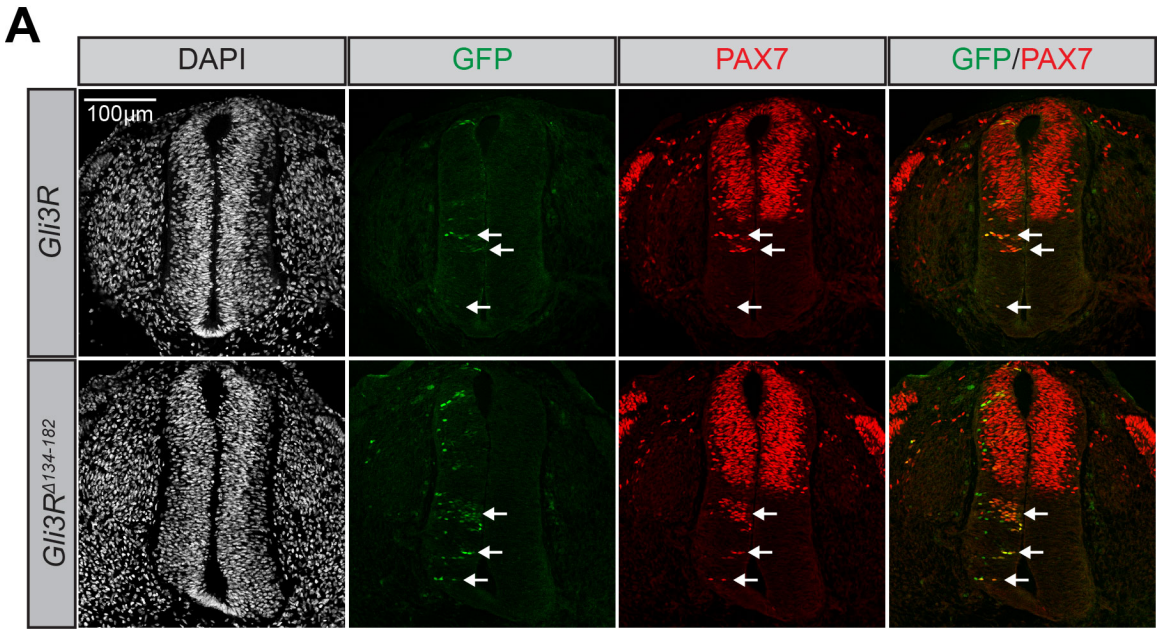

Figure 2.11. KAP3 binding does not alter GLI3R activity in vivo.
(A) Transverse sections of Hamburger-Hamilton stage 21-22 chicken neural tubes electroporated with Gli3R (top row) or Gli3Δ134-182 (bottom row) stained with antibodies raised against PAX7 (red). GFP expressing cells (green) denote electroporated cells. DAPI marks nuclei. Arrows indicate ectopic PAX7 expression. Scale bar, 100μm.

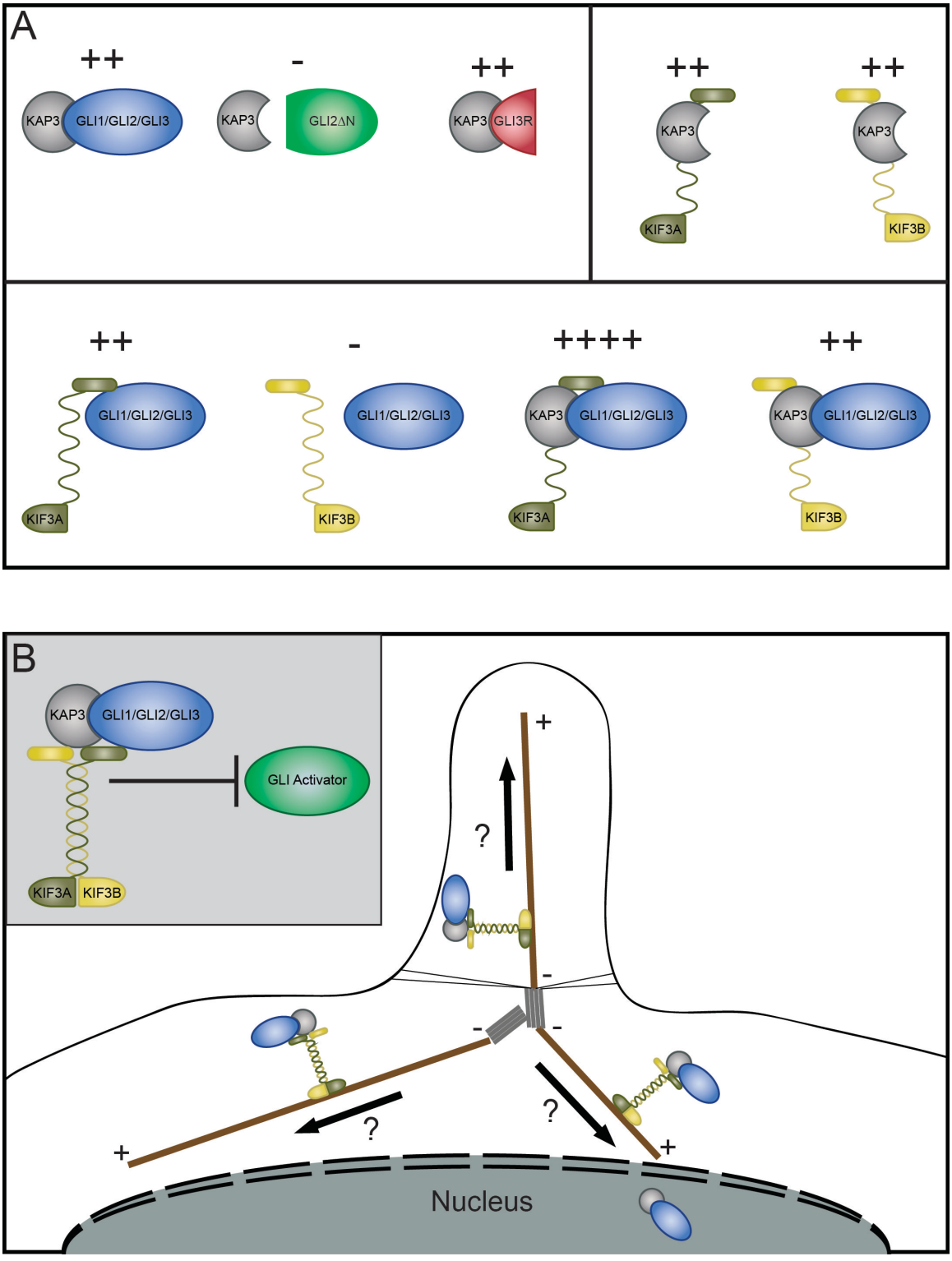

Figure 2.12. Model of GLI/kinesin-2 complex interactions and subcellular localization. (A) Schematic summary of biochemical interactions between GLI proteins (blue), KAP3 (grey), KIF3A (dark green), and KIF3B (yellow). Truncated versions of GLI proteins, GLI2ΔN and GLI3R, are represented in light green and red, respectively. Plus (+) and minus (-) represent the relative strength of interaction based on the immunoprecipitation studies with (-) indicating no

interaction and (++++) denoting the strongest interaction. (B) Graphic representation of the functional consequence of the KAP3-GLI interaction on GLI activator (green) and subcellular localization of the GLI (blue)/KAP3 (grey)/KIF3A (dark green)/ KIF3B (yellow) complex. The primary cilium is represented by microtubules (brown) extending from basal bodies (grey) with the ciliary barrier depicted by thin black lines. Plus (+) and minus (-) depict microtubule directionality. Question marks denote putative plus-end trafficking roles for KIF3A/KIF3B/KAP3 in regulating GLI proteins based on biochemical, immunofluorescence and signaling studies.

2.9 References

Allen, B.L., J.Y. Song, L. Izzi, I.W. Althaus, J.-S. Kang, F. Charron, R.S. Krauss, and A.P. McMahon. 2011. Overlapping Roles and Collective Requirement for the Coreceptors GAS1, CDO, and BOC in SHH Pathway Function. *Developmental Cell*. 20:775–787. doi:10.1016/j.devcel.2011.04.018.

Altaba, A.R.I. 1999. Gli proteins encode context-dependent positive and negative functions: implications for development and disease. *Development*.

Aza-Blanc, P., H.Y. Lin, A. Ruiz i Altaba, and T.B. Kornberg. 2000. Expression of the vertebrate Gli proteins in Drosophila reveals a distribution of activator and repressor activities. *Development*. 127:4293–4301.

Bai, C.B., and A.L. Joyner. 2001. Gli1 can rescue the in vivo function of Gli2. *Development*. 128:5161–5172.

Bai, C.B., D. Stephen, and A.L. Joyner. 2004. All mouse ventral spinal cord patterning by hedgehog is Gli dependent and involves an activator function of Gli3. *Developmental Cell*. 6:103–115.

Bai, C.B., W. Auerbach, J.S. Lee, D. Stephen, and A.L. Joyner. 2002. Gli2, but not Gli1, is required for initial Shh signaling and ectopic activation of the Shh pathway. *Development*.

Baldari, C.T., and J. Rosenbaum. 2010. Intraflagellar transport: it's not just for cilia anymore. *Current opinion in cell biology*.

Barnfield, P.C., X. Zhang, V. Thanabalasingham, M. Yoshida, and C.-C. Hui. 2005. Negative regulation of Gli1 and Gli2 activator function by Suppressor of fused through multiple mechanisms. *Differentiation*. 73:397–405. doi:10.1111/j.1432-0436.2005.00042.x.

Bhogaraju, S., B.D. Engel, and E. Lorentzen. 2013. Intraflagellar transport complex structure and cargo interactions. *Cilia*. 2:10. doi:10.1186/2046-2530-2-10.

Briscoe, J., and P.P. Thérond. 2013. The mechanisms of Hedgehog signalling and its roles in development and disease. *Nat Rev Mol Cell Biol*.

Brown, C.L., K.C. Maier, T. Stauber, L.M. Ginkel, L. Wordeman, I. Vernos, and T.A. Schroer. 2005. Kinesin-2 is a motor for late endosomes and lysosomes. *Traffic*. 6:1114–1124. doi:10.1111/j.1600-0854.2005.00347.x.

Chen, C.H., D.P. von Kessler, W. Park, B. Wang, Y. Ma, and P.A. Beachy. 1999. Nuclear trafficking of Cubitus interruptus in the transcriptional regulation of Hedgehog target gene expression. *Cell*. 98:305–316.

Cheung, H.O.-L., X. Zhang, A. Ribeiro, R. Mo, S. Makino, V. Puviindran, K.K.L. Law, J. Briscoe, and C.-C. Hui. 2009. The Kinesin Protein Kif7 Is a Critical Regulator of Gli Transcription Factors in Mammalian Hedgehog Signaling. *Sci Signal*. 2:ra29.

doi:10.1126/scisignal.2000405.

Cole, D.G., S.W. Chinn, K.P. Wedaman, K. Hall, and T. Vuong. 1993. Novel heterotrimeric kinesin-related protein purified from sea urchin eggs. *Nature*.

Ding, Q., J. Motoyama, S. Gasca, R. Mo, H. Sasaki, J. Rossant, and C.C. Hui. 1998. Diminished Sonic hedgehog signaling and lack of floor plate differentiation in Gli2 mutant mice.

Endoh-Yamagami, S., M. Evangelista, D. Wilson, X. Wen, J.-W. Theunissen, K. Phamluong, M. Davis, S.J. Scales, M.J. Solloway, F.J. de Sauvage, and A.S. Peterson. 2009. The Mammalian Cos2 Homolog Kif7 Plays an Essential Role in Modulating Hh Signal Transduction during Development. *Current Biology*. 19:1320–1326. doi:10.1016/j.cub.2009.06.046.

Finetti, F., S.R. Paccani, M.G. Riparbelli, and E. Giacomello. 2009. Intraflagellar transport is required for polarized recycling of the TCR/CD3 complex to the immune synapse. *Nature cell ...*.

Gindhart, J.G., and L.S. Goldstein. 1996. Armadillo repeats in the SpKAP115 subunit of kinesin-II. *Trends Cell Biol.* 6:415–416.

Goetz, S.C., and K.V. Anderson. 2010. The primary cilium: a signalling centre during vertebrate development. *Nat. Rev. Genet.* 11:331–344. doi:10.1038/nrg2774.

Hao, L., E. Efimenko, P. Swoboda, and J.M. Scholey. 2011. The retrograde IFT machinery of C. elegans cilia: two IFT dynein complexes? *PLoS ONE*. 6:e20995. doi:10.1371/journal.pone.0020995.

Haycraft, C.J., B. Banizs, Y. Aydin-Son, Q. Zhang, E.J. Michaud, and B.K. Yoder. 2005. Gli2 and Gli3 localize to cilia and require the intraflagellar transport protein polaris for processing and function. *PLoS Genet.* 1:e53. doi:10.1371/journal.pgen.0010053.

He, M., R. Subramanian, F. Bangs, T. Omelchenko, K.F. Liem Jr, T.M. Kapoor, and K.V. Anderson. 2014. The kinesin-4 protein Kif7 regulates mammalian Hedgehog signalling by organizing the cilium tip compartment. *Nat. Cell Biol.* 16:663–672. doi:doi:10.1038/ncb2988.

Hirokawa, N. 2000. Stirring up Development with the Heterotrimeric Kinesin KIF3. *Traffic*. 1:29–34. doi:10.1034/j.1600-0854.2000.010105.x.

Hirokawa, N., Y. Noda, Y. Tanaka, and S. Niwa. 2009. Kinesin superfamily motor proteins and intracellular transport. *Nat Rev Mol Cell Biol*. 10:682–696. doi:10.1038/nrm2774.

Hsu, S.-H.C., X. Zhang, C. Yu, Z.J. Li, J.S. Wunder, C.-C. Hui, and B.A. Alman. 2011. Kif7 promotes hedgehog signaling in growth plate chondrocytes by restricting the inhibitory function of Sufu. *Development*. 138:3791–3801. doi:10.1242/dev.069492.

Huang, C.-J., C.-C. Huang, and C.-C. Chang. 2011. Association of the testis-specific

TRIM/RBCC protein RNF33/TRIM60 with the cytoplasmic motor proteins KIF3A and KIF3B. *Mol Cell Biochem*. 360:121–131. doi:10.1007/s11010-011-1050-8.

Huangfu, D., A. Liu, A.S. Rakeman, N.S. Murcia, L. Niswander, and K.V. Anderson. 2003. Hedgehog signalling in the mouse requires intraflagellar transport proteins. *Nature*. 426:83–87. doi:10.1038/nature02061.

Hui, C.-C., and S. Angers. 2011. Gli Proteins in Development and Disease. *Annu. Rev. Cell Dev. Biol.* 27:513–537. doi:10.1146/annurev-cellbio-092910-154048.

Insinna, C., N. Pathak, B. Perkins, and I. Drummond. 2008. The homodimeric kinesin, Kif17, is essential for vertebrate photoreceptor sensory outer segment development. *Developmental …*.

Jimbo, T., Y. Kawasaki, R. Koyama, R. Sato, S. Takada, K. Haraguchi, and T. Akiyama. 2002. Identification of a link between the tumour suppressor APC and the kinesin superfamily. *Nat. Cell Biol.* 4:323–327. doi:10.1038/ncb779.

Keady, B.T., R. Samtani, K. Tobita, M. Tsuchya, J.T. San Agustin, J.A. Follit, J.A. Jonassen, R. Subramanian, C.W. Lo, and G.J. Pazour. 2012. IFT25 Links the Signal-Dependent Movement of Hedgehog Components to Intraflagellar Transport. *Developmental Cell*. 22:940–951. doi:10.1016/j.devcel.2012.04.009.

Kim, J., M. Kato, and P.A. Beachy. 2009. Gli2 trafficking links Hedgehog-dependent activation of Smoothened in the primary cilium to transcriptional activation in the nucleus. *Proc. Natl. Acad. Sci. U.S.A.* 106:21666–21671. doi:10.1073/pnas.0912180106.

Kogerman, P., T. Grimm, L. Kogerman, D. Krause, A.B. Undén, B. Sandstedt, R. Toftgård, and P.G. Zaphiropoulos. 1999. Mammalian suppressor-of-fused modulates nuclear-cytoplasmic shuttling of Gli-1. *Nat. Cell Biol.* 1:312–319. doi:10.1038/13031.

Li, Z.J., E. Nieuwenhuis, W. Nien, X. Zhang, J. Zhang, V. Puviindran, B.J. Wainwright, P.C.W. Kim, and C.-C. Hui. 2012. Kif7 regulates Gli2 through Sufu-dependent and -independent functions during skin development and tumorigenesis. *Development*. 139:4152–4161. doi:10.1242/dev.081190.

Liem, K.F., M. He, P.J.R. Ocbina, and K.V. Anderson. 2009. Mouse Kif7/Costal2 is a cilia-associated protein that regulates Sonic hedgehog signaling. *Proc. Natl. Acad. Sci. U.S.A.* 106:13377–13382. doi:10.1073/pnas.0906944106.

Liu, A., B. Wang, and L.A. Niswander. 2005. Mouse intraflagellar transport proteins regulate both the activator and repressor functions of Gli transcription factors. *Development*. 132:3103–3111. doi:10.1242/dev.01894.

Liu, Y.C., A.L. Couzens, A.R. Deshwar, L.D. B McBroom-Cerajewski, X. Zhang, V. Puviindran, I.C. Scott, A.-C. Gingras, C.-C. Hui, and S. Angers. 2014. The PPFIA1-PP2A protein complex promotes trafficking of Kif7 to the ciliary tip and Hedgehog signaling. *Sci Signal*. 7:ra117. doi:10.1126/scisignal.2005608.

Marigo, V., R.A. Davey, Y. Zuo, and J.M. Cunningham. 1996. Biochemical evidence that patched is the Hedgehog receptor. ....

Marks, S.A., and D. Kalderon. 2011. Regulation of mammalian Gli proteins by Costal 2 and PKA in Drosophila reveals Hedgehog pathway conservation. *Development*. 138:2533–2542. doi:10.1242/dev.063479.

Matise, M.P., D.J. Epstein, H.L. Park, K.A. Platt, and A.L. Joyner. 1998. Gli2 is required for induction of floor plate and adjacent cells, but not most ventral neurons in the mouse central nervous system. *Development*. 125:2759–2770.

Maurya, A.K., J. Ben, Z. Zhao, R.T.H. Lee, W. Niah, A.S.M. Ng, A. Iyu, W. Yu, S. Elworthy, F.J.M. van Eeden, and P.W. Ingham. 2013. Positive and Negative Regulation of Gli Activity by Kif7 in the Zebrafish Embryo. *PLoS Genet.* 9:e1003955. doi:10.1371/journal.pgen.1003955.

McMahon, A.P., P.W. Ingham, and C.J. Tabin. 2003. Developmental roles and clinical significance of hedgehog signaling. *Curr. Top. Dev. Biol.* 53:1–114.

Megason, S.G., and A.P. McMahon. 2002. A mitogen gradient of dorsal midline Wnts organizes growth in the CNS.

Meyer, N.P., and H. Roelink. 2003. The amino-terminal region of Gli3 antagonizes the Shh response and acts in dorsoventral fate specification in the developing spinal cord. *Dev. Biol.* 257:343–355.

Morris, R.L., C.N. English, J.E. Lou, and F.J. Dufort. 2004. Redistribution of the kinesin-II subunit KAP from cilia to nuclei during the mitotic and ciliogenic cycles in sea urchin embryos. *Developmental* ....

Morsci, N.S., and M.M. Barr. 2011. Kinesin-3 KLP-6 regulates intraflagellar transport in male-specific cilia of Caenorhabditis elegans. *Curr. Biol.* 21:1239–1244. doi:10.1016/j.cub.2011.06.027.

Nonaka, S., Y. Tanaka, Y. Okada, S. Takeda, A. Harada, Y. Kanai, M. Kido, and N. Hirokawa. 1998. Randomization of left-right asymmetry due to loss of nodal cilia generating leftward flow of extraembryonic fluid in mice lacking KIF3B motor protein. *Cell*. 95:829–837.

Norman, R.X., H.W. Ko, V. Huang, C.M. Eun, L.L. Abler, Z. Zhang, X. Sun, and J.T. Eggenschwiler. 2009. Tubby-like protein 3 (TULP3) regulates patterning in the mouse embryo through inhibition of Hedgehog signaling. *Hum. Mol. Genet.* 18:1740–1754. doi:10.1093/hmg/ddp113.

Nozawa, Y.I., C. Lin, and P.-T. Chuang. 2013. Hedgehog signaling from the primary cilium to the nucleus: an emerging picture of ciliary localization, trafficking and transduction. *Curr. Opin. Genet. Dev.* 23:429–437. doi:10.1016/j.gde.2013.04.008.

Nybakken, K., S.A. Vokes, T.-Y. Lin, A.P. McMahon, and N. Perrimon. 2005. A genome-wide

RNA interference screen in Drosophila melanogaster cells for new components of the Hh signaling pathway. *Nat Genet*. 37:1323–1332. doi:10.1038/ng1682.

Ocbina, P.J.R., J.T. Eggenschwiler, I. Moskowitz, and K.V. Anderson. 2011. Complex interactions between genes controlling trafficking in primary cilia. *Nat Genet*. doi:10.1038/ng.832.

Oosterveen, T., S. Kurdija, Z. Alekseenko, C.W. Uhde, M. Bergsland, M. Sandberg, E. Andersson, J.M. Dias, J. Muhr, and J. Ericson. 2012. Mechanistic differences in the transcriptional interpretation of local and long-range Shh morphogen signaling. *Developmental Cell*. 23:1006–1019. doi:10.1016/j.devcel.2012.09.015.

Pan, Y., C.B. Bai, A.L. Joyner, and B. Wang. 2006. Sonic hedgehog signaling regulates Gli2 transcriptional activity by suppressing its processing and degradation. *Molecular and Cellular Biology*. 26:3365–3377. doi:10.1128/MCB.26.9.3365-3377.2006.

Pedersen, L.B., and J.L. Rosenbaum. 2008. Intraflagellar transport (IFT) role in ciliary assembly, resorption and signalling. *Curr. Top. Dev. Biol.* 85:23–61. doi:10.1016/S0070-2153(08)00802-8.

Peterson, K.A., Y. Nishi, W. Ma, A. Vedenko, L. Shokri, X. Zhang, M. McFarlane, J.-M. Baizabal, J.P. Junker, A. van Oudenaarden, T. Mikkelsen, B.E. Bernstein, T.L. Bailey, M.L. Bulyk, W.H. Wong, and A.P. McMahon. 2012. Neural-specific Sox2 input and differential Gli-binding affinity provide context and positional information in Shh-directed neural patterning. *Genes & Development*. 26:2802–2816. doi:10.1101/gad.207142.112.

Phang, H.-Q., J.-L. Hoon, S.-K. Lai, Y. Zeng, K.-H. Chiam, H.-Y. Li, and C.-G. Koh. 2014. POPX2 phosphatase regulates the KIF3 kinesin motor complex. *J. Cell. Sci.* 127:727–739. doi:10.1242/jcs.126482.

Qin, H., D.R. Diener, S. Geimer, D.G. Cole, and J.L. Rosenbaum. 2004. Intraflagellar transport (IFT) cargo: IFT transports flagellar precursors to the tip and turnover products to the cell body. *J. Cell Biol.* 164:255–266. doi:10.1083/jcb.200308132.

Qin, J., Y. Lin, R.X. Norman, H.W. Ko, and J.T. Eggenschwiler. 2011. Intraflagellar transport protein 122 antagonizes Sonic Hedgehog signaling and controls ciliary localization of pathway components. *Proceedings of the …*

Robbins, D.J., K.E. Nybakken, R. Kobayashi, and J.C. Sisson. 1997. Hedgehog elicits signal transduction by means of a large complex containing the kinesin-related protein costal2. *Cell*.

Roessler, E., A.N. Ermilov, D.K. Grange, A. Wang, M. Grachtchouk, A.A. Dlugosz, and M. Muenke. 2005. A previously unidentified amino-terminal domain regulates transcriptional activity of wild-type and disease-associated human GLI2. *Hum. Mol. Genet.* 14:2181–2188. doi:10.1093/hmg/ddi222.

Ruiz i Altaba, A. 2011. Hedgehog Signaling and the Gli Code in Stem Cells, Cancer, and

Metastases. *Sci Signal*. 4:pt9. doi:10.1126/scisignal.2002540.

Sasaki, H., Y. Nishizaki, C. Hui, M. Nakafuku, and H. Kondoh. 1999. Regulation of Gli2 and Gli3 activities by an amino-terminal repression domain: implication of Gli2 and Gli3 as primary mediators of Shh signaling. *Development*. 126:3915–3924.

Scholey, J.M. 2003. Intraflagellar transport. *Annu. Rev. Cell Dev. Biol.* 19:423–443. doi:10.1146/annurev.cellbio.19.111401.091318.

Scholey, J.M. 2013. Kinesin-2: A Family of Heterotrimeric and Homodimeric Motors with Diverse Intracellular Transport Functions. *Annu. Rev. Cell Dev. Biol.*

Sisson, J.C., K.S. Ho, K. Suyama, and M.P. Scott. 1997. Costal2, a novel kinesin-related protein in the Hedgehog signaling pathway. *Cell*.

Snow, J.J., G. Ou, A.L. Gunnarson, M.R.S. Walker, H.M. Zhou, I. Brust-Mascher, and J.M. Scholey. 2004. Two anterograde intraflagellar transport motors cooperate to build sensory cilia on C. elegans neurons. *Nat. Cell Biol.* 6:1109–1113. doi:10.1038/ncb1186.

Stamataki, D. 2005. A gradient of Gli activity mediates graded Sonic Hedgehog signaling in the neural tube. *Genes & Development*. 19:626–641. doi:10.1101/gad.325905.

Stone, D.M., M. Hynes, M. Armanini, T.A. Swanson, and Q. Gu. 1996. The tumour-suppressor gene patched encodes a candidate receptor for Sonic hedgehog. *Nature*.

Takeda, S., Y. Yonekawa, Y. Tanaka, Y. Okada, S. Nonaka, and N. Hirokawa. 1999. Left-right asymmetry and kinesin superfamily protein KIF3A: new insights in determination of laterality and mesoderm induction by kif3A-/- mice analysis. *J. Cell Biol.* 145:825–836.

Tanuma, N., M. Nomura, M. Ikeda, I. Kasugai, Y. Tsubaki, K. Takagaki, T. Kawamura, Y. Yamashita, I. Sato, M. Sato, R. Katakura, K. Kikuchi, and H. Shima. 2008. Protein phosphatase Dusp26 associates with KIF3 motor and promotes N-cadherin-mediated cell–cell adhesion. *Oncogene*. 28:752–761. doi:10.1038/onc.2008.431.

Teng, J., T. Rai, Y. Tanaka, Y. Takei, T. Nakata, M. Hirasawa, A.B. Kulkarni, and N. Hirokawa. 2005. The KIF3 motor transports N-cadherin and organizes the developing neuroepithelium. *Nat. Cell Biol.* 7:474–482. doi:10.1038/ncb1249.

Tukachinsky, H., L.V. Lopez, and A. Salic. 2010. A mechanism for vertebrate Hedgehog signaling: recruitment to cilia and dissociation of SuFu-Gli protein complexes. *J. Cell Biol.* 191:415–428. doi:10.1083/jcb.201004108.

Vokes, S.A., H. Ji, S. McCuine, T. Tenzen, S. Giles, S. Zhong, W.J.R. Longabaugh, E.H. Davidson, W.H. Wong, and A.P. McMahon. 2007. Genomic characterization of Gli-activator targets in sonic hedgehog-mediated neural patterning. *Development*. 134:1977–1989. doi:10.1242/dev.001966.

Wang, B., J.F. Fallon, and P.A. Beachy. 2000. Hedgehog-regulated processing of Gli3 produces

an anterior/posterior repressor gradient in the developing vertebrate limb. *Cell*. 100:423–434.

Wang, C., Y. Pan, and B. Wang. 2010. Suppressor of fused and Spop regulate the stability, processing and function of Gli2 and Gli3 full-length activators but not their repressors.

Wedaman, K.P. 1996. Sequence and submolecular localization of the 115-kD accessory subunit of the heterotrimeric kinesin-II (KRP85/95) complex. *J. Cell Biol.* 132:371–380. doi:10.1083/jcb.132.3.371.

Wen, X., C.K. Lai, M. Evangelista, J.A. Hongo, F.J. de Sauvage, and S.J. Scales. 2010. Kinetics of Hedgehog-Dependent Full-Length Gli3 Accumulation in Primary Cilia and Subsequent Degradation. *Molecular and Cellular Biology*. 30:1910–1922. doi:10.1128/MCB.01089-09.

Yamazaki, H., T. Nakata, Y. Okada, and N. Hirokawa. 1995. KIF3A/B: a heterodimeric kinesin superfamily protein that works as a microtubule plus end-directed motor for membrane organelle transport. *J. Cell Biol.* 130:1387–1399.

Yamazaki, H., T. Nakata, Y. Okada, and N. Hirokawa. 1996. Cloning and characterization of KAP3: a novel kinesin superfamily-associated protein of KIF3A/3B. *Proc. Natl. Acad. Sci. U.S.A.* 93:8443–8448.

Yang, Z., and L.S. Goldstein. 1998. Characterization of the KIF3C neural kinesin-like motor from mouse. *Mol. Biol. Cell*. 9:249–261.

Yang, Z., E.A. Roberts, and L.S. Goldstein. 2001. Functional analysis of mouse kinesin motor Kif3C. *Molecular and Cellular Biology*. 21:5306–5311. doi:10.1128/MCB.21.16.5306-5311.2001.

CHAPTER III:

Investigation of KIF17 interactions with GLI proteins and its role in regulating Hedgehog signaling

3.1 Abstract

GLI (Glioblasoma) proteins are the transcriptional effector molecules of the Hedgehog (HH) signaling pathway that function to activate and repress Hedgehog (HH) target gene expression. GLI proteins traffic between multiple subcellular compartments including the cytoplasm, nucleus, and primary cilium. Disrupting GLI intracellular trafficking results in defects in GLI protein activity; however, the mechanisms regulating GLI protein trafficking are incomplete. Kinesin-2 motor proteins regulate both ciliary and non-ciliary transport of cargo and have been implicated in HH signaling for over a decade, but how these motor complexes regulate GLI proteins directly is still unclear. In Chapter II, I identified direct interactions between heterotrimeric kinesin-2 motor complexes and GLI proteins that selectively restrict GLI activator function. Here I examine a role for the homodimeric kinesin-2 motor, KIF17, in regulating GLI activity. Using a combination of biochemical, cell signaling, and *in vivo* experimental approaches I show that KIF17 co-localizes and interacts with GLI proteins. Further, I show that GLI1 protein expression is decreased in cells stably expressing a dominant-negative version of KIF17. Finally, I provide evidence that KIF17 and GLI are expressed in overlapping cell layers

in the developing cerebellum, and that *Kif17*$^{-/-}$ mice have smaller cerebella. These data suggest a model in which KIF17 is playing a tissue specific role in regulating HH signaling through interactions with GLI proteins.

3.2 Introduction

GLI proteins are the transcriptional effector molecules of the Hedgehog (HH) signaling pathway (Hui and Angers, 2011). Among the three mammalian GLI proteins, GLI2 and GLI3 are the first responders to the HH signal. GLI2 and GLI3 both contain N-terminal repressor and C-terminal activation domains that modulate their function (Sasaki et al., 1999; Aza-Blanc et al., 2000; Stamataki, 2005). In the absence of HH signaling, GLI2 and GLI3 are proteolytically processed into N-terminal repressors that inhibit HH target gene transcription (Sasaki et al., 1999; Wang et al., 2000; Aza-Blanc et al., 2000; Stamataki, 2005). Conversely, HH ligand stimulation promotes the accumulation of full-length GLI2 and GLI3 that activate HH target gene transcription (Pan et al., 2006). Once activated, GLI2 and GLI3 induce expression of the third GLI protein family member, GLI1, which functions exclusively as a transcriptional activator that is dispensable for mammalian development (Bai et al., 2002).

GLI2 and GLI3 are indispensible for normal development and adult tissue homeostasis (reviewed by Hui and Angers, 2011). Despite the importance of GLI2 and GLI3 in embryonic development, the mechanisms regulating their protein function are incomplete. Over the past decade, several studies have shown that all mammalian GLI proteins localize to primary cilia in a regulated process and that this localization is enriched in the presence of HH signaling (Haycraft et al., 2005; Liu et al., 2005; Chen et al., 2009; Wen et al., 2010; Zeng et al., 2010). Loss of primary cilia, or mutations that prevent GLI2 and/or GLI3 proteins from trafficking to primary

cilia, cause defects in both GLI processing and activation (Haycraft et al., 2005; Liu et al., 2005; 2015; Santos and Reiter, 2014). Although an increasing body of evidence now suggest that GLI protein ciliary trafficking is essential for proper GLI function, a major question remains unresolved: What molecules directly regulate GLI protein trafficking, and to what extent do these molecules affect GLI protein function?

Intraflagellar transport (IFT) complexes traffic cargo within primary cilia through interactions with microtubule-based anterograde (kinesin-2) and retrograde (dynein) motor proteins (Pedersen and Rosenbaum, 2008; Goetz and Anderson, 2010). Although mutations in genes that encode for components of retrograde motors (*Dync2h1*), IFT A complexes (*Ift122*), or IFT B complexes (*Ift25* and *Ift27*) disrupt GLI protein ciliary localization and correlate with aberrant HH signaling (Ocbina et al., 2011; Qin et al., 2011; Keady et al., 2012; Yang et al.), the mechanisms of how GLI proteins are trafficked within and between subcellular compartments remain poorly understood.

Kinesin-2 motor proteins traffic protein cargos toward the plus-ends of microtubules both in the cytoplasm and within primary cilia making them presumptive candidates for directly regulating GLI protein trafficking. Within the kinesin-2 motor protein family there are two major motor complexes: a heterotrimeric complex consisting of KIF3A, KIF3B and the kinesin-associated protein, KAP3; and second, a homodimeric KIF17 motor complex (Scholey, 2013). I recently demonstrated that the heterotrimeric KIF3A/KIF3B/KAP3 motor complex directly interacts with and regulates GLI transcriptional activity (Carpenter et al., 2015). More specifically, I show that all mammalian GLI proteins interact with KAP3 and that this interaction is important for regulating the transcriptional activation of GLI2, but is dispensable for GLI3 repressor function. (Carpenter et al., 2015). While this study implicates the heterotrimeric

KIF3A/KIF3B/KAP3 motor complex in directly regulating GLI transcriptional activity, a role for the homodimeric KIF17 motor complex has not been addressed. Here, I investigate a role for KIF17 in interacting with and regulating GLI protein trafficking and function, specifically in HH-dependent cerebellar proliferation.

Kif17$^{-/-}$ mice are viable, fertile and display a grossly normal body plan (our own observations and (Setou et al., 2000). However, recent studies have revealed that loss of KIF17 leads to neurological defects including impaired learning and memory in mice and is associated with schizophrenia in humans (Wong-Riley and Besharse, 2012; Tarabeux et al., 2010; Yin et al., 2012). KIF17 is abundantly expressed in neuronal tissue and plays important roles in regulating NMDA receptor subunit 2B (NR2B) in hippocampal dendrites, cyclic nucleotide–gated (CNG) channels in olfactory sensory cilia, and microtubule stabilization in epithelial cells (Setou et al., 2000; Yin et al., 2012; Jaulin and Kreitzer, 2010). Similar to KIF17, GLI proteins are expressed in multiple neuronal tissues and play important roles in regulating brain growth and development ((Ruiz i Altaba et al., 2002). Whether KIF17 and GLI proteins are expressed in the same neuronal tissues is unknown, and whether KIF17, like the heterotrimeric KIF3A/KIF3B/KAP3 motor complex, can physically interact with GLI proteins and regulate their function has yet to be tested. Here, I use a combination of biochemical, cell culture, and *in vivo* mouse genetic experimental approaches to show that KIF17 co-localizes and interacts with all mammalian GLI proteins. In addition, I provide evidence that GLI1 protein expression is decreased in cells stably expressing a dominant-negative version of KIF17 (DNKIF17) that lacks the motor domain. Finally, I show that KIF17 and GLI proteins are expressed in overlapping cell layers in the developing cerebellum, and that *Kif17*$^{-/-}$ mice have smaller cerebella.

3.3 Results

KIF17 co-localizes with GLI proteins in vitro

To initially assess whether GLI proteins co-localize with KIF17, I compared the cellular distribution of an epitope-tagged KIF17 (KIF17::HA) with endogenous GLI2 and GLI3 in NIH/3T3 cells (Figure 3.1). Consistent with previous work, KIF17::HA localizes to multiple subcellular compartments including the cytoplasm, nucleus, and primary cilia (Verhey and Hammond, 2009; Dishinger et al., 2010)(Figure 3.1A and 3.1B). Similarly, endogenous GLI2 and GLI3 distribute across multiple cellular compartments and co-localize with KIF17::HA in primary cilia (Figure 3.1A and Figure 3.1B). These data suggest that, like KAP3, KIF17 co-localizes with GLI proteins in primary cilia.

Since KIF17 and GLI proteins localize to the same subcellular compartments, we performed co-immunoprecipitation experiments in COS-7 cells to determine whether KIF17 and GLI proteins physically interact (Figure 3.2). COS-7 cells were co-transfected with MYC::GLI2 and KIF17::HA followed by immunoprecipitation and western blot analysis (Figure 3.2A). I find that KIF17::HA co-precipitates with MYC::GLI2 (Figure 3.2A). The physical association of GLI2 with KIF17 prompted me to assess whether KIF17 interacts with the other full-length mammalian proteins, GLI1 and GLI3. Similar to GLI2, I find that KIF17 co-precipitates with both GLI1 and GLI3 (Figure 3.2B). Taken together, these data indicate that KIF17 physically interacts with all three mammalian GLI proteins.

DNKIF17 does not disturb ciliary localization of GLI2 and GLI3

Motorless KIF17 and KIF3A proteins are predicted to exert dominant-negative effects on kinesin-2 dependent cargo trafficking (Brown et al., 2005; Jiang et al., 2015; Guillaud et al.,

2003). To determine whether GLI localization is perturbed in the presence of motorless KIF17, I generated NIH/3T3 Flp-In cells (Sauer, 1994) stably expressing EGFP-tagged full-length KIF17 (KIF17::EGFP), dominant-negative KIF17 (DNKIF17::EGFP), and dominant-negative KIF3A (DNKIFA::EGFP). Similar to transiently transfected KIF17::HA, KIF17::EGFP localizes to multiple subcellular compartments including the cytoplasm and nucleus (compare Figure 3.1A and 3.1B to Figure 3.3A and 3.3B, top rows). However, unlike KIF17::HA, KIF17::EGFP is not detected in primary cilia (Figure 3.3A, top rows, white arrows). While KIF17::EGFP is absent from primary cilia, endogenous GLI2 and GLI3 localize normally to the tips of primary cilia (Figure 3.3A and 3.3B, top rows, white arrow).

I next assessed localization of endogenous GLI2 and GLI3 in cells expressing a dominant-negative version of KIF17, DNKIF17::EGFP, which lacks the conserved motor domain (Figure 3.3A and 3.3B, middle rows). Similar to KIF17::EGFP, DNKIF17::EGFP localizes to nuclear and cytoplasmic compartments (Figure 3.3A and 3.3B, middle rows). However, in contrast to KIF17::EGFP, DNKIF17::EGFP co-localizes with GLI2 and GLI3 in the tips of primary cilia (Figure 3.3A and 3.3B, middle rows, white arrows). In addition to DNKIF17::EGFP, I assessed GLI2 and GLI3 localization in a NIH/3T3 Flp-In cells stably expressing dominant-negative KIF3A (DNKIF3A::EGFP; Figure 3.3A and 3.3B, bottom rows). NIH/3T3 cells expressing motorless KIF3A have been reported to display defects in HH signaling due to perturbed ciliogenesis (Kim et al., 2009). Similar to DNKIF17, DNKIF3A::EGFP localizes to the nucleus and cytoplasm (Figure 3.3A and 3.3B, bottom rows). In contrast to what has been previously reported (Kim et al., 2009), primary cilia appear to be normal in these cells, and DNKIF3A::EGFP co-localizes with GLI2 and GLI3 in the tips of primary cilia (Figure 3.3A and 3.3B, bottom rows, white arrows). Taken together, these data

suggest that stably expressing low levels of either DNKIF17 or DNKIF3A does not disrupt endogenous GLI2 and GLI3 ciliary localization and that both DNKIF17 and DNKIF3A co-localize with GLI2 and GLI3 at the tips of primary cilia.

GLI1 expression is decreased in cells expressing DNKIF17

Despite no obvious defects in GLI2 and GLI3 trafficking in cells expressing DNKIF17 and DNKIF3A, I was curious whether HH target gene expression and GLI3 processing were affected in these cell lines. To assess HH-responsiveness, I analyzed GLI1 protein expression via western blotting and quantified our findings (Figure 3.4A and Figure 3.4B). After 48 hours of SAG treatment to activate the HH signaling pathway (REF- for SAG), GLI1 protein expression was similar between the parental NIH/3T3 Flp-In cells and in cells expressing full-length KIF17::EGFP (Figure 3.4A, lanes 1 and 2; quantified in Figure 3.4B). In contrast to the parental cells, cells expressing DNKIF17::EGFP show reduced GLI1 protein expression (Figure 3.4A, compare lanes 1 vs. 3; quantified in Figure 3.4B). Similar to DNKIF17::EGFP expressing cells, DNKIF3A::EGFP cells show reduced GLI1 expression compared to the parental cells (Figure 3.4A, compare lanes 1 vs. 4; quantified in Figure 3.4B).

Decreased GLI1 expression levels in cells expressing DNKIF17 and DNKIF3A prompted me to test whether this could be explained by defects in GLI3 processing. To examine GLI3 processing in cells expressing DNKIF17 and DNKIF3A, I assessed GLI3 full-length (GLI3FL) and GLI3 repressor (GLI3R) protein levels in each cell line (Fig 3.4C). GLI3FL and GLI3R levels are similar between parental cells and cells expressing KIF17::EGFP, DNKIF17::EGFP, and DNKIF3A::EGFP (Figure3.4C). Importantly, the apparently decreased level of GLI3FL in KIF17::EGFP-expressing cells observed in this experiment (Figure 3.4C, compare lane 2 to lane

4) is more similar to parent cells in repeated experiments (data not shown). Overall, these data suggest that GLI1 protein expression levels are decreased in cells stably expressing DNKIF17 and DNKIF3A; however, this decrease cannot be explained by altered GLI3 processing.

KIF17 is dispensable for HH-dependent neural patterning

Due to defects in GLI1 protein expression in cells expressing DNKIF17, I assessed whether loss of KIF17 affects HH-dependent neural tube patterning. To do this, I performed immunofluorescence experiments on *Kif17*$^{-/-}$ neural tubes at E10.5 (Figure 3.5A). Using a combination of dorsal and ventral neural progenitor markers, I show that both *Kif17*$^{+/-}$ (Figure 3.5A, left panels) and *Kif17*$^{-/-}$ (Figure 3.5A, right panels) neural tubes show no apparent defects in neural patterning and are indistinguishable from *wildtype* E10.5 neural tubes (data not shown).

The lack of phenotype in *Kif17*$^{-/-}$ E10.5 neural tubes prompted me to determine whether KIF17 is expressed in E10.5 embryos. To assess KIF17 expression in E10.5 embryos, I performed whole-mount X-Gal staining on *Kif17*$^{+/+}$, *Kif17*$^{+/-}$, and *Kif17*$^{-/-}$ embryos (Figure 3.5B). No X-Gal staining was observed in either *Kif17*$^{+/-}$ or *Kif17*$^{-/-}$ at E10.5 (Figure 3.5B). These data suggest that KIF17 is dispensable for HH-dependent neural patterning, likely due to a lack of *Kif17* expression in the developing neural tube.

KIF17 is expressed in the developing cerebellum

Previous reports on vertebrate KIF17 expression showed high-level mRNA expression in adult mouse brain tissue (Setou et al., 2000). This led me to test where KIF17 is expressed in adult mouse brains. To do so, I performed whole-mount X-Gal staining on *Kif17*$^{+/+}$ (Figure 3.6A, left panel) and *Kif17*$^{+/-}$ (Figure 3.6A, right panel) adult mouse brains. Specific X-Gal staining in

Kif17$^{+/-}$ brains is observed in multiple compartments including the cerebral cortex (Cx), thalamus (Th), and cerebellum (Cb) (Figure 3.6A, right panel).

In mice, cerebellar proliferation continues up to 2 to 3 weeks after birth and is dependent on HH signaling (Wechsler-Reya and Scott, 1999). This prompted me to perform a more detailed time course of *Kif17* expression to determine whether *Kif17* is also expressed in the developing cerebellum during this time frame (Figure 3.6B). At P4, no X-Gal staining is observed in *Kif17*$^{+/+}$, *Kif17*$^{+/-}$, or *Kif17*$^{-/-}$ cerebella; however, specific staining is present in the adjacent ependymal cell lining in *Kif17*$^{+/-}$and *Kif17*$^{-/-}$ (Figure 3.6Bi, middle and bottom panels, black asterisk). By P8, X-Gal is detectable in the posterior most lobules of both *Kif17*$^{+/-}$ and *Kif17*$^{-/-}$ cerebellum with stronger X-Gal staining observed in *Kif17*$^{-/-}$ cerebellum (Figure 3.6Bii, middle and bottom panels, black arrows). From P14 to P21, X-Gal staining intensifies in *Kif17*$^{+/-}$ and *Kif17*$^{-/-}$ cerebella, and is also present at lower levels in every lobe of the cerebellum (Figure 3.6Biii and 3.6Biv, middle and bottom panels). Taken together, these data suggest that KIF17 is expressed during postnatal cerebellar development.

KIF17 and GLI proteins co-localize in Purkinje cell layer

GLI proteins interact with KIF17 *in vitro* and are expressed in distinct layers of the cerebellum (Figure 3.2; (Corrales et al., 2004). This prompted me to determine if KIF17 and GLIs are expressed in overlapping cell layers within the developing cerebellum. By performing X-Gal staining on P21 *Kif17*$^{-/-}$ cerebellum sections, I found that X-Gal staining is present in a cell layer located between the inner granule layer (IGL) and external granule layer (EGL) presumed to be the Purkinje cell layer (PCL) (Figure 3.7A). Co-staining with a Purkinje cell

marker (LIM1/2) and an antibody against β-Galactosidase (β-Gal) confirmed that KIF17 is expressed in the PCL (Figure 3.7B, bottom panels, inset).

Both GLI1 and GLI2 are expressed in the PCL by P21 (Corrales et al., 2004). To confirm these reports and to determine whether KIF17 and GLI proteins display overlapping expression in the PCL, I performed whole-mount X-Gal staining on *Kif17*$^{+/-}$, *Gli1*$^{+/-}$, and *Gli2*$^{+/-}$ P21 cerebellum (Fig 3.8A). X-Gal staining on *Gli1*$^{+/-}$ cerebella at P21 showed that, similar to KIF17 expression, GLI1 expression is restricted to the PCL (Figure 3.8A, compare top and middle panels, dotted line in insets). In both *Kif17*$^{+/-}$ and *Gli1*$^{+/-}$, X-Gal staining is strongest in the PCL; however, lower levels of X-Gal are also present in the molecular cell layer (MCL) in *Kif17*$^{+/-}$ animals (Figure 3.8A, top panel, inset). No X-Gal staining is observed in the EGL of either *Kif17*$^{+/-}$ or *Gli1*$^{+/-}$ cerebella. Similar to *Kif17*$^{+/-}$ and *Gli1*$^{+/-}$, X-Gal staining is strongest in the PCL of *Gli2*$^{+/-}$ cerebella at P21 (Figure 3.8A, compare top, middle, and bottom panels, dotted line in insets). However, unlike *Kif17*$^{+/-}$ and *Gli1*$^{+/-}$, X-Gal staining in *Gli2*$^{+/-}$ cerebella are also present in the IGL (Figure 3.8A, bottom panel, inset). Taken together, these data suggest that *Kif17*, *Gli1*, and *Gli2* display distinct and overlapping expression in the developing cerebellum. Interestingly, *Kif17*, *Gli1*, and *Gli2* all display overlapping expression in the PCL.

Mice lacking KIF17 display decreased cerebellum size

During the process of analyzing KIF17 expression in the developing cerebellum, I noticed *Kif17*$^{-/-}$ cerebella appeared smaller compared to wildtype littermates. This observation prompted me to compare the size of wildtype vs. *Kif17*$^{-/-}$ adult cerebella (Figure 3.9A). I confirmed my initial observations that *Kif17*$^{-/-}$ cerebella are smaller compared to wildtype cerebella (Figure 3.9A, compare dotted line in left panels vs. dotted line in right panels). These

data, though preliminary, suggest that cerebellum development is perturbed in mice lacking KIF17.

3.4 Discussion

GLI proteins interact with multiple kinesin-2 motor complexes

Here I provide evidence that the homodimeric KIF17 motor complex interacts with all mammalian GLI proteins. These data are interesting in light of my recent work showing that the heterotrimeric KIF3A/KIF3B/KAP3 complex also interacts with all mammalian GLI proteins (Carpenter et al., 2015). Taking these two studies together, my data suggest a model in which both kinesin-2 motor complexes share GLI proteins as cargo. KAP3 interacts with GLI proteins directly in the absence of IFT particles (Carpenter et al., 2015), but whether KIF17 binds GLI proteins directly has yet to be tested. It is possible that KIF17 may interact with GLI proteins via IFT particles or some unknown protein scaffolds. In support of this idea, it has been reported that immunoprecipitation of either KIF17 or KIF3A/KIF3B/KAP3 motor complexes from mouse retinal extracts co-immunoprecipitates equal amounts of an IFT complex B protein, IFT88 (Insinna et al., 2009). In the same study, the authors further show that immunoprecipitation of KIF17 co-immunoprecipitates KIF3A, KIF3B, and KAP3, suggesting that in addition to interacting with IFT88, KIF17 also interacts with a complex containing KIF3A/KIF3B and KAP3 (Insinna et al., 2009). More experiments are required to test whether KIF17 and GLI proteins form separate complexes from KIF3A/KIF3B/KAP3 and whether these interactions are direct. To my knowledge, the finding that both kinesin-2 motor complexes interact with GLI proteins provides a rare example where the homodimeric KIF17 and heterotrimeric

KIF3A/KIF3B/KAP3 motor complexes interact redundantly with a protein cargo other than IFT protein machinery.

DNKIF17 perturbs GLI1 expression, but does not alter GLI cilia localization

KIF17 localizes with GLI2 and GLI3 in primary cilia when transiently transfected in NIH/3T3 cells; however, I do not detect co-localization of KIF17 with either GLI2 or GLI3 in primary cilia when KIF17 is stably expressed at lower levels. This contrasting finding is likely due to the fact cells stably expressing KIF17 simply do not have enough KIF17 protein in the primary cilia to detect using our standard immunofluorescence protocol. To assess whether KIF17 is trafficking through primary cilia at barely detectable levels, one approach would be to assess whether KIF17 accumulates in primary cilia in *Dync2h* $^{lln/lln}$ mouse embryonic fibroblasts (MEFs) (Ocbina et al., 2011) that are defective in retrograde trafficking of ciliary proteins. However, further experiments are required to test this possibility.

In contrast to full-length KIF17, DNKIF17 co-localizes with GLI2 and GLI3 at the tips of primary cilia. I also observe an increase in DNKIF17 nuclear localization compared to cells stably expressing full-length KIF17. These observations are consistent with published studies showing that C-terminal truncated versions of KIF17 display increased nuclear localization due to exposure of an N-terminal sequence that interacts with import protein, Importin-β2, and is important for both cilia and nuclear localization of KIF17 (Dishinger et al., 2010). It is possible that without the motor domain, DNKIF17 is localized to both the nuclear and ciliary compartments via interactions with other proteins, like Importin- β2 for example. Regardless, GLI2 and GLI3 localize to primary cilia normally in the presence of stably expressed DNKIF17.

Transiently expressing DNKIF3A in NIH/3T3 cells causes defects ciliogenesis (Kim et al., 2009) and our unpublished observations); however, I show that NIH/3T3 cells stably expressing low levels of DNKIF3A display no defects in ciliogenesis and that DNKIF3A localizes to the tips of cilia. Further, stable expression of DNKIF3A does not alter GLI2 and GLI3 cilia localization. Despite no affects on GLI2 and Gli3 cilia localization, I find that GLI1 protein expression is significantly decreased in cells stably expressing DNKIF3A and DNKIF17. The defect in GLI1 expression could not be explained by defects in GLI3 processing as neither DNKIF17 nor DNKIF3A expressing cells display defects in GLI3 processing. One possibility is that DNKIF17 and DNKIF3A disrupt non-ciliary GLI protein trafficking. Evidence in support of this comes from a study where specifically disrupting non-ciliary dynamic microtubules by nocodazole (Noc) treatment decreases HH transcriptional response in a dose dependent manner (Tukachinsky et al., 2010). More studies are needed to determine how DNKIF17 regulates GLI1 protein expression and if this is consistent with other HH target proteins, like PTCH1.

KIF17 co-expresses with GLI proteins in Purkinje cell layer of the developing cerebellum

HH signaling is required for proper cerebellar development and GLI2 is the major activator driving HH-dependent cerebellar proliferation (Corrales et al., 2004; 2006; Wechsler-Reya and Scott, 1999; Blaess et al., 2006). Here I show that KIF17 is expressed in the posterior lobes of the developing cerebellum by P8 and that this expression is detected broadly throughout the cerebellum by P21. At P21, KIF17 is expressed in the Purkinje cell layer (PCL) along with GLI1 and GLI2. While co-localization with Purkinje cells (PCs) marker, LIM1/2, shows that KIF17 is expressed in PCs, whether GLI1 and GLI2 are present in PCs at P21 is not clear. It has been reported that in GLI1 and GLI2 cerebella at P5 and P10, respectively that both GLI1 and

GLI2 are expressed in Bergman glia cells (BG) that are present along with PCs within PCL (Corrales et al., 2004); however, whether they overlap with KIF17 in PCs with KIF17 at P21 has not been tested. BG are intimately associated with PCs in the PCL and are important for regulating PC structure in the adult cerebellum (Yamada and Watanabe, 2002). A more in-depth analysis of KIF17 expression by co-staining with BG markers is required to confirm that KIF17 expression is indeed restricted to PCs. Regardless, why GLI proteins are co-expressed with KIF17 in the PCL in adult cerebellum and whether KIF17 and GLI proteins are involved in maintenance of BG and/or PCs provide important questions to investigate. It will also be important to assess a role for KIF17 in regulating HH-dependent cerebellar development by performing cerebellar granule cell progenitor (CGNP) cell proliferation assays (Izzi et al., 2011).

While more experiments are needed to confirm whether KIF17 is regulating HH-dependent cerebellar development, I show here that mice lacking KIF17 display smaller cerebellum. Interestingly, I further show that KIF17 is expressed during the time window of HH-dependent cerebellar proliferation and in the same cell layers as the major activators driving cerebellum proliferation, GLI proteins. As a whole, this investigation supports a model that implicates yet another kinesin-2 motor, KIF17, in the regulation of HH signaling via interactions with GLI proteins.

3.5 Materials and Methods

DNA Constructs

Hemagglutinin (HA)-tagged h*KIF17* and h*KIF3A* constructs and variants were generated from full-length human *KIF17* cDNA (provided by Kristen J. Verhey, University of Michigan Ann Arbor, MI). Briefly, full-length *hKIF17* (cDNA, base pairs) 1 to 3,081; protein, amino acis 1-

1027), *hDNKIF17* (cDNA, base pairs 1,393 to 3,081; protein, amino acids 464-1027) and *hDNKif3A* (cDNA, base pairs 1,033 to 2,106; protein, amino acids 345-702)-were cloned into pGIG (Megason and McMahon, 2002) using standard molecular biology techniques. To generate 6X MYC-tagged *Gli* constructs, m*Gli1*, h*Gli2*, h*Gli3* were cloned into pCDNA3 as previously described (Carpenter et al., 2015).

Immunoprecipitation and Western Blot Analysis

COS-7 cells were transiently transfected with the relevant DNA constructs using Lipofectamine 2000 (Invitrogen, Cat. #11668). The cells were lysed 48 hr after transfection in HEPES lysis buffer (25mM HEPES pH 7.4, 115mM KOAc, 5mM NaOAc, 5mM $MgCl_2$, 0.5mM EGTA, and 1% TX-100) containing protease inhibitor (Roche, Cat. #11836153001). Cell lysates were then subjected to centrifugation at 14,000 x *g* for 15 min to remove the insoluble fraction and protein concentrations were determined using a BCA Assay Kit (Pierce, Cat. #23225). Cell lysates (1mg) were then pre-cleared with Protein G agarose beads (Roche, Cat. #11719416001) for 1 hr at 4°C. MYC- or HA-tagged proteins were immunoprecipitated from pre-cleared lysates using either anti-MYC (1:150; Santa Cruz, Cat. #sc-40) or anti-HA (1:300; Covance, Cat. #MMS-101) antibodies for 2 hr at 4°C. Following immunoprecipitation, the lysates were incubated with Protein G agarose beads for 1 hr at 4°C. The Protein G agarose beads were washed 5 x 8 min in HEPES lysis buffer and re-suspended in 30 µl of 1x PBS and 6x Laemmli buffer. The samples were boiled for 10 minutes and proteins were separated using SDS-PAGE and analyzed by western blotting. Anti-MYC (1:1000) and anti-HA (1:1000) primary antibodies, peroxidase-conjugated AffiniPure goat anti-mouse light chain secondary antibody (1:50,000; Jackson ImmunoResearch, Cat. # 115-035-174), and a Konica Minolta SRX-101A medical film

processor were used to visualize tagged proteins. For detecting endogenous GLI1 and GLI3, whole cell lysates were collected in RIPA lysis buffer (50mM Tris pH 7.2, 150mM NaCl, 0.1% SDS, 1% TX-100, 1% sodium deoxycholate, 5mM EDTA) containing protease inhibitor. HH signaling was stimulated by adding 300 nM SAG in low serum for 48 hrs. Anti-GLI1 (Cell Signaling (L42B10), Cat. #2643; 1:1000) and anti-GLI3 (R&D, Cat. # AF3690; 1:200) primary antibodies and either peroxidase-conjugated AffiniPure goat anti-mouse light chain secondary antibody, or peroxidase-conjugated AffiniPure Donkey anti-goat light chain secondary antibody (1:50,000; Jackson ImmunoResearch, Cat. # 705-035-147) were used to detect GLI1 and GLI3, respectively. Western blots were quantified using ImageJ software.

Immunofluorescence staining

NIH/3T3 fibroblasts were seeded at a density of 1.5 x 10^5 cells/well in 6 well plates. Cells were transfected 24 hr later with either empty vector (pCIG) or with a DNA construct encoding KIF17::HA using Lipofectamine 2000. Cells were grown in low-serum media starting 8 hr after transfection, fixed 48 hr post-transfection in 4% paraformaldehyde for 10 min at room temperature, and permeabilized with a 5 min incubation in 0.2% Triton X-100 in PBS. Neural tube and cerebellum immunofluorescence was performed essentially as previously described (Allen et al., 2011). Neural patterning analysis was performed at the forelimb level in E10.5 embryos. Immunostaining was performed using the following primary antibodies: mouse anti-acetylated tubulin (1:2500; Sigma), rabbit anti-GFP (1:1000; Invitrogen), rabbit anti-gamma tubulin (1:2500; Sigma), rabbit anti-ARL13B (1:500; Proteintech), mouse anti-HA (1:1000; Covance), guinea pig anti-GLI2 (1:300; a gift from Dr. J.T. Eggenschwiler, University of Georgia), mouse anti-GLI3 (1:1000; obtained from Dr. S.J. Scales, Genentech), mouse IgG1

anti-NKX6.1 (1:20, Developmental Studies Hybridoma Bank [DSHB]), mouse IgG2a anti-PAX3 (1:20, DSHB), rabbit IgG anti-DBX1 (1:1000, gift from Dr. Yasushi Nagakawa), mouse IgG1 anti-FOXA2 (1:20, DSHB), rabbit IgG anti-FOXA2 (1:500, Cell Signaling), mouse IgG2b anti-NKX2.2 (1:20, DSHB), rabbit IgG anti-OLIG2 (1:1000, Millipore), rabbit anti- β-Galactosidase (1:500, MP Biomedical), mouse IgG1 anti-LIM1/2 (1:20; DSHB) . The following secondary antibodies were used at a dilution of 1:500: Alexa 488 goat anti-guinea pig IgG, Alexa 488 goat anti-mouse IgG2b, Alexa 555 goat anti-mouse IgG1, Alexa 633 goat anti-rabbit IgG. To visualize nuclei, DAPI (Invitrogen) was incubated for 5 min at a dilution of 1:30,000. Cells and neural tube sections were imaged using a Leica Upright SP5X White Light Laser Confocal Microscope. Images were processed using Adobe Photoshop and Illustrator.

Stable cell line generation

Stable NIH/3T3 cells lines expressing low levels of EGFP fused KIF17, DNKIF17, and DNKIF3A were generated using the Flp-In method exactly according to the manufacturer's recommendations (Life Technologies). Briefly, NIH/3T3 Flp-In cells were co-transfected with pOG44 and the pCDNA5/FRT vector containing *KIF17*, *DNKIF17*, or *DNKIF3A* fused to *EFGP*. After 48 hrs, the cells were reseeded at low density and the culture media was supplemented with Hygromycin B (Invitrogen) for stable integrant selection. Stable cell lines were passaged in Hygromycin B supplemented media every other passage to preserve selection pressure and prevent silencing of the transgene.

Whole-mount X-Gal staining

Mouse embryos were dissected and fixed in 4% paraformaldehyde for 1hr at room temperature and then washed 3x 5 minutes in PBS. Embryos were then stained overnight using 1mg/ml X-Gal substrate (Gold Biotechnology) in PBS solution containing 5mM $K_3Fe(CN)_6$, $K_4Fe(CN)_6$, 2mM $MgCl_2$, 0.01% sodium deoxycholate, and 0.02% NP-40. Following staining, embryos were washed in PBS and post-fixed in 4% paraformaldehyde for 20 minutes at room temperature. Embryos were then cleared over night in PBS and photographed in PBS on a stereoscopic microscope (SMZ1500: Nikon) using a Nikon objective (type: HR Plan Apochromat; NA 0.13) with a camera (Digital Sight DS-Ri1; Nikon). Images were acquired using the NIS Elements software (Nikon).

Mice

Mice were housed in specific pathogen-free facilities of the University of Michigan Comprehensive Cancer Center. This study was approved by the University of Michigan University Committee on Use and Care of Animals guidelines. *Gli1*^{lacZ}, *Gli2*^{lacZ}, and *Gli3*^{lacZ} mice were obtained from Dr. A. Joyner (MSKCC) and were maintained on a mixed C57BL/6 and 129/SvJ genetic background. *Kif17*^{LacZ} mice were obtained from Dr. J Besharse (Medical College of Wisconsin) and maintained on a mixed C57BL/6 background.

3.6 Acknowledgements

We thank Drs. S. Scales (Genentech) and J. Eggenschwiler (University of Georgia) for sharing anti-GLI3 and anti-GLI2 antibodies, respectively. We are grateful to Drs. B. Yoder (University of Alabama-Birmingham) and A. Dlugosz (University of Michigan) for the full-

length *Gli* constructs. We also thank Dr. J. Besharse (Medical College of Wisconsin) for providing the KIF17 mice. We thank members of the Allen lab for insightful comments and helpful suggestions. The NKX2.2 and NKX6.1 antibodies were obtained from the Developmental Studies Hybridoma Bank developed under the auspices of the NICHD and maintained by The University of Iowa, Department of Biological Sciences, Iowa City, IA. Confocal microscopy was performed in the Microscopy and Image Analysis Laboratory at the University of Michigan. This work was supported by an EBS EDGE award to B.S.C., The University of Michigan Center for Organogenesis, an American Heart Association scientist development grant (11SDG6380000) and by NIH grants (R21 CA167122 and R01 DC014428) to B.L.A.

3.7 Author contributions

B.S.C. and B.L.A. conceived and designed the experiments. B.S.C. executed the experiments and collected the data. T.L.B. aided in DNKIF17 immunofluorescence experiments. K.J.V. provided kinesin-2 constructs, as well as technical advice, experimental suggestions and aided with manuscript preparation and editing. B.S.C. and B.L.A. wrote and edited the manuscript.

3.8 Figures

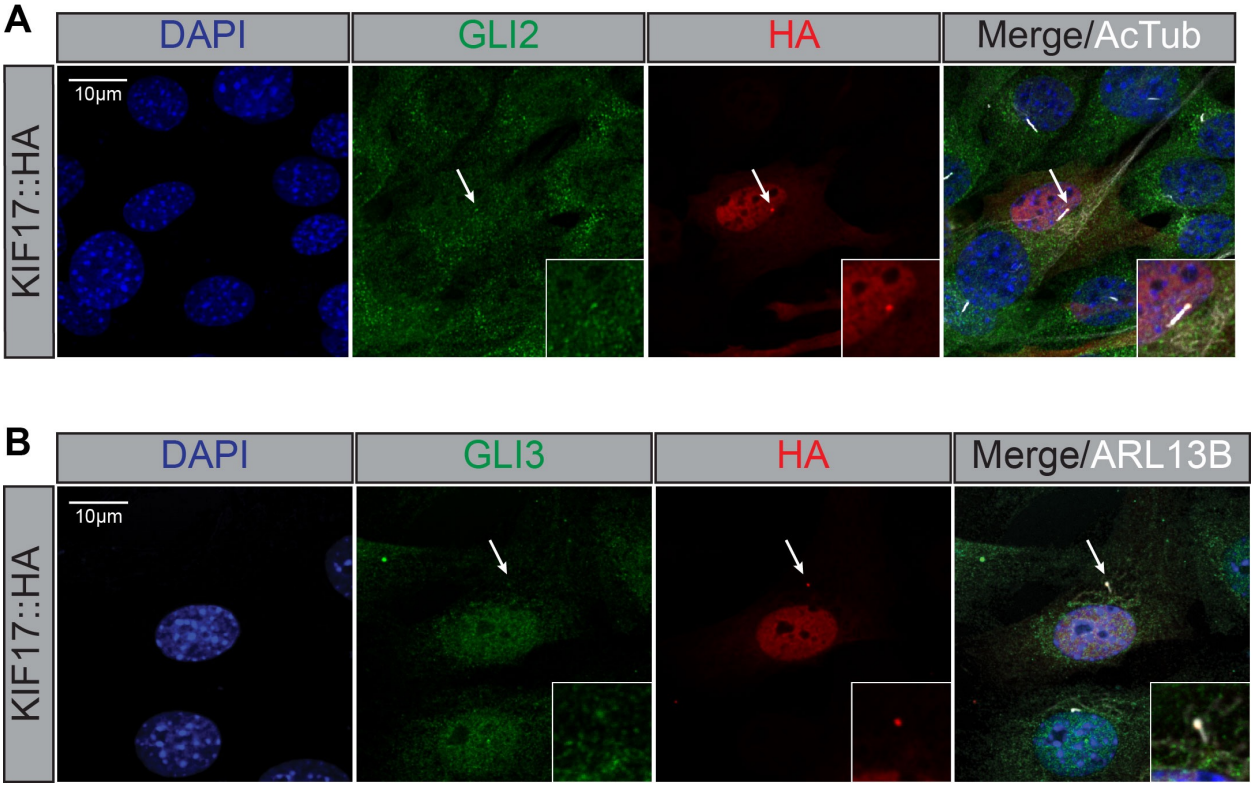

Figure 3.1. KIF17 co-localizes with endogenous GLI2 and GLI3 in NIH/3T3 cells.
(A) Antibody detection of endogenous GLI2 in NIH/3T3 cells (top row; green) expressing HA-tagged KIF17 (KIF17::HA, red). Primary cilia are identified using antibodies directed against Acetylated-tubulin (AcTub; grey). (B) Antibody detection of endogenous GLI3 in NIH/3T3 cells expressing HA-tagged KIF17 (KIF17::HA, red). Primary cilia are identified using antibodies directed against ARL13B (ARL13B; grey). DAPI denotes nuclei (blue). Insets represent high magnification images of primary cilia. Scale bar, 10μm.

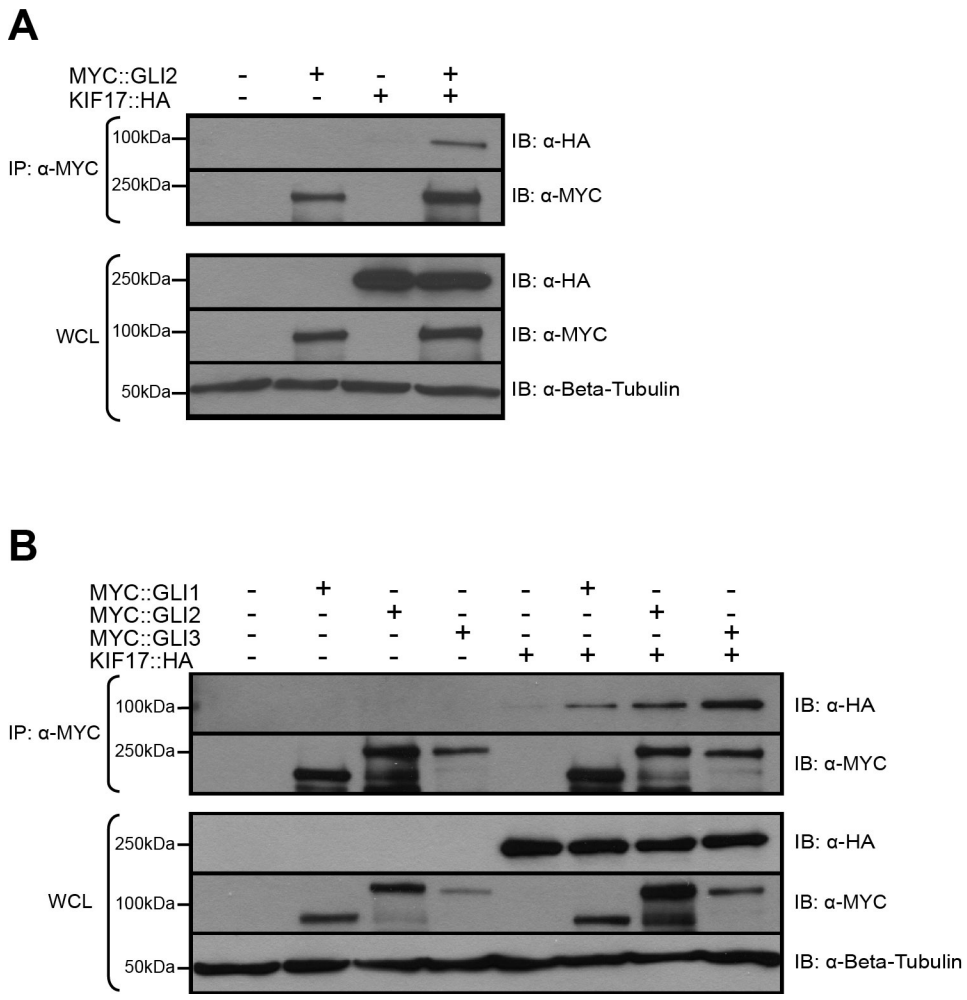

Figure 3.2. KIF17 interacts with all mammalian GLI proteins.
(A) Immunoprecipitation of MYC-tagged GLI2 (MYC::GLI2) from COS-7 cells expressing HA-tagged KIF17 (KIF17::HA). (B) Immunoprecipitation of MYC::GLI1-3 from COS-7 cells co-expressing KIF17::HA. Immunoprecipitates (IP) and whole cell lysates (WCL) were subjected to SDS-PAGE and western blot analysis (IB) using antibodies directed against MYC (α-MYC) and HA (α-HA). Antibody detection of Beta-Tubulin (α-Beta-Tubulin) was used to confirm equal loading across lanes. The molecular weights (in kDa) of protein standards are indicated at the left of each blot.

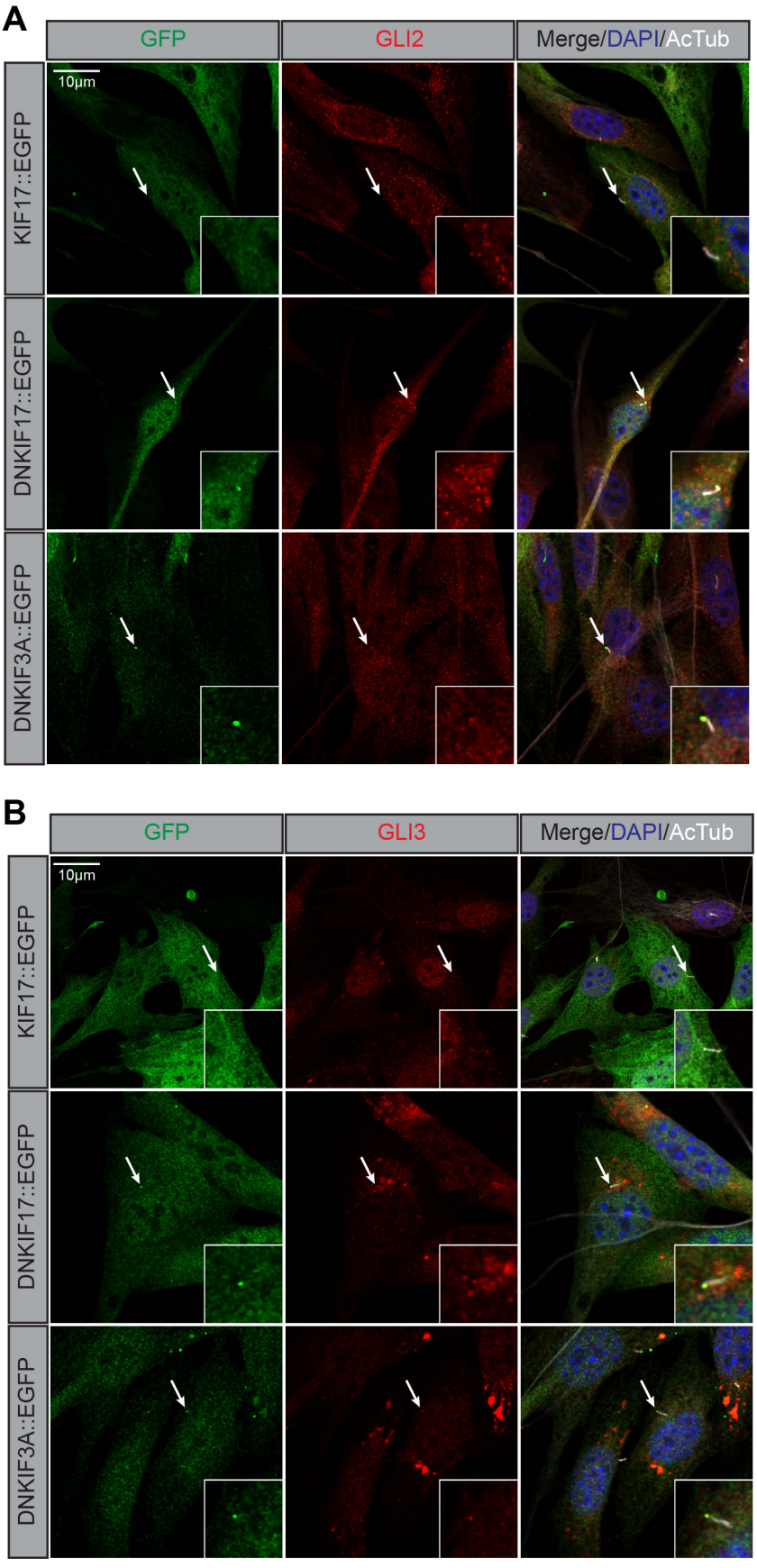
A
GFP
GLI2
Merge/DAPI/AcTub
10μm
KIF17::EGFP
DNKIF17::EGFP
DNKIF3A::EGFP
B
GFP
GLI3
Merge/DAPI/AcTub
10μm
KIF17::EGFP
DNKIF17::EGFP
DNKIF3A::EGFP

Figure 3.3. Endogenous GLI2 and GLI3 localize to primary cilia in NIH/3T3 cells expressing DNKIF17.(A) Antibody detection of endogenous GLI2 (red) in NIH/3T3 cells stably expressing KIF17::EGFP (top row), DNKIF17::EGFP (middle row), or DNKIF3A::EGFP (bottom row). DAPI denotes nuclei (blue) and an antibody directed against GFP is used to detect EGFP constructs (GFP; green). Primary cilia are identified using antibodies directed against Acetylated-tubulin (AcTub; grey). (B) Antibody detection of endogenous GLI3 (red) in NIH/3T3 cells stably expressing KIF17::EGFP (top row), DNKIF17::EGFP (middle row), or DNKIF3A::EGFP (bottom row). Primary cilia are identified using antibodies directed against ARL13B (ARL13B; grey). DAPI denotes nuclei (blue) and an antibody directed against GFP was used to detect EGFP constructs (GFP; green). Insets represent high magnification images of primary cilia. Scale bar, 10μm.

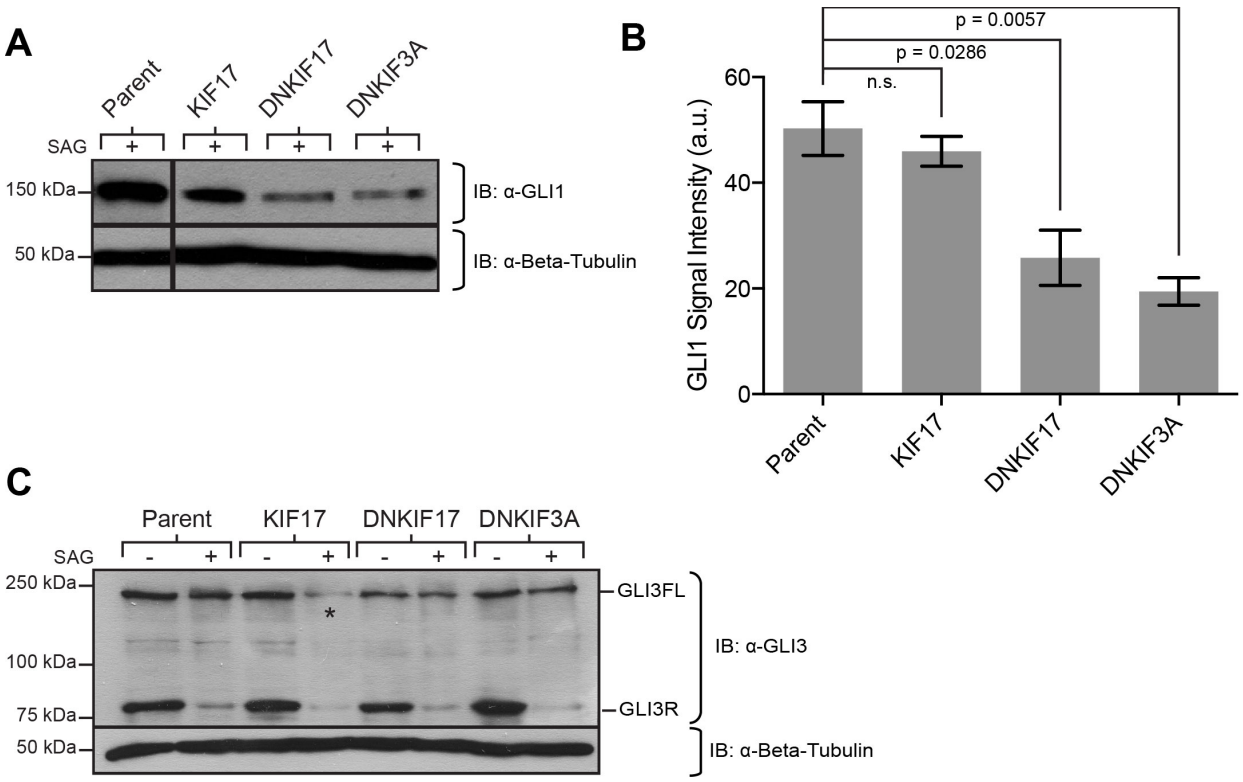

Figure 3.4. DNKIF17 alters GLI1 expression, but does not affect GLI3 processing.
(A) GLI1 protein expression in NIH/3T3 cells stably expressing KIF17::EGFP, DNKIF17::EGFP , or DNKIF3A::EGFP after 48 hr SAG treatment (+). GLI1 expression in the parental cell line (Parent) was cropped from same experimental blot used to visualize GLI1 expression in stable cell lines in (A) (see lane 1). Whole cell lysates (WCL) were subjected to SDS-PAGE and western blot analysis (IB) using an antibody directed against GLI1 (α-GLI1) . Antibody detection of Beta-Tubulin (α-Beta-Tubulin) was used to confirm equal loading across lanes. The molecular weights (in kDa) of protein standards are indicated at the left of each blot. (B) Quantification of GLI1 signal intensity in parental vs. stable cell lines. Error bars represent the mean +/- the standard error for three seperate experiments; p-values are indicated above the relevant treatment groups (Student's unpaired t-test); n.s., not significant ($p>0.05$). (C) GLI3 protein expression in NIH/3T3 cells stably expressing KIF17::EGFP, DNKIF17::EGFP , or DNKIF3A::EGFP plus (+) or minus (-) 48 hr SAG treatment. Similar to (A), GLI3 expression in the parental cell line (Parent) was compared to GLI3 expression in the stable cell lines. GLI3 full-length (GLI3FL) and GLI3 repressor (GLI3R) are labeled on the right of the blot. Asterick (*) denotes lower GLI3FL expression in the KIF17::EGFP expressing cell line. Whole cell lysates (WCL) were subjected to SDS-PAGE and western blot analysis (IB) using an antibody directed against GLI3 (α-GLI3). Antibody detection of Beta-Tubulin (α-Beta-Tubulin) was used to confirm equal loading across lanes. The molecular weights (in kDa) of protein standards are indicated at the left of each blot.

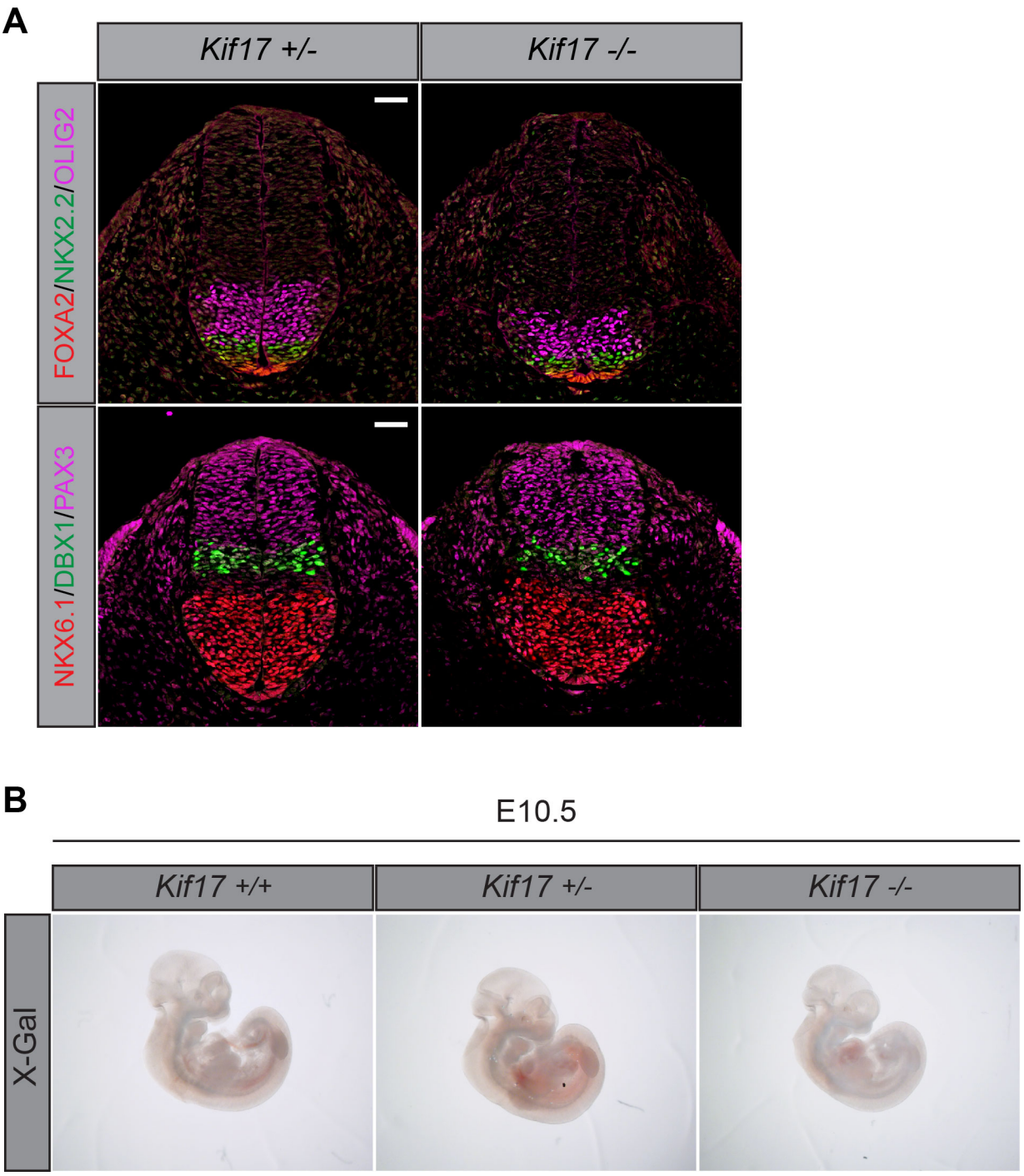

Figure 3.5. KIF17 is dispensable for HH-dependent neural patterning and not expressed in the early embryo.
(A) Immunofluorescent analysis of neural patterning in E10.5 *Kif17* $^{+/-}$ (left panels) and *Kif17*$^{-/-}$ (right panels) mouse forelimb sections. FOXA2, NKX2.2, and OLIG2 (red, green, magenta, respectively) expression is detected in the top panels, and NKX6.1, DBX1, and PAX3 (expression red, green, magenta, respectively) is detected in the bottom panels. Scale bars: 100 μm. (B) Whole-mount X-Gal staining of E10.5 *Kif17*$^{+/+}$, *Kif17* $^{+/-}$, and *Kif17*$^{-/-}$ mouse embryos.

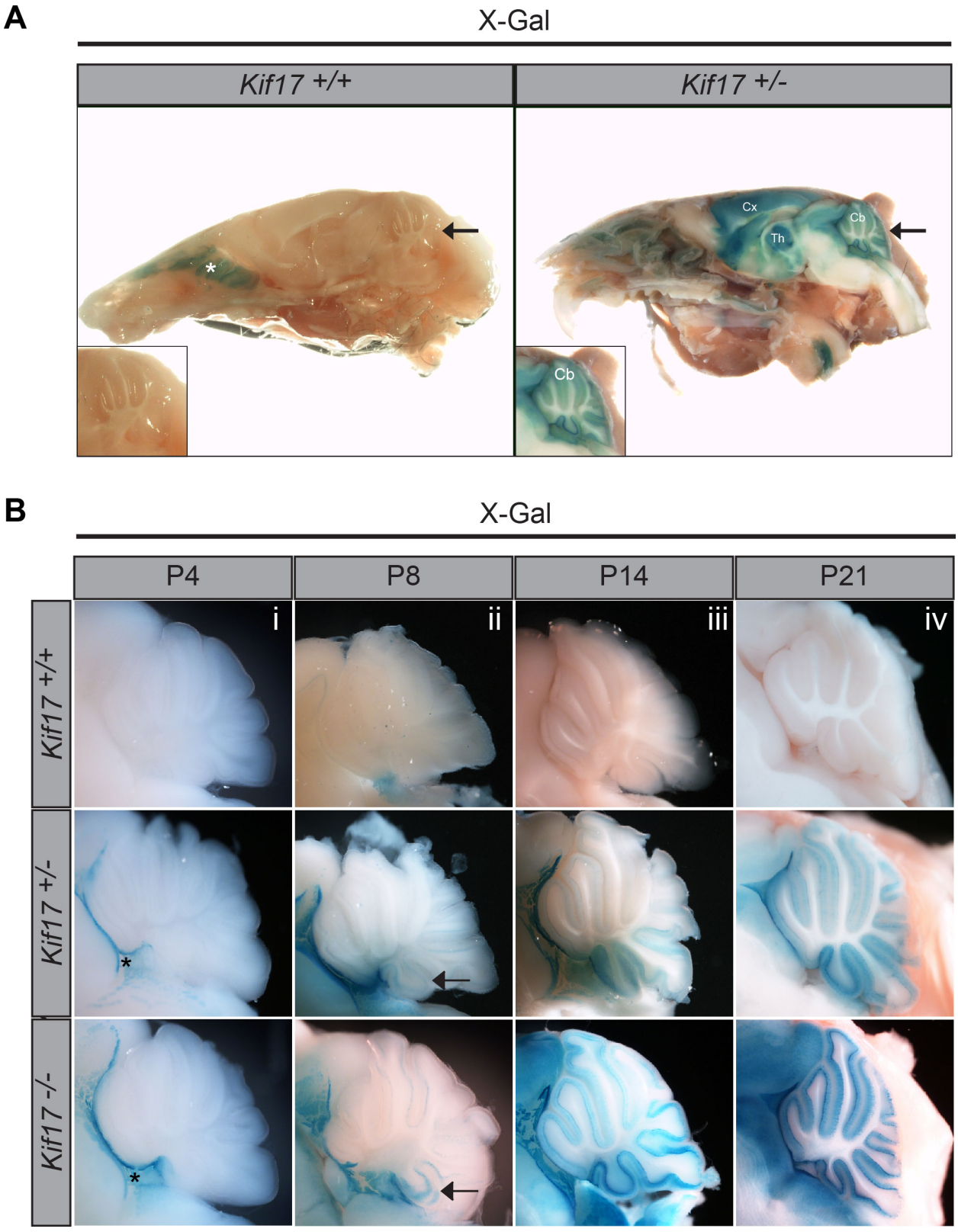
A
X-Gal
Kif17 +/+
Kif17 +/-
Cx
Th
Cb
Cb
B
X-Gal
P4
P8
P14
P21
i
ii
iii
iv
Kif17 +/+
Kif17 +/-
Kif17 -/-

Figure 3.6. KIF17 expressed in the developing mouse cerebellum.
(A) Whole-mount X-Gal staining of *Kif17* $^{+/+}$ (left) and *Kif17*$^{+/-}$ (right) adult mouse brains. Cx, cerebral cortex; Cb, cerebellum; Th, thalamus. White asterisk (*) denotes non-specific X-Gal staining. Insets represent a high magnification the cerebellum denoted by black arrows. (B) Whole-mount X-Gal staining of mouse cerebellum from stages P4 to P21 in *Kif17* $^{+/+}$ (top row), *Kif17*$^{+/-}$ (middle row), and *Kif17*$^{-/-}$ (bottom row). Black Asterisks (*) denote X-Gal staining in the ependymal cell lining. Black arrows indicate initial X-Gal staining observed in cerebellum.

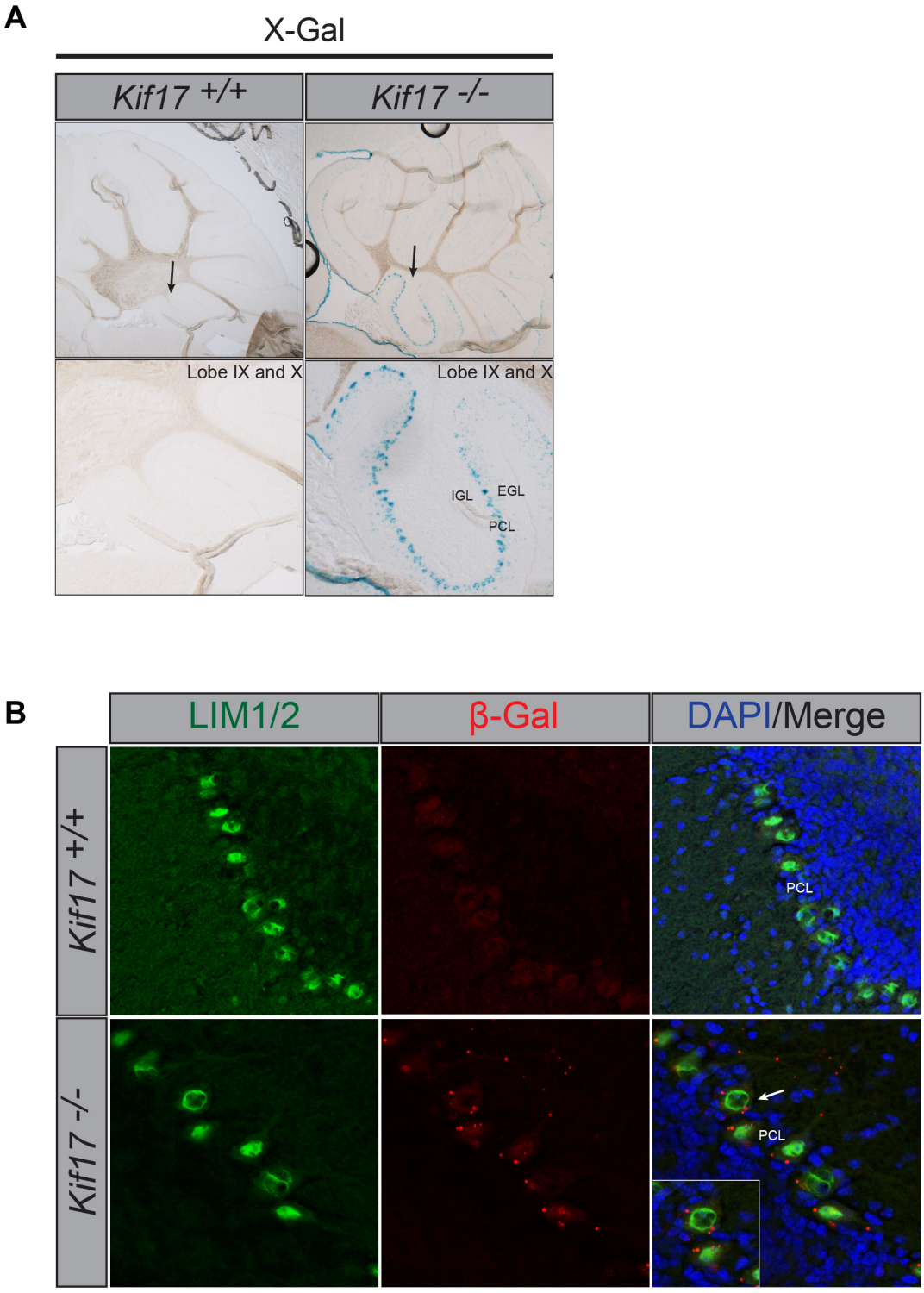

Figure 3.7. KIF17 expressed in the Purkinje cell layer of the cerebellum.
(A) Whole-mount X-Gal staining on sagittal sections of *Kif17*$^{+/+}$ (left panels) and *Kif17*$^{-/-}$ (right panels) P21 mouse cerebellum. Bottom panels represent higher magnification images of lobules IX and X indicated by black arrows in the top panels. Purkinje cell layer (PCL); inner granule layer (IGL); external granule layer (EGL). (B) Immunofluorescent staining on sagittal sections of

Kif17$^{+/+}$ (top panels) and *Kif17*$^{-/-}$ (bottom panels) P21 mouse cerebellum. Images represent high magnification of Lobe IX. Purkinje cells are labeled using an antibody directed against LIM1/2 (green); β-Gal (red) and DAPI (blue). Inset represents high magnification image of Purkinje cells indicated by white arrow.

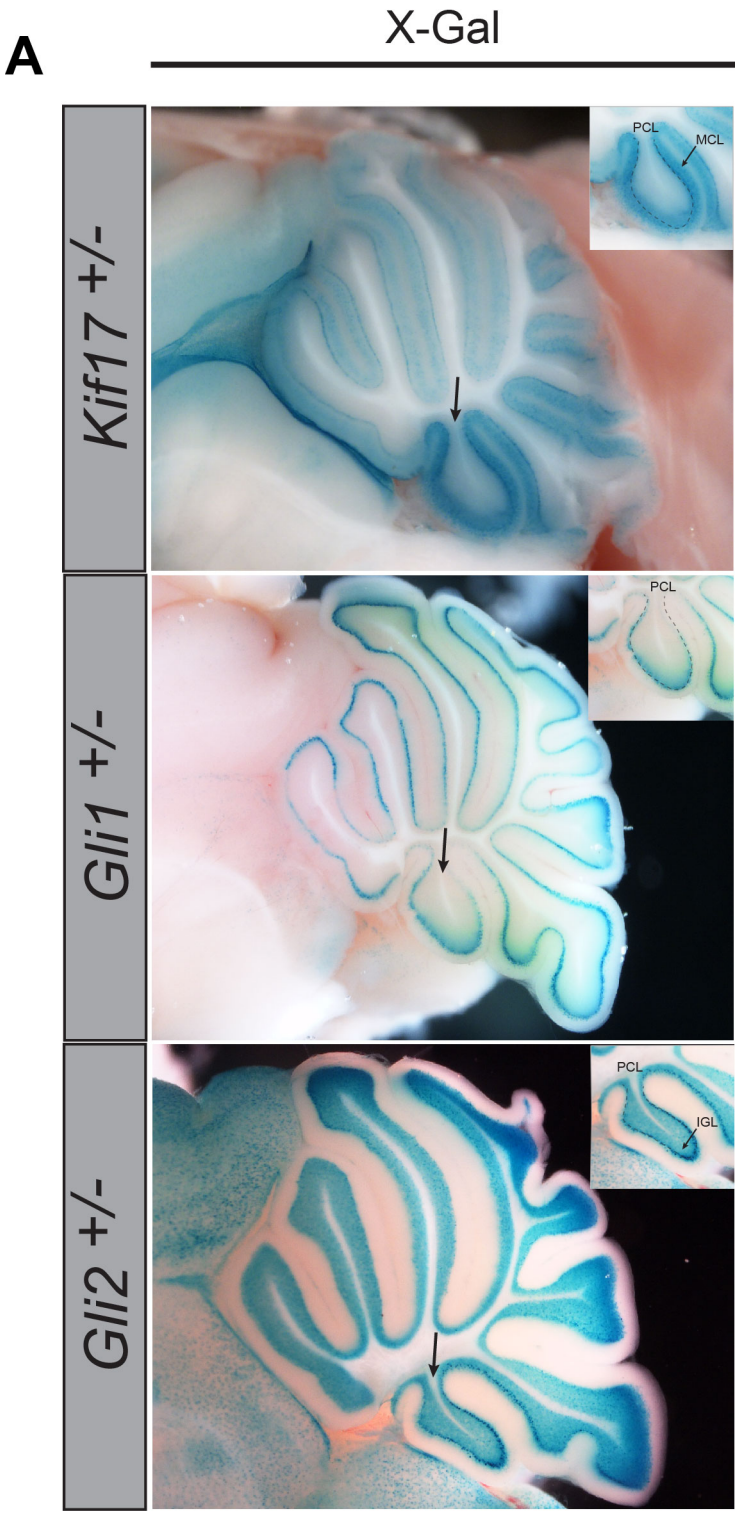

Figure 3.8. KIF17 expression overlaps with GLI1 and GLI2 in the Purkinje cell layer of the cerebellum. (A) Whole-mount X-Gal staining on *Kif17*$^{+/-}$, *Gli1*$^{+/-}$, and *Gli2*$^{+/-}$ P21 cerebellum. Insets represent high magnifications of lobe X indicated by black arrows. Purkinje cell layer (PCL); inner granule layer (IGL); external granule layer (EGL); molecular cell layer (MCL). Dotted lines in insets denote the PCL.

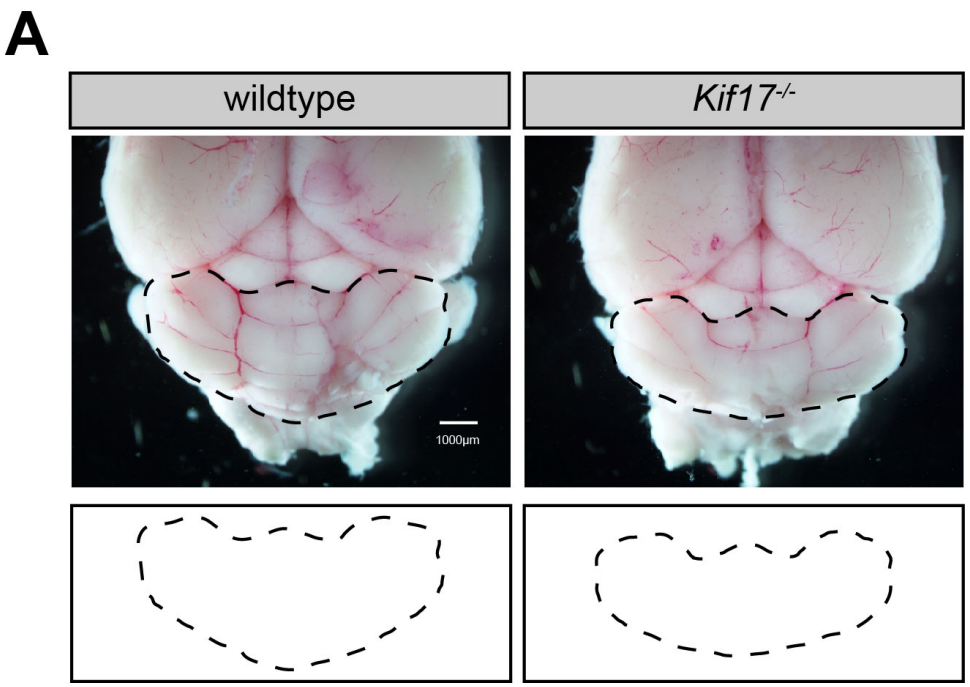

Figure 3.9. *Kif17*$^{-/-}$ mice display decreased cerebellum size.
(A) Whole-mount images of wildtype (top left) and *Kif17*$^{-/-}$ (top right) adult mouse brains. Dotted outlines highlight the difference in size between wiltdtype (bottom left) and *Kif17*$^{-/-}$ (bottom right) cerebellum. Scale bar, 1000 µm.

3.9 References

Allen, B.L., J.Y. Song, L. Izzi, I.W. Althaus, J.-S. Kang, F. Charron, R.S. Krauss, and A.P. McMahon. 2011. Overlapping Roles and Collective Requirement for the Coreceptors GAS1, CDO, and BOC in SHH Pathway Function. *Developmental Cell*. 20:775–787. doi:10.1016/j.devcel.2011.04.018.

Aza-Blanc, P., H.Y. Lin, A. Ruiz i Altaba, and T.B. Kornberg. 2000. Expression of the vertebrate Gli proteins in Drosophila reveals a distribution of activator and repressor activities. *Development*. 127:4293–4301.

Bai, C.B., W. Auerbach, J.S. Lee, D. Stephen, and A.L. Joyner. 2002. Gli2, but not Gli1, is required for initial Shh signaling and ectopic activation of the Shh pathway. *Development*.

Blaess, S., J.D. Corrales, and A.L. Joyner. 2006. Sonic hedgehog regulates Gli activator and repressor functions with spatial and temporal precision in the mid/hindbrain region. *Development*. 133:1799–1809. doi:10.1242/dev.02339.

Brown, C.L., K.C. Maier, T. Stauber, L.M. Ginkel, L. Wordeman, I. Vernos, and T.A. Schroer. 2005. Kinesin-2 is a motor for late endosomes and lysosomes. *Traffic*. 6:1114–1124. doi:10.1111/j.1600-0854.2005.00347.x.

Carpenter, B.S., R.L. Barry, K.J. Verhey, and B.L. Allen. 2015. The heterotrimeric kinesin-2 complex interacts with and regulates GLI protein function. *J. Cell. Sci.* 128:1034–1050. doi:10.1242/jcs.162552.

Chen, M.-H., C.W. Wilson, Y.-J. Li, K.K.L. Law, C.-S. Lu, R. Gacayan, X. Zhang, C.-C. Hui, and P.-T. Chuang. 2009. Cilium-independent regulation of Gli protein function by Sufu in Hedgehog signaling is evolutionarily conserved. *Genes & Development*. 23:1910–1928. doi:10.1101/gad.1794109.

Corrales, J.D., G.L. Rocco, S. Blaess, Q. Guo, and A.L. Joyner. 2004. Spatial pattern of sonic hedgehog signaling through Gli genes during cerebellum development. *Development*. 131:5581–5590. doi:10.1242/dev.01438.

Corrales, J.D., S. Blaess, E.M. Mahoney, and A.L. Joyner. 2006. The level of sonic hedgehog signaling regulates the complexity of cerebellar foliation. *Development*. 133:1811–1821. doi:10.1242/dev.02351.

Dishinger, J.F., H.L. Kee, P.M. Jenkins, S. Fan, T.W. Hurd, J.W. Hammond, Y.N.-T. Truong, B. Margolis, J.R. Martens, and K.J. Verhey. 2010. Ciliary entry of the kinesin-2 motor KIF17 is regulated by importin-beta2 and RanGTP. *Nat. Cell Biol.* 12:703–710. doi:10.1038/ncb2073.

Goetz, S.C., and K.V. Anderson. 2010. The primary cilium: a signalling centre during vertebrate development. *Nat. Rev. Genet.* 11:331–344. doi:10.1038/nrg2774.

Guillaud, L., M. Setou, and N. Hirokawa. 2003. KIF17 dynamics and regulation of NR2B trafficking in hippocampal neurons. *J. Neurosci.* 23:131–140.

Haycraft, C.J., B. Banizs, Y. Aydin-Son, Q. Zhang, E.J. Michaud, and B.K. Yoder. 2005. Gli2 and Gli3 localize to cilia and require the intraflagellar transport protein polaris for processing and function. *PLoS Genet.* 1:e53. doi:10.1371/journal.pgen.0010053.

Hui, C.-C., and S. Angers. 2011. Gli Proteins in Development and Disease. *Annu. Rev. Cell Dev. Biol.* 27:513–537. doi:10.1146/annurev-cellbio-092910-154048.

Insinna, C., M. Humby, T. Sedmak, U. Wolfrum, and J.C. Besharse. 2009. Different roles for KIF17 and kinesin II in photoreceptor development and maintenance. *Dev. Dyn.* 238:2211–2222. doi:10.1002/dvdy.21956.

Izzi, L., M. Lévesque, S. Morin, D. Laniel, B.C. Wilkes, F. Mille, R.S. Krauss, A.P. McMahon, B.L. Allen, and F. Charron. 2011. Boc and Gas1 Each Form Distinct Shh Receptor Complexes with Ptch1 and Are Required for Shh-Mediated Cell Proliferation. *Developmental Cell*. 20:788–801. doi:10.1016/j.devcel.2011.04.017.

Jaulin, F., and G. Kreitzer. 2010. KIF17 stabilizes microtubules and contributes to epithelial morphogenesis by acting at MT plus ends with EB1 and APC. *J. Cell Biol.* 190:443–460. doi:10.1083/jcb.201006044.

Jiang, L., B.M. Tam, G. Ying, S. Wu, W.W. Hauswirth, J.M. Frederick, O.L. Moritz, and W. Baehr. 2015. Kinesin family 17 (osmotic avoidance abnormal-3) is dispensable for photoreceptor morphology and function. *FASEB J.* doi:10.1096/fj.15-275677.

Keady, B.T., R. Samtani, K. Tobita, M. Tsuchya, J.T. San Agustin, J.A. Follit, J.A. Jonassen, R. Subramanian, C.W. Lo, and G.J. Pazour. 2012. IFT25 Links the Signal-Dependent Movement of Hedgehog Components to Intraflagellar Transport. *Developmental Cell*. 22:940–951. doi:10.1016/j.devcel.2012.04.009.

Kim, J., M. Kato, and P.A. Beachy. 2009. Gli2 trafficking links Hedgehog-dependent activation of Smoothened in the primary cilium to transcriptional activation in the nucleus. *Proc. Natl. Acad. Sci. U.S.A.* 106:21666–21671. doi:10.1073/pnas.0912180106.

Liu, A., B. Wang, and L.A. Niswander. 2005. Mouse intraflagellar transport proteins regulate both the activator and repressor functions of Gli transcription factors. *Development*. 132:3103–3111. doi:10.1242/dev.01894.

Liu, J., H. Zeng, and A. Liu. 2015. The loss of Hh responsiveness by a non-ciliary Gli2 variant. *Development*. doi:10.1242/dev.119669.

Megason, S.G., and A.P. McMahon. 2002. A mitogen gradient of dorsal midline Wnts organizes growth in the CNS.

Ocbina, P.J.R., J.T. Eggenschwiler, I. Moskowitz, and K.V. Anderson. 2011. Complex interactions between genes controlling trafficking in primary cilia. *Nat Genet*. doi:10.1038/ng.832.

Pan, Y., C.B. Bai, A.L. Joyner, and B. Wang. 2006. Sonic hedgehog signaling regulates Gli2

transcriptional activity by suppressing its processing and degradation. *Molecular and Cellular Biology*. 26:3365–3377. doi:10.1128/MCB.26.9.3365-3377.2006.

Pedersen, L.B., and J.L. Rosenbaum. 2008. Intraflagellar transport (IFT) role in ciliary assembly, resorption and signalling. *Curr. Top. Dev. Biol.* 85:23–61. doi:10.1016/S0070-2153(08)00802-8.

Qin, J., Y. Lin, R.X. Norman, H.W. Ko, and J.T. Eggenschwiler. 2011. Intraflagellar transport protein 122 antagonizes Sonic Hedgehog signaling and controls ciliary localization of pathway components. *Proceedings of the …*.

Ruiz i Altaba, A., V. Palma, and N. Dahmane. 2002. Hedgehog-Gli signalling and the growth of the brain. *Nat. Rev. Neurosci.* 3:24–33. doi:10.1038/nrn704.

Santos, N., and J.F. Reiter. 2014. A central region of Gli2 regulates its localization to the primary cilium and transcriptional activity. *J. Cell. Sci.* 127:1500–1510. doi:10.1242/jcs.139253.

Sasaki, H., Y. Nishizaki, C. Hui, M. Nakafuku, and H. Kondoh. 1999. Regulation of Gli2 and Gli3 activities by an amino-terminal repression domain: implication of Gli2 and Gli3 as primary mediators of Shh signaling. *Development*. 126:3915–3924.

Sauer, B. 1994. Site-specific recombination: developments and applications. *Curr. Opin. Biotechnol.* 5:521–527.

Scholey, J.M. 2013. Kinesin-2: A Family of Heterotrimeric and Homodimeric Motors with Diverse Intracellular Transport Functions. *Annu. Rev. Cell Dev. Biol.*

Setou, M., T. Nakagawa, D.H. Seog, and N. Hirokawa. 2000. Kinesin superfamily motor protein KIF17 and mLin-10 in NMDA receptor-containing vesicle transport. *Science*. 288:1796–1802.

Stamataki, D. 2005. A gradient of Gli activity mediates graded Sonic Hedgehog signaling in the neural tube. *Genes & Development*. 19:626–641. doi:10.1101/gad.325905.

Tarabeux, J., N. Champagne, E. Brustein, F.F. Hamdan, J. Gauthier, M. Lapointe, C. Maios, A. Piton, D. Spiegelman, É. Henrion, B. Millet, J.L. Rapoport, L.E. DeLisi, R. Joober, F. Fathalli, É. Fombonne, L. Mottron, N. Forget-Dubois, M. Boivin, J.L. Michaud, R.G. Lafrenière, P. Drapeau, M.-O. Krebs, and G.A. Rouleau. 2010. De Novo Truncating Mutation in Kinesin 17 Associated with Schizophrenia. *Biological Psychiatry*. 68:649–656. doi:10.1016/j.biopsych.2010.04.018.

Tukachinsky, H., L.V. Lopez, and A. Salic. 2010. A mechanism for vertebrate Hedgehog signaling: recruitment to cilia and dissociation of SuFu-Gli protein complexes. *J. Cell Biol.* 191:415–428. doi:10.1083/jcb.201004108.

Verhey, K.J., and J.W. Hammond. 2009. Traffic control: regulation of kinesin motors. *Nat Rev Mol Cell Biol*. 10:765–777. doi:10.1038/nrm2782.

Wang, B., J.F. Fallon, and P.A. Beachy. 2000. Hedgehog-regulated processing of Gli3 produces an anterior/posterior repressor gradient in the developing vertebrate limb. *Cell*. 100:423–434.

Wechsler-Reya, R.J., and M.P. Scott. 1999. Control of Neuronal Precursor Proliferation in the Cerebellum by Sonic Hedgehog. *Neuron*. 22:103–114. doi:10.1016/S0896-6273(00)80682-0.

Wen, X., C.K. Lai, M. Evangelista, J.A. Hongo, F.J. de Sauvage, and S.J. Scales. 2010. Kinetics of Hedgehog-Dependent Full-Length Gli3 Accumulation in Primary Cilia and Subsequent Degradation. *Molecular and Cellular Biology*. 30:1910–1922. doi:10.1128/MCB.01089-09.

Wong-Riley, M.T.T., and J.C. Besharse. 2012. The kinesin superfamily protein KIF17: one protein with many functions. *Biomol Concepts*. 3:267–282. doi:10.1515/bmc-2011-0064.

Yamada, K., and M. Watanabe. 2002. Cytodifferentiation of Bergmann glia and its relationship with Purkinje cells. *Anat Sci Int*. 77:94–108. doi:10.1046/j.0022-7722.2002.00021.x.

Yang, N., L. Li, T. Eguether, J.P. Sundberg, G.J. Pazour, and J. Chen. Intraflagellar transport 27 is essential for hedgehog signaling but dispensable for ciliogenesis during hair follicle morphogenesis. *proxy.lib.umich.edu*.

Yin, X., X. Feng, Y. Takei, and N. Hirokawa. 2012. Regulation of NMDA receptor transport: a KIF17-cargo binding/releasing underlies synaptic plasticity and memory in vivo. *J. Neurosci.* 32:5486–5499. doi:10.1523/JNEUROSCI.0718-12.2012.

Zeng, H., J. Jia, and A. Liu. 2010. Coordinated translocation of mammalian Gli proteins and suppressor of fused to the primary cilium. *PLoS ONE*. 5:e15900. doi:10.1371/journal.pone.0015900.

CHAPTER IV:

Discussion and Future Directions

4.1 Regulation of GLI protein function by the heterotrimeric kinesin-2 complex

4.1.1 GLI proteins specifically interact with distinct members of the heterotrimeric kinesin-2 complex

Despite their implication in HH signaling for more than a decade, in Chapter II I provide the first evidence that the heterotrimeric KIF3A/KIF3B/KAP3 complex physically interacts with all mammalian GLI proteins. Interestingly, I demonstrate that GLI2 specifically interacts with KIF3A, but not KIF3B, and I further detect synergistic interactions between GLI2, KIF3A and KAP3. These findings provide another example of how the heterotrimeric kinesin-2 motor complex interacts with specific protein cargos, an area that still remains poorly understood. Since it is largely accepted that KIF3A and KIF3B exist as a heterodimer(Yamazaki et al., 1995), it is interesting that GLI2 interacts with KIF3A and KAP3, but not KIF3B. It will be important to determine whether this is the general mechanism by which the heterotrimeric kinesn-2 complexes bind cargo, or whether this is distinct interaction with KIF3A and KAP3 is specific to GLI proteins. Further, it will also be important to test whether GLI1 and GLI3 also fail to interact with KIF3B. Future biochemical studies with GLI proteins and additional protein cargos

will help define how the heterotrimeric kinesin-2 complex interacts with cargo and how these interactions regulate protein cargo function.

Anderson and colleagues eloquently showed that KIF7 lacks plus-end-directed microtubule trafficking capabilities (He et al., 2014); based on my findings in Chapter II, I propose that the heterotrimeric kinesin-2 motor complex regulates GLI trafficking toward the plus-ends of microtubules. These findings are particularly interesting given that it is largely accepted that kinesin-2 cargo anterograde trafficking is mediated by IFT particles (Scholey, 2003; Qin et al., 2004; Bhogaraju et al., 2013). Our findings are consistent with emerging reports showing that the heterotrimeric kinesin-2 complex directly interacts with and regulates anterograde trafficking of dynein motors independent of IFT proteins (Hao et al., 2011). Together these findings suggest a new paradigm where the heterotrimeric kinesin-2 complex interacts with protein cargo through interactions with distinct complex members independent of IFT particles to mediate plus-end-directed microtubule trafficking. While I provide evidence that GLI proteins interact with KAP3 in the absence of IFT particles using in vitro binding assays, it will be important to perform additional biochemical studies to determine whether IFT particles can also interact with GLI proteins to mediate both ciliary and non-ciliary trafficking.

Through extensive structure-function biochemical analyses, I demonstrate that KAP3 binds a specific 47 amino-acid N-terminal sequence that is conserved between GLI2 and GLI3. While deleting this domain in full-length GLI2 and the C-terminally truncated GLI3 repressor (GLI3R) prevents KAP3 binding, GLI1 lacks the conserved 47 amino-acid N-terminal KAP3 binding sequence but still robustly interacts with KAP3. Furthermore, fusing the conserved 47 amino-acid KAP3 binding domain to the N-terminally truncated constitutive GLI activator (GLI2ΔN) is not sufficient to rescue the KAP3 interaction (Figure 4.1). Together these data

suggest that KAP3 may interact with GLI proteins through multiple motifs, but further biochemical studies are required to identify additional KAP3 binding domains. Similar mapping experiments that I used to identify the KAP3 binding domain within GLI2 are necessary to determine whether KIF3A interacts with GLI2 and GLI3 via the same motif as KAP3. In chapter II, I also showed that KAP3 interacts with GLI2 via it armadillo repeats and that the motor domain of KIF3A is dispensable for GLI2 interaction. It will be important to further map domains within both KAP3 and KIF3A that mediate interactions with GLI proteins. By identifying interaction domains within all three mammalian GLI proteins, KIF3A, and KAP3 that mediate complex formation, we will improve our understanding of how these kinesin-2 motor complexes dynamically interact with protein cargos, like GLI proteins.

In Chapter II, I show that GLI2 interacts with KIF3A and KAP3 units of the heterotrimeric kinesin-2 complex but a major unanswered question is where do these interactions take place within the cell. Further microscopy experiments are required to determine if the interactions between KIF3A, KAP3, and GLI proteins occur within primary cilia, cytoplasmic trafficking to and from the cilium, and/or during nuclear entry. One way to assess this would be to use CRISPR technologies (Singh et al., 2015) to generate mice that endogenously express both GFP-tagged GLI2 and mCherry-tagged KAP3 or KIF3A. Once generated, these provide excellent tools to assess co-localization of GLI2::GFP with KAP3::mCherry or KIF3A::mCherry in a wide range of HH responsive tissues, including the neural tube, using live cell imaging and confocal microscopy. These tools will not only aid in visualizing the subcellular co-localization of GLI2 with KAP3 and KIF3A, but will also provide information on how the heterotrimeric complex regulates ciliary and/or non-ciliary trafficking of GLI2.

Biochemical and functional assessment of the interactions between GLI proteins and heterotrimeric complex members were performed in the absence of HH pathway activation, largely due to the fact that in the absence of HH ligand GLI proteins still traffic between multiple subcellular compartments including the primary cilia. To determine whether the interaction between GLI proteins and KAP3 are altered in the presence of HH pathway activation, I would perform the same biochemical assays from Chapter II in a HH-responsive cell type (i.e. NIH/3T3 cells) in the presence of HH ligand. Furthermore, whether primary cilia are required for the interaction between GLI2 and KIF3A and KIF3B has not been tested. Performing additional biochemical experiments in *Ift88*$^{-/-}$ mouse embryonic fibroblast (MEFs) that are defective in cilia formation, will determine whether cilia are necessary for these interactions. HH pathway activation promotes the dissociation of SUFU and GLI complexes and this dissociation requires primary cilia (Humke et al., 2010; Tukachinsky et al., 2010). The proposed experiments will test whether, like SUFU, the interactions between KAP3 and GLI proteins are altered by HH pathway activation and primary cilia.

4.1.2 KAP3 interacts with GLI proteins and regulates GLI activator function

In addition to identifying physical interactions between GLI proteins and the heterotrimeric kinesin-2 complex, I further show in Chapter II that the interaction between KAP3 and GLI proteins specifically regulates GLI2 activator, but not GLI3 repressor activity, suggesting that the interaction between GLI proteins and the kinesin-2 components are necessary for proper transcriptional activity of GLI proteins. While these findings suggest that the heterotrimeric kinesin-2 complex regulates GLI activator function, more work is required to determine the mechanism that underlies this regulation.

Deleting the KAP3 binding domain from GLI2 and GLI3R results in an increase in GLI2 transcriptional activity, but has no affect on GLI3 repressor activity. These findings are strikingly similar to those observed with SUFU (Wang et al., 2010). In these studies, SUFU interacts with both GLI2 and GLI3, however GLI3 repressor is able to rescue the ventralized neural tube phenotype in *Sufu*$^{-/-}$ embryos (Wang et al., 2010). It is interesting to speculate that, like SUFU, KAP3 may regulate GLI activator proteins as they traffic to the nucleus. Furthermore, immunoprecipitation of GLI2 from COS-7 cells transiently expressing GLI2 and either SUFU or KAP3 robustly co-immunoprecipitates SUFU and KAP3, respectively (Figure 4.2A lanes 5 and 6). However, immunoprecipitating GLI2 from lysates transiently transfected with GLI2, SUFU, and KAP3 decreases the amount of KAP3 that co-immunoprecipitates with GLI2 (Figure 4.2A, lane 8). These results suggest that either GLI2 exists in a complex with KAP3 distinct from its complex with SUFU or that SUFU and KAP3 compete for the same GLI2 binding domain (**Figure 4.2B**). One way to distinguish between these two possibilities is to immunoprecipitate SUFU from cells transiently expressing GLI2, SUFU, and KAP3 and assess whether KAP3 co-immunoprecipitates with SUFU. In addition, it will be interesting to test whether the GLI2 mutant lacking the KAP3 binding domain (GLI2Δ61-108) can interact with SUFU. While this site does not overlap with the published SYGH SUFU-binding motif (Dunaeva et al., 2003) it is possible that the close proximity of the SUFU and KAP3 binding sites may prevent simultaneous interactions of SUFU and KAP3 with GLI proteins. Similar to the in vitro binding assays in Chapter II used to assess direct interactions between KAP3 and GLI1, it will also be important to purify SUFU and GLI2 and perform in vitro binding assays to determine whether these interactions are also direct. In addition to the GFP-tagged GLI2 and mCherry-tagged KAP3 described above, I would also propose utlizing CRISPR techniques to replace the endogenous

Gli2 locus with a GFP-tagged GLI2Δ61-108 allele that is deficient in KAP3 binding. Along with assessing the cellular distribution of GLI2Δ61-108, we could also gain insights into the function of this construct in HH-dependent tissue patterning.

Similar to SUFU, KIF7 interactions with GLI proteins both positively and negatively regulate their function (Maurya et al., 2013; Cheung et al., 2009). Further, KIF7 organizes the ciliary tip compartment through the regulation of microtubule dynamics (He et al., 2014). Like KAP3 and SUFU, KIF7 interacts with GLI proteins but these domains have not been precisely mapped (Marks and Kalderon, 2011). It is possible that KAP3 competes for KIF7 binding to GLI proteins, thus limiting dissociation of GLI-SUFU complexes and restricting GLI protein function. Moving forward, it will be important to identify the domains where KIF7 interacts with GLI2 and whether these sites are distinct or overlap with the KAP3 binding motif. Another possibility is that KAP3-GLI protein interactions are disrupted in *Kif7* mutant cells due to the disorganized ciliary tip compartments. It will be particularly important to test these interactions in KIF7-deficient cells, and to assess the role of KIF7 in mediating kinesin-2 interactions with GLI proteins both in the presence and absence of HH pathway activation. More detailed biochemical mapping and live cell imaging will help decipher whether KAP3 is mediating GLI activator function through distinct or shared roles with SUFU and KIF7.

4.2 Role of the homodimeric kinesin-2 complex in regulating GLI protein function

4.2.1 KIF17 regulation of HH signaling through interactions with GLI proteins

Unlike the heterotrimeric KIF3A/KIF3B/KAP3 complex, the homodimeric KIF17 motor complex is dispensable for mammalian ciliogenesis and has not been implicated in HH signaling (Jenkins et al., 2006; Scholey, 2013). In Chapter III, I investigate the potential role for KIF17 in

HH signaling through interactions with GLI proteins. Here I show that, like KAP3, KIF17 interacts with all three mammalian GLI proteins. These findings suggest that both homodimeric and heterotrimeric knesin-2 motor complexes regulate HH signaling, and that KIF17 may regulate GLI trafficking and function through physical interactions. Extensive biochemical experiments are necessary to map the domains in each of the GLI proteins that mediate interactions with KIF17. Furthermore, though it is suggested that KIF17 interacts with cargo via the C-terminal tail domain (Setou et al., 2000), it will also be important to determine whether GLI proteins also interact with KIF17 via the tail domain. It will also be important to test the functional consequences of these interactions using a combination of cell-based and in vivo functional assays similar to the ones performed with the KAP3 binding-deficient GLI2 mutant (GLI2Δ61-108) in Chapter II.

In Chapter III, I show that stable expression of a dominant-negative version of KIF17 that lacks the motor domain KIF17 (KIF17_466-1029) causes a decrease in GLI1 expression; however, GLI localization and GLI3 processing are not altered in these cells. In contrast to low-level expression of a motorless version of KIF17, high-level expression of the KIF17 tail-domain (KIF17_801-1029) disrupts GLI2 localization, yet does not affect on HH signaling in cell-based luciferase assays (Figure 4.3). One explanation for normal GLI localization in the presence of low-level motorless KIF17 is that there is simply not enough mutant KIF17 present to exert a dominant negative effect on endogenous KIF17 motor function. Because not all cells were expressing the KIF17 tail domain due to transient transfections, I was unable to test whether the KIF17 tail domain alters GLI1 protein expression in whole cell lysates. Fortunately, the p*CIG* vector used to clone the KIF17 tail domain construct contains a nuclear GFP sequence and can be used to sort the cells expressing the dominant-negative KIF17 tail domain construct using

flow cytometry. By doing so, I will be able to determine whether GLI1 protein expression is similarly affected in high-expressing versus low-expressing dominant–negative KIF17 cells. It will also be important to perform these experiments using the same dominant negative KIF17 constructs. It is possible that the KIF17 tail domain construct, which lacks the motor domain and the coiled-coiled domain that is important in homodimerization (Setou et al., 2000), and the KIF17 construct that lacks only the motor domain may affect GLI localization and function differentially. While these findings implicate KIF17 as a potential regulator of GLI ciliary localization and HH target gene expression, more experiments are necessary to elucidate whether KIF17 regulates HH target gene expression directly through trafficking of GLI proteins or through additional mechanisms. For example, KIF17 stabilizes microtubules in epithelial cells and could be indirectly altering GLI activity and/or HH target gene expression by modulating microtubule dynamics (Jaulin and Kreitzer, 2010).

4.2.2 Investigation of a role for KIF17 in regulating HH-dependent cerebellar proliferation

Examining KIF17 expression during pre- and postnatal development led to the exciting finding in Chapter III that KIF17 is expressed in the developing cerebellum. These findings support initial reports that characterized KIF17 as a "brain-specific" homodimeric kinesin-2 motor complex (Setou et al., 2000). Further, the finding that KIF17 expression is largely restricted to postnatal neuronal tissues may explain how KIF17 could be playing a major role in regulating GLI protein trafficking and function, yet *Kif17*$^{-/-}$ mice are viable and display grossly normal body plans. Based on my expression analysis of KIF17, the cerebellum is the only tissue where both KIF17 and GLI proteins are co-expressed together at high levels (our observations and (Corrales et al., 2004). These finding are particularly interesting since cerebellar

proliferation depends on proper HH signaling and GLI protein function (Wechsler-Reya and Scott, 1999; Corrales et al., 2004; 2006). Furthermore, we observe that *Kif17*$^{-/-}$ mice display smaller cerebella and that *Kif17* co-localizes with *Gli1* and *Gli2* in the Purkinje cell layer (PCL) during cerebellum development. While these observations are interesting, further experiments are required to determine if KIF17 regulates HH-dependent cerebellar proliferation. SHH is secreted from Purkinje cells (PC) within the PCL and induces proliferation of granule progenitor cells (GCP) located with the external granule layer (EGL) (Wechsler-Reya and Scott, 1999; Dahmane and Ruiz i Altaba, 1999; Wallace and Raff, 1999). As a first step in determining whether KIF17 is required for HH-dependent cerebellar proliferation, I would assess GCP cell proliferation and apoptosis in wildtype versus *Kif17*$^{-/-}$ cerebella using markers for Ki67 and cleaved caspase-3, respectively. To further determine whether the defects in cerebellar proliferation observed in *Kif17*$^{-/-}$ mice are dependent on HH signaling, I would isolate GCPs and perform proliferation assays using recombinant SHH ligand (Izzi et al., 2011; Wechsler-Reya and Scott, 1999).

More in depth immunofluorescence experiments, including co-staining with additional PC and Bergman glia (BG) cell markers, will confirm whether *Kif17* is expressed in PCs or in BGs within the PCL. However, my preliminary co-staining experiments with the PC marker, LIM1/2, suggest that *Kif17* is specifically expressed in PCs. This is particularly interesting because SHH is produced and secreted by PCs, where as *Gli1* and *Gli2* appear to be restricted to BGs during cerebellar proliferation (Corrales et al., 2004; Wechsler-Reya and Scott, 1999). BGs are intimately associated with PCs in the PCL and are important for regulating PC structure in the adult cerebellum (Yamada and Watanabe, 2002). While *Gli*s do not appear to be highly expressed in PCs (Corrales et al., 2004), these results are unclear. Further experiments are

required to determine whether *Gli*s, *Shh*, and *Kif17* are present in the same or distinct cell types within the PCL. Interestingly, *GLI*s and *Kif17* remain highly expressed in the PCL in adult mice yet it remains unclear whether HH signaling contributes to maintenance of the adult cerebellum. Future experiments are necessary to test this possibility and whether KIF17 regulates HH dependent cerebellar proliferation and/or maintenance of the adult cerebellum through direct interactions with GLI proteins.

4.3 Conclusion

Here, I define novel interactions between the effector molecules of the HH signaling pathway, the GLI proteins, and kinesin-2 motors, namely the heterotrimeric KIF3A/KIF3B/KAP3 and homodimeric KIF17 motor complexes. In doing so, I improve our understanding of how GLI proteins are regulated by microtubule-based motor proteins; in addition, I provide details into how kinesin-2 motors interact with protein cargo. In particular, I map a novel domain within GLI2 and GLI3 that mediates KAP3 interaction and show that this interaction specifically regulating GLI activator function, but not GLI repressor function. It will be imperative to determine the subcellular location of the interactions between GLI proteins and kinesin-2 motors and to test whether these interactions require primary cilium. In addition to KAP3, I show that GLI proteins interact with KIF3A and KIF17, yet how these interactions affect GLI transcriptional activity require further investigation. Future mapping experiments are necessary to determine whether kinesin-2 motor complexes interact with and regulate GLI proteins function through the same or distinct domains (Figure 4.4) Once a more complete map of GLI-kinesin-2 interactions is available, CRISPR technology can be used to generate mice replacing endogenous *Gli2* with versions that are defective in interacting with specific or various

combinations of kinesin-2 motor proteins (Figure 4.4). Mouse mutants expressing *Gli2* variants that selectively interact with distinct kinesin-2 motor proteins could be used to test the consequences of GLI and kinesin-2 interactions throughout vertebrate embryonic development and during adult tissue maintenance. Together, my experimental findings define novel interactions between GLI2 and kinesin-2 proteins thereby providing the framework for future studies aimed at elucidating the complex mechanisms by which kinesin-2 motor complexes regulate GLI protein trafficking and function.

4.4 Materials and Methods

DNA Constructs

To generate 6X MYC-tagged constructs h*Gli2*, h*Gli2ΔN*, cDNAs were cloned into pCDNA3 using standard molecular biology techniques. To generate a version of hGLI2 lacking amino acids 61-108 (h*Gli2*$\Delta^{61\text{-}108}$), we amplified h*Gli2* using forward (5'-TCTTGCCACCATTCCATGCGGCTGGCCCTGGGGAGTCCCC- 3') and reverse (5'-GGGGACTCCCCAGGGCCAGCCGCATGGAATGGTGGCAAGA-3') mutagenesis primers. To generate a version of h*GLI2*Δ*N* fused to amino acids 61-108 (61_108_h*Gli2*Δ*N*) we amplified h*Gli2* using forward (5'-GGCTTTCCCCGCACCCGGCTATGGCCCTCACCTCCATCAA -3') and reverse (5'- TTGATGGAGGTGAGGGCCATAGCCGGGTGCGGGGAAAGCC-3') mutagenesis primers. Hemagglutinin (HA)-tagged h*KIF17* construct and variants were generated from full-length human *KIF17* cDNA (provided by Kristen J. Verhey, University of Michigan Ann Arbor, MI). Briefly, full-length *hKIF17* (amino acids 1-1027) and DNKIF17 (amino acids 801-1027), were cloned into pGIG (Megason and McMahon, 2002) using standard molecular biology techniques.

Immunoprecipitation and Western Blot Analysis

COS-7 cells were transiently transfected with the relevant DNA constructs using Lipofectamine 2000 (Invitrogen, Cat. #11668). The cells were lysed 48 hr after transfection in HEPES lysis buffer (25mM HEPES pH 7.4, 115mM KOAc, 5mM NaOAc, 5mM $MgCl_2$, 0.5mM EGTA, and 1% TX-100) containing protease inhibitor (Roche, Cat. #11836153001). Cell lysates were then subjected to centrifugation at 14,000 x *g* for 15 min to remove the insoluble fraction and protein concentrations were determined using a BCA Assay Kit (Pierce, Cat. #23225). Cell lysates (1mg) were then pre-cleared with Protein G agarose beads (Roche, Cat. #11719416001) for 1 hr at 4°C. MYC- or HA-tagged proteins were immunoprecipitated from pre-cleared lysates using either anti-MYC (1:150; Santa Cruz, Cat. #sc-40) or anti-HA (1:300; Covance, Cat. #MMS-101) antibodies for 2 hr at 4°C. Following immunoprecipitation, the lysates were incubated with Protein G agarose beads for 1 hr at 4°C. The Protein G agarose beads were washed 5 x 8 min in HEPES lysis buffer and re-suspended in 30 µl of 1x PBS and 6x Laemmli buffer. The samples were boiled for 10 minutes and proteins were separated using SDS-PAGE and analyzed by western blotting. Anti-MYC (1:1000), anti-FLAG (1:1000) and anti-HA (1:1000) primary antibodies, peroxidase-conjugated AffiniPure goat anti-mouse light chain secondary antibody (1:50,000; Jackson ImmunoResearch, Cat. # 115-035-174), and a Konica Minolta SRX-101A medical film processor were used to visualize tagged proteins.

Immunofluorescence staining

NIH/3T3 fibroblasts were seeded at a density of 1.5 x 10^5 cells/well in 6 well plates. Cells were transfected 24 hr later with either empty vector (pCIG) or with a DNA construct encoding

KIF17::HA or KIF17(801-1029) using Lipofectamine 2000. Cells were grown in low-serum media starting 8 hr after transfection, fixed 48 hr post-transfection in 4% paraformaldehyde for 10 min at room temperature, and permeabilized with a 5 min incubation in 0.2% Triton X-100 in PBS. Immunostaining was performed using the following primary antibodies: mouse anti-acetylated tubulin (1:2500; Sigma), mouse anti-HA (1:1000; Covance), guinea pig anti-GLI2 (1:300; a gift from Dr. J.T. Eggenschwiler, University of Georgia). The following secondary antibodies were used at a dilution of 1:500: Alexa 488 goat anti-guinea pig IgG, Alexa 555 goat anti-mouse IgG1, Alexa 633 goat anti-rabbit IgG2b. To visualize nuclei, DAPI (Invitrogen) was incubated for 5 min at a dilution of 1:30,000. Cells were imaged using a Leica Upright SP5X White Light Laser Confocal Microscope. Images were processed using Adobe Photoshop and Illustrator. GLI2 fluorescence at the ciliary tip was quantified across multiple experiments using imageJ.

Cell Culture and Luciferase Assays

NIH/3T3 cells were cultured at 37°C, 5% CO_2, 95% humidity in Dulbecco's modified eagle medium (DMEM; Gibco, Cat. #11965-092) containing 10% bovine calf serum (ATCC; Cat. #30-2030) and penicillin/streptomycin/glutamine (Gibco, Cat. #10378-016). Luciferase assays were performed by plating 2.5 x 10^4 cells/well in 24 well plates. The next day cells were co-transfected using Lipofectamine 2000 with the DNA constructs indicated in each experiment in addition to *Ptc*Δ136-GL3 (Chen et al., 1999; Nybakken et al., 2005) and pSV-Beta-galactosidase (Promega) constructs to report HH pathway activation and normalize transfections, respectively. Cells were changed to low-serum media (DMEM supplemented with 0.5% bovine calf serum and penicillin/streptomycin/glutamine) 48 hr after transfection and cultured at 37°C in

5%$C0_2$ for an additional 48 hr. NSHH-conditioned medium was added immediately after low-serum change where relevant to activate the HH pathway. Cells were harvested and luciferase and beta-galactosidase activities were measured using Luciferase Assay System (Promega Cat. # E1501) and BetaFluor β-gal assay kit (Novagen, Cat. #70979-3). Multiple assays were performed and each sample was assayed in triplicate.

4.5 Figures

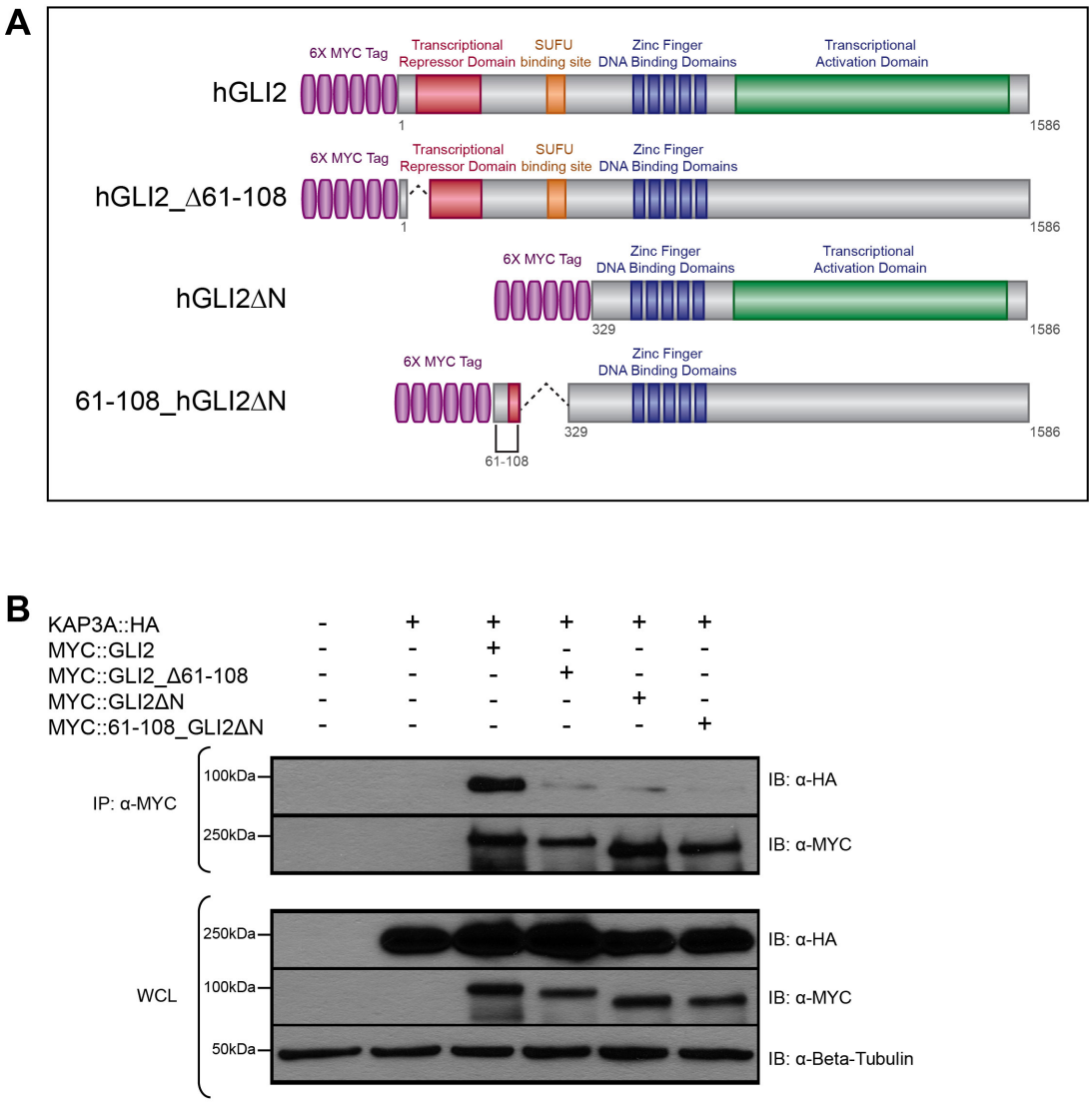

Figure 4.1. 61-108_GLI2ΔN does not rescue GLI2 interaction with KAP3A.
(A) Graphic representation of full-length and truncated human GLI2 proteins. A 6X MYC epitope tag (purple) is present at the N-terminus of each GLI2 protein. Highly conserved GLI2 protein sequences include a transcriptional repressor domain (red, absent from hGLI2ΔN), SUFU binding site (orange, absent from hGLI2ΔN), five zinc-finger DNA binding domains (dark blue), and a transcriptional activation domain (green). (B) Immunoprecipitation of MYC::GLI2, MYC::GLI2ΔN, MYC::GLI2Δ61_108, or MYC::61_108GLI2ΔN from COS-7 cells co-expressing KAP3A::HA. Immunoprecipitates (IP) and whole cell lysates (WCL) were subjected to SDS-PAGE and western blot analysis (IB) using antibodies directed against MYC (α-MYC) and HA (α-HA). Antibody detection of Beta-Tubulin (α-Beta-Tubulin) was used to confirm equal loading across lanes. The molecular weights (in kDa) of protein standards are indicated at the left of each blot

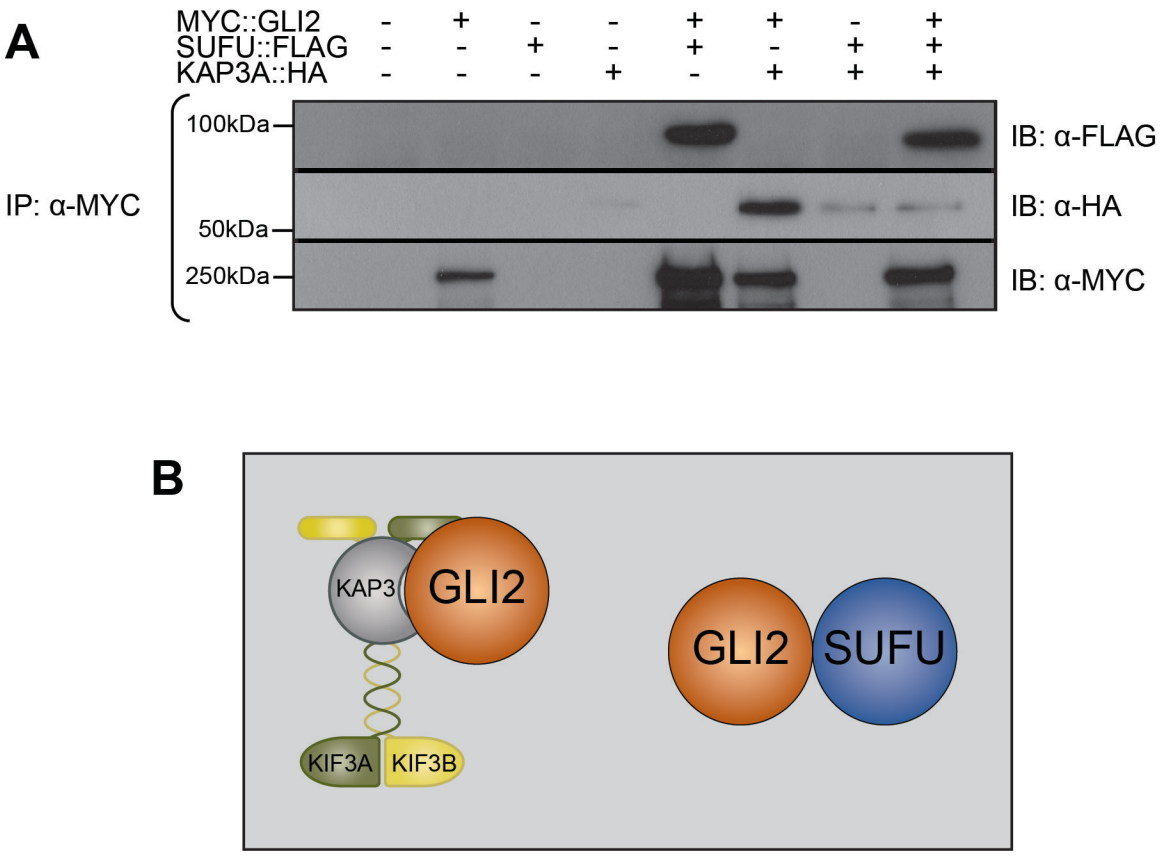

Figure 4.2. SUFU and KAP3 form distinct complexes with GLI2.
(A) Immunoprecipitation of MYC::GLI2 from COS-7 cells co-expressing KAP3A::HA and SUFU::FLAG. Immunoprecipitates (IP) subjected to SDS-PAGE and western blot analysis (IB) using antibodies directed against MYC (α-MYC) and HA (α-HA). The molecular weights (in kDa) of protein standards are indicated at the left of each blot (B) Graphic representation of two separate complexes containing GLI2. (Left) GLI2 (orange) interacts with KAP3 (grey) and KIF3A (dark green) in a complex that also contains KIF3B. (Right) GLI2 (orange) interacts with SUFU (blue) in a complex that does not include KAP3.

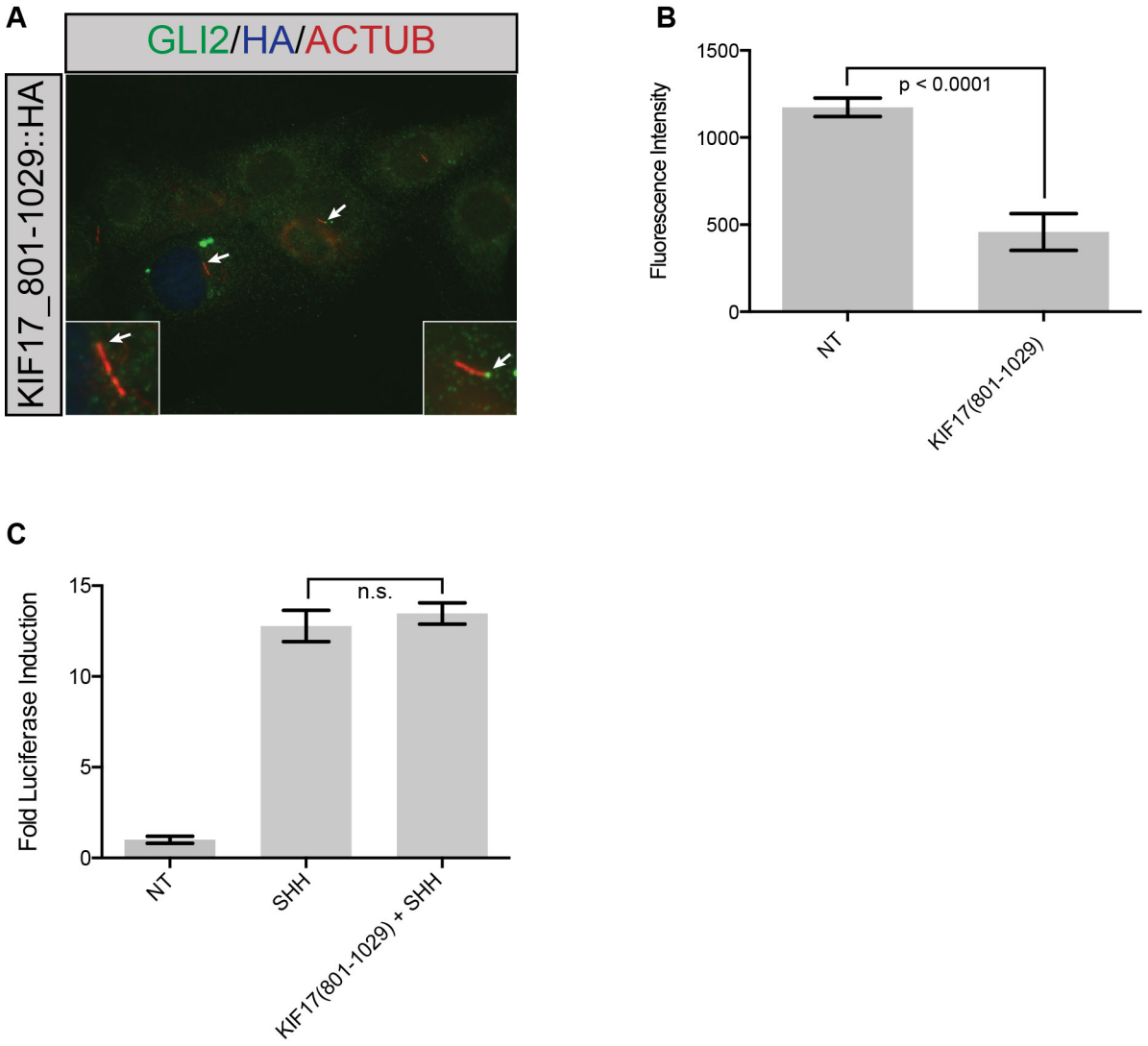

Figure 4.3. Transient transfection of DNKIF17 perturbs GLI2 cilia localization but does not affect HH signaling. (A) Antibody detection of endogenous GLI2 (green) in NIH/3T3 cells expressing HA-tagged KIF17 tail domain (KIF17_801-1029::HA; blue). Primary cilia are identified with antibodies against acetylated tubulin (ACTUB; red). White arrow denote cilia and insets represent high magnifications of cells transfected (left) and untransfected (right) with KIF17_801-1029::HA. (B) Quantification of GLI2 ciliary fluorescence intensity in cells in transfected and untransfected cells. Error bars represent the mean +/- the standard error across three separate experiments; p-values are indicated above the relevant treatment groups (Student's unpaired t-test); n.s., not significant ($p>0.05$). Immunofluorescence experiments in (A) and quantification in (B) were performed by Lynne Blasius. (C) Luciferase activity readout of HH signaling following treatment of NIH/3T3 fibroblasts with NSHH (SHH) after transfection with either empty vector (No Treatment) or KIF17_801-1029::HA. HH pathway activity is measured as fold luciferase induction. Error bars represent the mean +/- S.D. for triplicate samples from a single experiment and are representative of three independent experiments; p-values are indicated above the relevant treatment groups (Student's unpaired *t*-test).

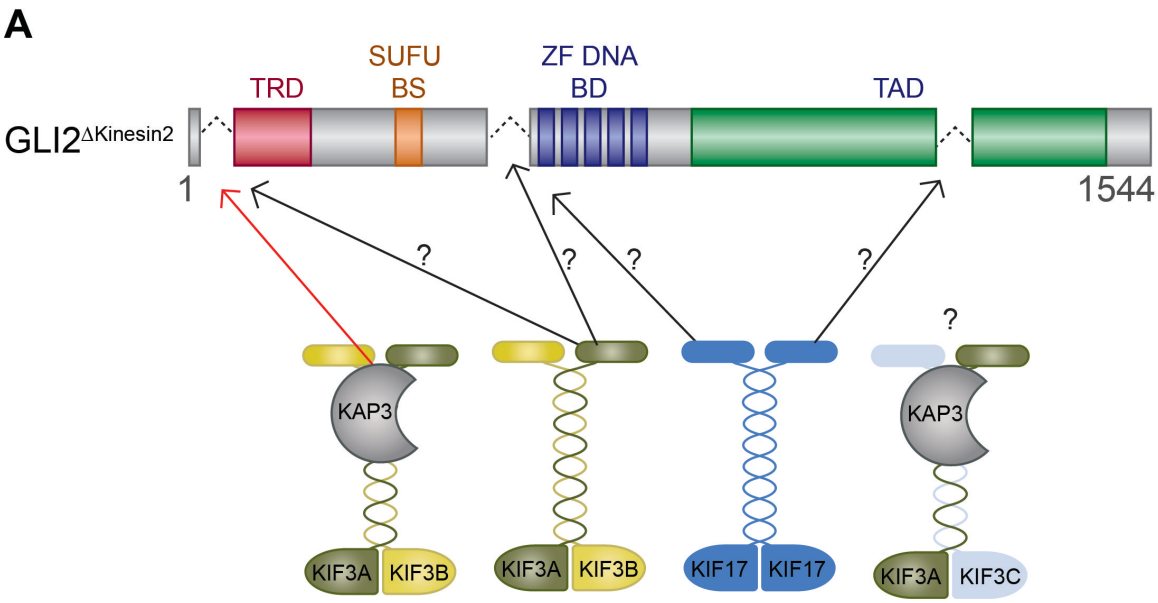

Figure 4.4. Proposed model for defining novel kinesin-2 motor binding domains within GLI2. (A) Graphic illustration of a hypothetical full-length GLI2 protein containing deletions in mapped and unmapped kinesin-2 binding motifs. Highly conserved GLI2 protein sequences include a transcriptional repressor domain (red), SUFU binding site (orange), five zinc-finger DNA binding domains (dark blue), and a transcriptional activation domain (green). Putative kinesin-2 complexes including the heterotrimeric KIF3A/KIF3B/KAP3 complex, heterodimeric KIF3A/KIF3B complex, homodimeric KIF17 complex, and the heterotrimeric KIF3A/KIF3B/KAP3 complex are depicted below with black arrows indicating unmapped binding motifs with unknown function. Red arrow represents experimentally mapped domain required for KAP3 binding that negatively regulates GLI activator function.

4.6 References

Bhogaraju, S., B.D. Engel, and E. Lorentzen. 2013. Intraflagellar transport complex structure and cargo interactions. *Cilia*. 2:10. doi:10.1186/2046-2530-2-10.

Chen, C.H., D.P. von Kessler, W. Park, B. Wang, Y. Ma, and P.A. Beachy. 1999. Nuclear trafficking of Cubitus interruptus in the transcriptional regulation of Hedgehog target gene expression. *Cell*. 98:305–316.

Cheung, H.O.-L., X. Zhang, A. Ribeiro, R. Mo, S. Makino, V. Puviindran, K.K.L. Law, J. Briscoe, and C.-C. Hui. 2009. The Kinesin Protein Kif7 Is a Critical Regulator of Gli Transcription Factors in Mammalian Hedgehog Signaling. *Sci Signal*. 2:ra29. doi:10.1126/scisignal.2000405.

Corrales, J.D., G.L. Rocco, S. Blaess, Q. Guo, and A.L. Joyner. 2004. Spatial pattern of sonic hedgehog signaling through Gli genes during cerebellum development. *Development*. 131:5581–5590. doi:10.1242/dev.01438.

Corrales, J.D., S. Blaess, E.M. Mahoney, and A.L. Joyner. 2006. The level of sonic hedgehog signaling regulates the complexity of cerebellar foliation. *Development*. 133:1811–1821. doi:10.1242/dev.02351.

Dahmane, N., and A. Ruiz i Altaba. 1999. Sonic hedgehog regulates the growth and patterning of the cerebellum. *Development*.

Dunaeva, M., P. Michelson, P. Kogerman, and R. Toftgard. 2003. Characterization of the physical interaction of Gli proteins with SUFU proteins. *J. Biol. Chem.* 278:5116–5122. doi:10.1074/jbc.M209492200.

Hao, L., E. Efimenko, P. Swoboda, and J.M. Scholey. 2011. The retrograde IFT machinery of C. elegans cilia: two IFT dynein complexes? *PLoS ONE*. 6:e20995. doi:10.1371/journal.pone.0020995.

He, M., R. Subramanian, F. Bangs, T. Omelchenko, K.F. Liem Jr, T.M. Kapoor, and K.V. Anderson. 2014. The kinesin-4 protein Kif7 regulates mammalian Hedgehog signalling by organizing the cilium tip compartment. *Nat. Cell Biol.* 16:663–672. doi:doi:10.1038/ncb2988.

Humke, E.W., K.V. Dorn, L. Milenkovic, M.P. Scott, and R. Rohatgi. 2010. The output of Hedgehog signaling is controlled by the dynamic association between Suppressor of Fused and the Gli proteins. *Genes & Development*. 24:670–682. doi:10.1101/gad.1902910.

Izzi, L., M. Lévesque, S. Morin, D. Laniel, B.C. Wilkes, F. Mille, R.S. Krauss, A.P. McMahon, B.L. Allen, and F. Charron. 2011. Boc and Gas1 Each Form Distinct Shh Receptor Complexes with Ptch1 and Are Required for Shh-Mediated Cell Proliferation. *Developmental Cell*. 20:788–801. doi:10.1016/j.devcel.2011.04.017.

Jaulin, F., and G. Kreitzer. 2010. KIF17 stabilizes microtubules and contributes to epithelial

morphogenesis by acting at MT plus ends with EB1 and APC. *J. Cell Biol.* 190:443–460. doi:10.1083/jcb.201006044.

Jenkins, P.M., T.W. Hurd, L. Zhang, D.P. McEwen, R.L. Brown, B. Margolis, K.J. Verhey, and J.R. Martens. 2006. Ciliary targeting of olfactory CNG channels requires the CNGB1b subunit and the kinesin-2 motor protein, KIF17. *Curr. Biol.* 16:1211–1216. doi:10.1016/j.cub.2006.04.034.

Marks, S.A., and D. Kalderon. 2011. Regulation of mammalian Gli proteins by Costal 2 and PKA in Drosophila reveals Hedgehog pathway conservation. *Development*. 138:2533–2542. doi:10.1242/dev.063479.

Maurya, A.K., J. Ben, Z. Zhao, R.T.H. Lee, W. Niah, A.S.M. Ng, A. Iyu, W. Yu, S. Elworthy, F.J.M. van Eeden, and P.W. Ingham. 2013. Positive and Negative Regulation of Gli Activity by Kif7 in the Zebrafish Embryo. *PLoS Genet.* 9:e1003955. doi:10.1371/journal.pgen.1003955.

Megason, S.G., and A.P. McMahon. 2002. A mitogen gradient of dorsal midline Wnts organizes growth in the CNS.

Nybakken, K., S.A. Vokes, T.-Y. Lin, A.P. McMahon, and N. Perrimon. 2005. A genome-wide RNA interference screen in Drosophila melanogaster cells for new components of the Hh signaling pathway. *Nat Genet*. 37:1323–1332. doi:10.1038/ng1682.

Qin, H., D.R. Diener, S. Geimer, D.G. Cole, and J.L. Rosenbaum. 2004. Intraflagellar transport (IFT) cargo: IFT transports flagellar precursors to the tip and turnover products to the cell body. *J. Cell Biol.* 164:255–266. doi:10.1083/jcb.200308132.

Scholey, J.M. 2003. Intraflagellar transport. *Annu. Rev. Cell Dev. Biol.* 19:423–443. doi:10.1146/annurev.cellbio.19.111401.091318.

Scholey, J.M. 2013. Kinesin-2: A Family of Heterotrimeric and Homodimeric Motors with Diverse Intracellular Transport Functions. *Annu. Rev. Cell Dev. Biol.*

Setou, M., T. Nakagawa, D.H. Seog, and N. Hirokawa. 2000. Kinesin superfamily motor protein KIF17 and mLin-10 in NMDA receptor-containing vesicle transport. *Science*. 288:1796–1802.

Singh, P., J.C. Schimenti, and E. Bolcun-Filas. 2015. A mouse geneticist's practical guide to CRISPR applications. *Genetics*. 199:1–15. doi:10.1534/genetics.114.169771.

Tukachinsky, H., L.V. Lopez, and A. Salic. 2010. A mechanism for vertebrate Hedgehog signaling: recruitment to cilia and dissociation of SuFu-Gli protein complexes. *J. Cell Biol.* 191:415–428. doi:10.1083/jcb.201004108.

Wallace, V.A., and M.C. Raff. 1999. A role for Sonic hedgehog in axon-to-astrocyte signalling in the rodent optic nerve. *Development*.

Wang, C., Y. Pan, and B. Wang. 2010. Suppressor of fused and Spop regulate the stability, processing and function of Gli2 and Gli3 full-length activators but not their repressors.

Wechsler-Reya, R.J., and M.P. Scott. 1999. Control of Neuronal Precursor Proliferation in the Cerebellum by Sonic Hedgehog. *Neuron*. 22:103–114. doi:10.1016/S0896-6273(00)80682-0.

Yamada, K., and M. Watanabe. 2002. Cytodifferentiation of Bergmann glia and its relationship with Purkinje cells. *Anat Sci Int*. 77:94–108. doi:10.1046/j.0022-7722.2002.00021.x.

Yamazaki, H., T. Nakata, Y. Okada, and N. Hirokawa. 1995. KIF3A/B: a heterodimeric kinesin superfamily protein that works as a microtubule plus end-directed motor for membrane organelle transport. *J. Cell Biol.* 130:1387–1399.

APPENDIX I:

Supplemental Materials

A1.1 Assessment of endogenous interactions between GLI proteins and KAP3

To test whether endogenous GLI proteins and KAP3 interact, I performed immunoprecipitation experiments using commercially available antibodies against GLI1, GLI3 and KAP3 in an attempt to co-precipitate endogenous GLI-KAP3 complexes (Figure A1.1). I was able to successfully IP endogenous KAP3 from both wildtype and *Gli2*$^{-/-}$*;Gli3*$^{-/-}$ MEFs, and could also specifically co-precipitate endogenous GLI3 in wildtype MEFs as determined by the absence of GLI3 protein in *Gli2;Gli3* double mutant MEFs (Figure A1.1A). However, upon repeating this experiment with additional controls, I determined that endogenous GLI3 non-specifically precipitates with beads alone (i.e. in the absence of KAP3 precipitation), nullifying our initial result. In addition, I performed the converse experiment, where I was able to immunoprecipitate endogenous GLI3; however, I did not detect the co-precipitation of endogenous KAP3 (Figure A1.1B). Further, the use of different lysis conditions did not alter this result (Figure A1.1B, top vs. bottom blots, data not shown). To attempt to enrich for GLI and KAP3 interactions, I performed similar experiments in *Dync2h1*$^{lln/lln}$ MEFs that are deficient in retrograde ciliary trafficking (Figure A1.1B, lane 3, top and bottom blots). However, I also failed to detect endogenous GLI and KAP3 interactions in this cell line.

Further, I attempted immunoprecipitation experiments with KAP3 and GLI1 in wildtype MEFs in the presence of SAG, a Smoothened agonist that stimulates GLI1 expression downstream of Hedgehog pathway activation (Chen et al., 2002). While these experiments successfully up-regulated endogenous GLI1 that I could detect by western blot, and could also successfully immunoprecipitate, I failed to co-precipitate endogenous KAP3. The converse experiment also failed to co-precipitate endogenous GLI1 (Figure A1.1C, top and bottom blots).

It is important to note, however, that the failure to detect endogenous GLI-KAP3 complexes biochemically is exactly what I would predict, especially given the limited amount of ciliary GLI protein within a cell at any given point in time. That is, current published estimates are that only 0.01% of total GLI3 protein is located within the primary cilium of Hedgehog-responsive cells (Wen et al., 2010). Thus, even if this estimate is inaccurate by several orders of magnitude the likelihood of detecting endogenous GLI-KAP3 interactions biochemically is daunting at best. Further, the GLI-KAP3 interactions are likely to be transient, again limiting their detection by standard immunoprecipitation protocols. Additional biochemical experiments are required (i.e. cross-linking GLI-KAP3 complexes prior to immunoprecipitation) to detect endogenous GLI-KAP3 complexes

A1.2 GLI proteins interact with KIF3A via a distinct domain from KAP3

In Chapter II, I show that GLI2 interacts KIF3A and KAP3, but not KIF3B. While I performed detailed mapping experiments to define the GLI2 motif required for KAP3 interaction, where KIF3A interacts with GLI proteins was not reported. Here, I performed an additional biochemical experiment using the epitope-tagged GLI2 and KIF3A proteins generated

in Chapter II to narrow the domain within GLI2 required for interaction with KIF3A (Figure A1.2).

Immunoprecipitation of full-length GLI2, but not GLI2ΔN, co-immunoprecipitates KIF3A (Figure A1.2; lanes 3 and 4). Interestingly, and in contrast to what I observed in Chapter II with KAP3A, immunoprecipitation of $GLI2^{\Delta 61\text{-}108}$ also co-immunoprecipitates KIF3A (Figure A1.2; lane 5). Further, immunoprecipitation of $GLI2^{108\text{-}1586}$ co-immunoprecipitates KIF3A, but this interaction is detected to a lesser degree when immunoprecipitating $GLI2^{154\text{-}1586}$ and $GLI2^{280\text{-}1586}$ (Figure A1.2; lanes 6,7, and 8). Importantly, these results suggest that KIF3A interacts via a domain within GLI2 that is distinct from the KAP3A binding motif that I defined in Chapter II. While these experiments show that two members of the heterotrimeric kinesin-2 complex interact with GLI2 through distinct motifs, more biochemical experiments are required to precisely map the domain within GLI2 required for KIF3A interaction.

A1.3 Full-length GLI3 lacking KAP3 binding motif interacts with KAP3

In Chapter II, I show that KAP3A interacts with a motif that is conserved between GLI2 and GLI3. Deletion of the KAP3 binding motif in either GLI2 or GLI3R results in loss of KAP3 binding. In contrast to GLI2 and GLI3R, deletion of the conserved KAP3 binding motif from full-length GLI3 does not perturb the interaction between GLI3 and KAP3 (Figure A1.3). This result suggests that additional motifs may exist within GLI3 that are important for interaction with KAP3. Interestingly, the finding that GLI1, which lacks the conserved KAP3 binding motif present in both GLI2 and GLI3, also interacts with KAP3 further supports the idea that GLI proteins interact with KAP3 via multiple binding motifs. Additional experiments are necessary to identify and test the functional consequence of these motifs on GLI protein activity.

A1.4 Mice lacking KIF17 display defects in cerebellum proliferation

In Chapter III, I show that *Kif17*$^{-/-}$ mice display smaller cerebella compared to *Kif7*$^{+/+}$. To determine whether this difference is due to defects in proliferation, I performed additional immunofluorescence experiments using markers for proliferation (Ki67) and apoptosis (caspase-3) (Figure A1.4). Strikingly, at P14, even at a time point when cerebellar proliferation has started to decrease (Espinosa and Luo, 2008), Ki67 staining is more abundantly distributed within the proliferative external granular layer (EGL) in *Kif17*$^{+/+}$ compared to *Kif17*$^{-/-}$ embryos (Figure A1.4A, high magnification images in middle panel). In contrast, no discernable difference is observed between *Kif17*$^{+/+}$ and *Kif17*$^{-/-}$ cerebella using an antibody against cleaved caspase-3 (Figure A1.4B). These results suggest that the smaller sized cerebella in *Kif17*$^{-/-}$ mice is likely due to defects in granular cell proliferation and not cell death. It will be important to perform similar immunofluorescence experiments on P8 *Kif17*$^{+/+}$ and *Kif17*$^{-/-}$ cerebella when granule cells are rapidly proliferating in response to the HH ligand (Corrales et al., 2004; Wechsler-Reya and Scott, 1999). Furthermore, isolating proliferating granular cells and performing proliferation assays using HH ligand will be required to determine whether the proliferation defect observed in *Kif17*$^{-/-}$ cerebella is due to a defect in HH signaling.

Figures

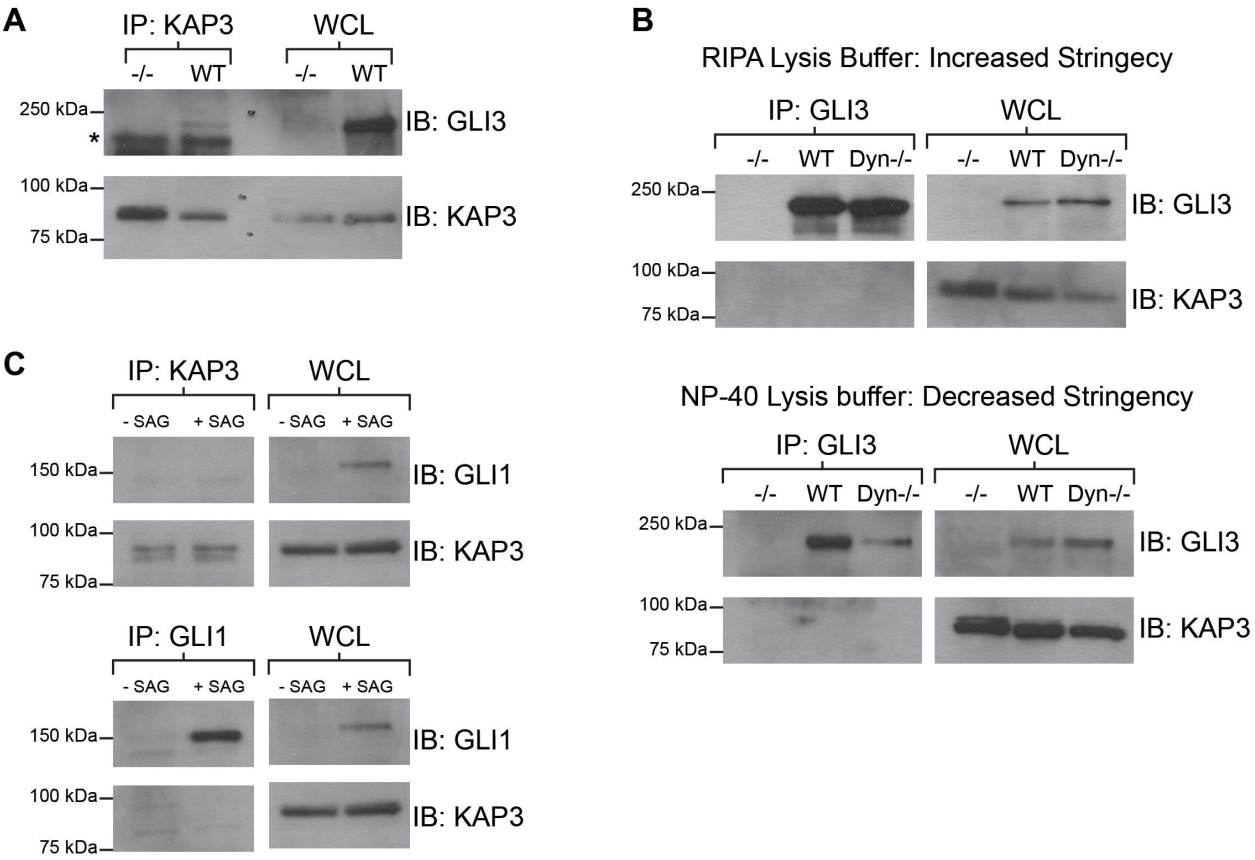

Figure A1.1. Endogenous KAP3 does not co-immunoprecipitate with endogenous GLI3 and GLI1. (A) Immunoprecipitation of endogenous KAP3 from *Gli2*$^{-/-}$*;Gli3*$^{-/-}$ (-/-) and wildtype (WT) MEFs. (*) denotes a non-specific band detected in both WT and -/- tissue. (B) Immunoprecipitation of endogenous GLI3 from *Gli2*$^{-/-}$*;Gli3*$^{-/-}$ (-/-), wildtype (WT), and Dynein (*Dync2h1*) mutant (Dyn-/-) MEFs. Whole cell lysates (WCL) were collected in either a high stringency RIPA lysis buffer (B, top) or a low stringency NP-40 lysis buffer (B, bottom). (C) Immunoprecipitation of either endogenous KAP3 (C, top) or GLI1 (C, bottom) from wildtype MEFs in the presence (+SAG) or absence (-SAG) of Smoothened agonist (SAG). Immunoprecipitates (IP) and whole cell lysates (WCL) were subjected to SDS-PAGE and western blot analysis (IB) using anti-KAP3, anti-GLI3, and/or anti-GLI1 antibodies. The molecular weights (in kDa) of protein standards are indicated at the left of each blot.

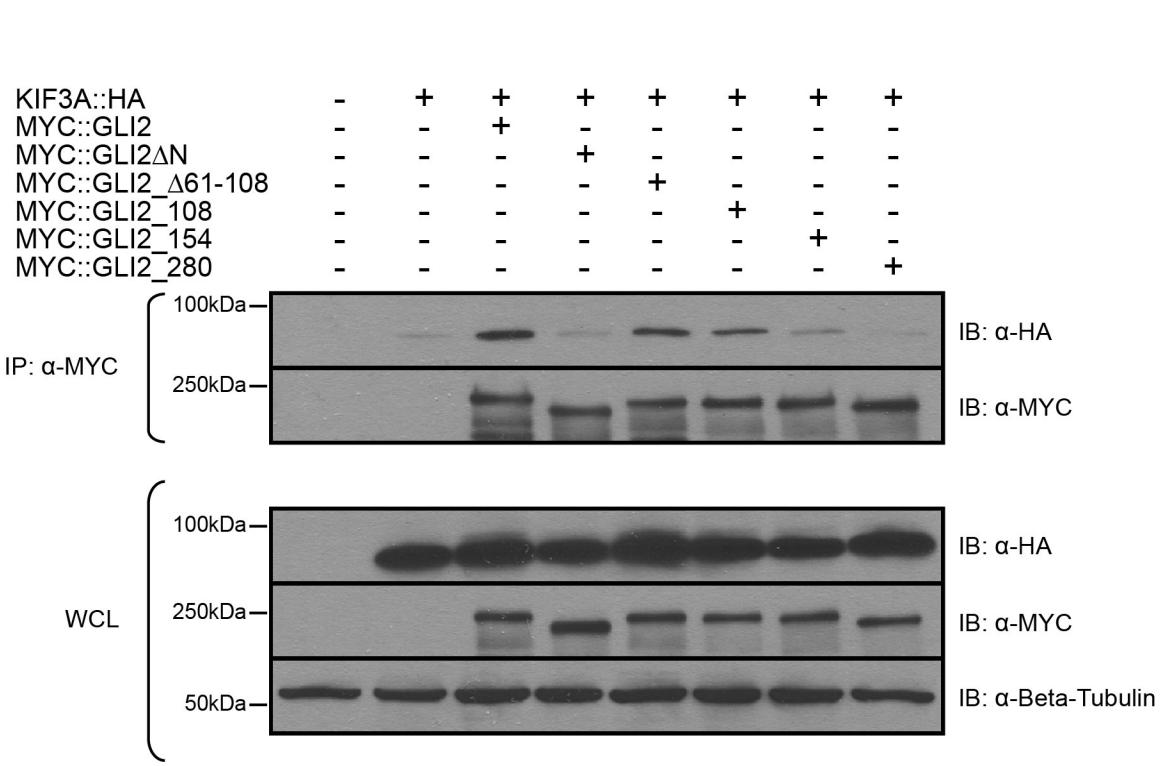

Figure A1.2. GLI2 interacts with KIF3A via a distinct domain from KAP3.
(A) Immunoprecipitation of MYC::GLI2, MYC::GLI2ΔN, MYC::GLI2_Δ61-108, MYC::GLI2_108-1586, MYC:GLI2_154-1586, or MYC:GLI2_280-1586 from COS-7 cells expressing KIF3A::HA. Immunoprecipitates (IP) and whole cell lysates (WCL) were subjected to SDS-PAGE and western blot analysis (IB) using antibodies directed against MYC (α-MYC) and HA (α-HA). Antibody detection of Beta-Tubulin (α-Beta-Tubulin) was used to confirm equal loading across lanes. The molecular weights (in kDa) of protein standards are indicated at the left of each blot.

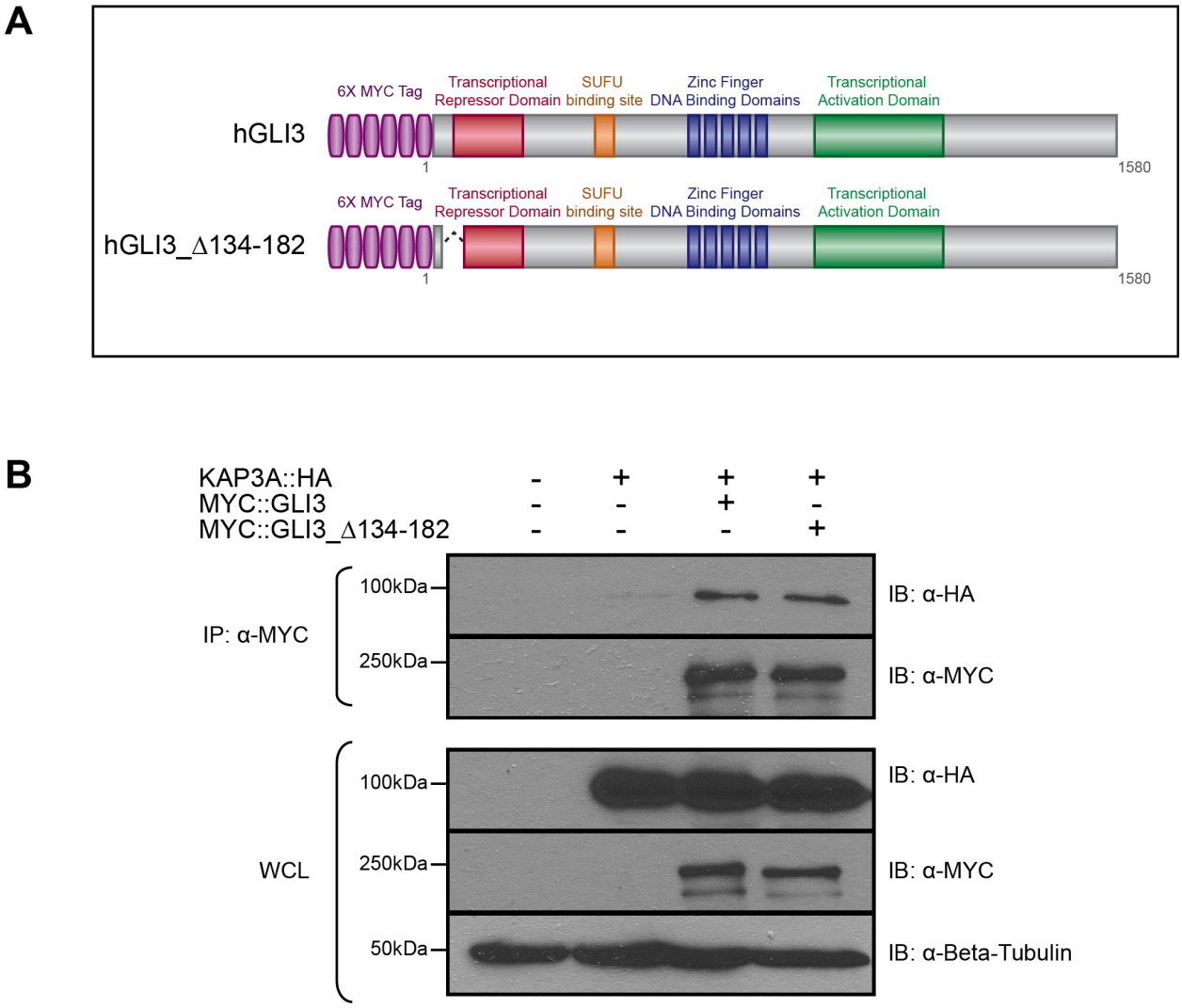

Figure A1.3. Full-length GLI3 lacking the KAP3 binding domain interacts with KAP3. (A) Graphic representation of full-length and mutant human GLI3 proteins. (B) Immunoprecipitation of MYC::GLI3 or MYC::GLI3Δ134-182 from COS-7 cells expressing KAP3A::HA. Immunoprecipitates (IP) and whole cell lysates (WCL) were subjected to SDS-PAGE and western blot analysis (IB) using antibodies directed against MYC (α-MYC) and HA (α-HA). Antibody detection of Beta-Tubulin (α-Beta-Tubulin) was used to confirm equal loading across lanes. The molecular weights (in kDa) of protein standards are indicated at the left of each blot.

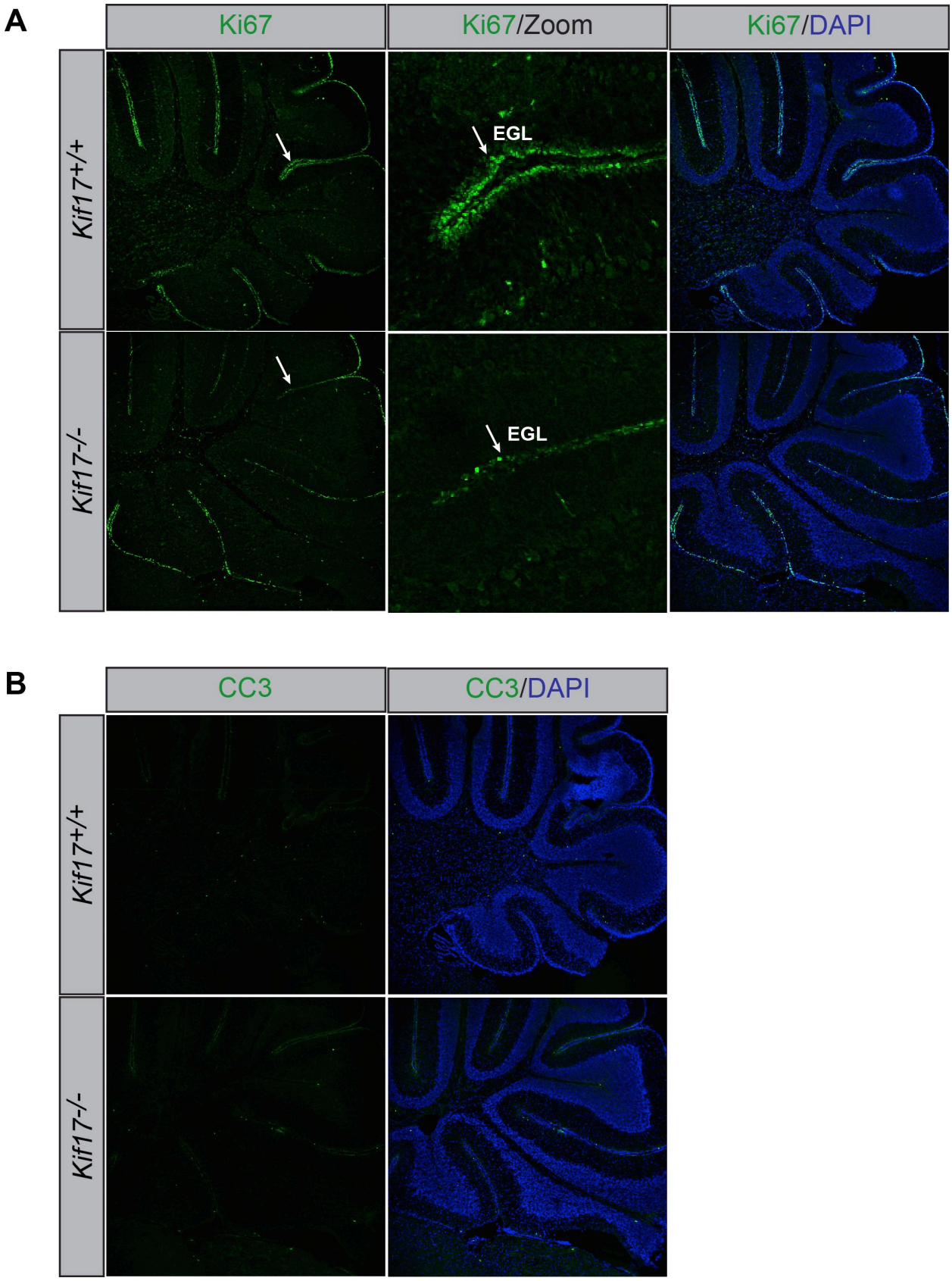
A
Ki67
Ki67/Zoom
Ki67/DAPI
Kif17+/+
Kif17-/-
EGL
EGL
B
CC3
CC3/DAPI
Kif17+/+
Kif17-/-

Figure A1.4. *Kif17*$^{-/-}$ mice display defects in cerebellar proliferation.
Immunofluorescence staining of *Kif17*$^{+/+}$ and *Kif17*$^{-/-}$ P14 mouse cerebella stained with markers for (A) proliferation (Ki67, green) and (B) apoptosis [cleave caspase-3 (CC3), green]. Nuclei are stained with DAPI (blue). Arrows in (A) highlight cerebellar lobule VIII that is magnified in the middle panels to highlight differences in proliferation of cells within the external granular layer (EGL).

References

Chen, J.K., J. Taipale, and K.E. Young. 2002. Small molecule modulation of Smoothened activity.

Corrales, J.D., G.L. Rocco, S. Blaess, Q. Guo, and A.L. Joyner. 2004. Spatial pattern of sonic hedgehog signaling through Gli genes during cerebellum development. *Development*. 131:5581–5590. doi:10.1242/dev.01438.

Espinosa, J.S., and L. Luo. 2008. Timing Neurogenesis and Differentiation: Insights from Quantitative Clonal Analyses of Cerebellar Granule Cells. *J. Neurosci.* 28:2301–2312. doi:10.1523/JNEUROSCI.5157-07.2008.

Wechsler-Reya, R.J., and M.P. Scott. 1999. Control of Neuronal Precursor Proliferation in the Cerebellum by Sonic Hedgehog. *Neuron*. 22:103–114. doi:10.1016/S0896-6273(00)80682-0.

Wen, X., C.K. Lai, M. Evangelista, J.A. Hongo, F.J. de Sauvage, and S.J. Scales. 2010. Kinetics of Hedgehog-Dependent Full-Length Gli3 Accumulation in Primary Cilia and Subsequent Degradation. *Molecular and Cellular Biology*. 30:1910–1922. doi:10.1128/MCB.01089-09.